REGULATION OF UBIQUITIN-MEDIATED ENDOCYTOSIS IN *SACCHAROMYCES CEREVISIAE*

A Dissertation

Presented to the Faculty of the Graduate School

of Cornell University

In Partial Fulfillment of the Requirements for the Degree of

Doctor of Philosophy

by

Pi-Chiang (Bi) Hsu

Augest 2012

© 2012 Pi-Chiang (Bi) Hsu

Regulation of Ubiquitin-mediated Endocytosis in *Saccharomyces Cerevisiae*

Pi-Chiang (Bi) Hsu, Ph. D.

Cornell University 2012

Endocytic downregulation plays an important role in the homeostasis of plasma membrane (PM) proteins. A key determinant of this process is ubiquitin modification, which targets surface proteins for endocytosis. In *Saccharomyces cerevisiae*, most PM proteins that have been studied undergo ubiquitin-dependent endocytic downregulation mediated by the ubiquitin ligase Rsp5. Previously, we identified a family of yeast arrestin-related trafficking adaptors, or ARTs that function as adaptors for Rsp5, targeting its ubiquitin ligase activity to specific proteins at cell surface.

The goal of my thesis research has been to understand how ART activity is regulated to control the composition of protein at cell surface. In the first part of my thesis, I demonstrate that the TORC1 kinase signaling pathway modulates the protein composition of the PM by regulating Art1 activity and ubiquitin-mediated endocytosis. This research elucidates a novel effector mechanism of TORC1, underscoring how TORC1 coordinates ubiquitin-mediated endocytosis with protein synthesis and autophagy in order to regulate cell growth. In the second part of my thesis, I demonstrate that the PP1 family Ppz phosphatases are involved in regulating PM cargo ubiquitination and endocytosis by mediating the Art1 phospho-regulatory cycle. This study provides a potential mechanism of

how Ppz phosphatases may activate different ART family proteins to trigger PM protein turnover. In the last part of my thesis, I show that a specialized secretion pathway at the Golgi complex plays a role in Art1 PM translocation, which is required for Art1-mediated cargo endocytosis. This research begins to dissect a potential mechanism for the Golgi-to-PM trafficking of Art1 during endocytic targeting. In conclusion, based on our various genetic, biochemical, and proteomic analyses, I propose that: 1) TORC1 kinase signaling regulates endocytosis by controlling ubiquitin ligase activity; 2) Art1 activity is tightly regulated by a complex phosphorylation cycle which involves in Npr1 kinase, Ppz phosphatases, as well as other potential phosphor-regulatory factors; and 3) the Golgi-to-PM trafficking machinery plays an important role in regulating PM protein endocytosis via mediating Art1 subcellular localization and activity.

Biographical Sketch of Pi-Chiang (Bi) Hsu

Pi-Chiang Hsu was born in Taipei, the capital city of Taiwan. He went to National Taiwan University for undergraduate study in 2000. In his sophomore year, he joined Dr. Zee-Fen Chang's laboratory for his undergraduate thesis study to understand the mechanism of death receptor-mediated apoptosis. In 2004, he accepted the offer from the Institute of Biochemistry and Molecular Biology, National Taiwan University, College of Medicine and continued his research at Dr. Zee-Fen Chang's laboratory for his master thesis study. He dissected the mechanism of Rho kinase (ROCK)-dependent repression of general transcription in a leukemia cell line. After graduated from his master study in 2006, he joined Dr. Yao-Ming Wu's laboratory at the Department of Surgery, National Taiwan University Hospital as a research assistant to study hepatic preconditioning for transplanted cell engraftment and proliferation. In the same year, he won the Taiwan Ministry of Education Graduate Fellowship in Biotechnology. Next year, he accepted an offer from the Biochemistry Molecular and Cell Biology program, Cornell University and started his Ph.D. study in 2008. He joined Dr. Scott Emr's laboratory in 2009 and began his Ph.D. thesis study on dissecting the regulatory mechanisms of a ubiquitin ligases adaptor, Art1. He published his work on Art1 in *Cell* in 2011 and the *Annual Review of Biochemistry* journal in 2012.

This work is dedicated to my grandmother Yueh-Yun HsuLo.
此書獻給我的阿嬤許駱月雲

ACKNOWLEDGEMENTS

If life was composed of different journeys, the journey of my Ph.D. study would be the most exciting and abundant one. Throughout this journey, I have witnessed beautiful sceneries and, of course, met many wonderful people. However, every journey has a beginning, and an end. I am very happy and proud to give thanks to those who have helped me mentally and scientifically throughout this entire journey.

First, I would like to give thanks to my best friend, Tsai-Ni Hsieh. She lives in Taipei where there is a 12-hour time difference from here in the United States, but her support has always been by my side. Tsai-Ni was the first person to visit me and warmed my heart when Ithaca was covered by the silent white of snow. We shared our sorrows and happiness every week like there was no distance between us. It would be extremely difficult and hard to imagine finishing my Ph.D. study without such a big support.

A person's success is also the success of his family. I am very lucky and grateful for having the best parents in the world. Their wisdoms guide me towards the right direction when I am in the darkest of places. Their cares comfort me to a peaceful rest when I am in the most anxious of moods. The journey of my Ph.D. study is just one small example of showing how much and how far their love has touched me.

Next, I am honored to thank my supervisor and mentor, Scott Emr. He lets me realize the ART of the SCIENCE. He always instructs and encourages me to reach new heights of scientific knowledge that I have never dreamed existed. As

my research is trying to dissect cellular pathways, Scott's advice is as strong as a lighthouse that guides me along the right route when I am lost in these pathways. Moreover, he is always very supportive and encouraging when I have any question to consult with him. The help he provides is the key to cultivating me towards my long-term goal of becoming an independent scientist.

I also want to express my deep and sincere appreciation to Jason MacGurn. If I could write down all the things he has helped me accomplished, it could very well be one of the chapters in my thesis. Jason himself is a perfect model of how an outstanding scientist should be like. I not only learned a voluminous amount of scientific- and nonscientific-related knowledge from him, but also enjoyed working with him over these past four years. His good influences have and will always push me to become a better researcher.

Finally, I would like to thank God for making everything possible. Every step in this Ph.D. study journey is a beautiful miracle!

TABLE OF CONTENTS

LIST OF FIGURES

LIST OF TABLES

Chapters 1, in part, material as it appears in *Annual Review of Biochemistry* 81:231-259, 2012. MacGurn J.A., **Hsu P.C.**, and Emr S.D.. Ubiquitin and membrane protein turnover: from cradle to grave. The dissertation author was the second author of this paper.

Chapter 2, in part, material as it appears in *Cell* 147(5): 1104-1117, 2011. MacGurn J.A., **Hsu P.C.**, and Emr S.D.. TORC1 regulates endocytosis via Npr1-mediated phosphoinhibition of a ubiquitin ligase adaptor. The dissertation author was the primary investigator and co-first author of this paper. In the paper list above, Pi-Chiang carried out a genetic screen using the yeast deletion mutant collection. He discovered a protein kinase Npr1 that regulates the activity of a ubiquitin ligase adaptor, Art1. Pi-Chiang's research contributions are presented in Figure 1, 2, 3 and 4. The other co-first author, Jason McGurn, carried out the Mass Spec studies included in the paper (Figure 5, 6 and 7).

Chapter 5, in part, material as it appears in *Cell* 147(5): 1104-1117, 2011. MacGurn J.A., **Hsu P.C.**, and Emr S.D.. TORC1 regulates endocytosis via Npr1-mediated phosphoinhibition of a ubiquitin ligase adaptor. The dissertation author was the primary investigator and co-first author of this paper.

Chapter 1

INTRODUCTION

Endocytic Downregulation of Plasma Membrane Proteins

Endocytic downregulation plays a pivotal role in the homeostasis of plasma membrane (PM) proteins in eukaryotic cells, influencing key cellular processes such as nutrient uptake and signaling for cell growth and differentiation (Ing et al., 2007). Failure to properly downregulate PM proteins via endocytosis has been implicated in the development of various diseases ranging from cancer to neurodegeneration. Different human diseases have been linked to the proper regulation of PM protein endocytosis. One example of these diseases is Liddle's syndrome. Patients with this syndrome cannot downregulate the PM epithelial Na^+ channel (ENaC) in the kidney and have abnormal reabsorption of sodium, resulting in hypertension (Warnock, 2001).

There are three major stages associated with the endocytic downregulation of PM proteins: 1) PM protein internalization by endocytosis and delivery to the endosome; 2) endosomal protein sorting into intralumenal vesicles, forming the multivesicular body (MVB); 3) fusion of the endosome with the lysosome and protein degradation (Figure 1.1) (Bonifacino and Weissman, 1998), (Katzmann et al., 2004). Although the trafficking processes that govern endocytic downregulation have been studied extensively, the diversity of PM proteins and complexity of extracellular signals make it difficult to study how cargo-specificity of endocytosis is achieved. One classic example is the downregulation of G protein-coupled receptors

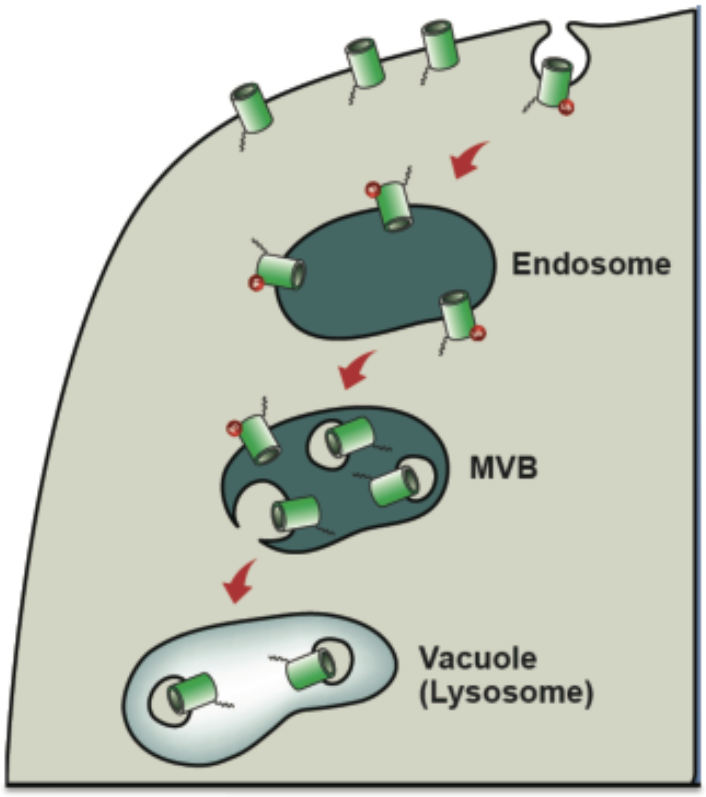

Figure 1-1

Figure 1.1. The three stages of endocytic pathway. There are three stages for plasma membrane proteins undergo endocytic turnover. After a specific stimulation, PM proteins are internalized by endocytic machinery and delivered to the endosome. Next, these endosomal proteins are sorted into MVB by the ESCRT machinery. Finally, the endosome is fused with lysosome and the proteins are degraded.

(GPCRs). There are more than 1000 different GPCRs encoded in the human genome, each with the potential to respond to different extracellular stimuli (Lefkowitz, 1998). Agonist-induced GPCR activation triggers both a signaling cascade and a negative feedback mechanism, which is required to attenuate the signaling process. Central to GPCR downregulation are arrestins. Following GPCR activation, GPCR kinases (GRKs) phosphorylate GPCRs, which creates a binding surface for arrestins (Moore et al., 2007). Arrestin not only sterically blocks G protein activation but also serves as an adaptor to recruit endocytic machinery (Kendall and Luttrell, 2009). Interestingly, the regulation of arrestins themselves is not well understood, although arrestin post-translational modifications, such as phosphorylation and ubiquitination, and subcellular localization all seem to have important regulatory roles.

Four well-studied human arrestins have been reported to regulate GPCR turnover (Gurevich and Gurevich, 2006). Two of them, visual and cone arrestins, are only expressed in retina cells and the other two, β-arrestin 1 and β-arrestin 2, are ubiquitously expressed. The crystal structures of these arrestins have been determined and all of them form a conserved β-sandwich ("arrestin fold") structure (Aubry et al., 2009). Interestingly, structural and bioinformatic analyses have indicated at least nine proteins exhibit the arrestin fold structure in mammalian cells. Although most of these proteins are not well studied, one of them, Vps26, has been demonstrated to be involved in the cargo recognition subcomplex in retromer, a protein complex that mediates cargo recycling from the endosome to Golgi (Collins et al., 2008). Thus, proteins harboring an arrestin fold structure may generally be

responsible for membrane protein recognition. While numerous studies have elucidated the mechanism of GPCR turnover, less is known about how other PM proteins are downregulated. It is important to improve our understanding of how different arrestin fold proteins recognize specific membrane cargos at the right time and right place.

A key determinant of endocytic downregulation of surface proteins is ubiquitin modification, which is thought to target plasma membrane proteins to conserved ubiquitin-binding domains of the endocytic machinery. In *Saccharomyces cerevisiae*, hundreds of PM cargos undergo ubiquitin-dependent endocytic downregulation mediated by the ubiquitin ligase Rsp5. Recently, a chemical-genetic screen led to the identification of a family of arrestin-related trafficking adaptors (or ARTs) in yeast that function as adaptors for Rsp5, targeting its ubiquitin ligase activity to specific PM cargos (Lin et al., 2008). Yeast ARTs direct ubiquitin ligase activity to specific PM cargoes and target them for endocytosis. Art1 was originally identified based on its hypersensitivity to canavanine, a toxic analog of arginine, indicating involvement in the endocytosis of the arginine transporter Can1. Interestingly, Art1 was shown to play a role in cargo-specific endocytic downregulation. Structural modeling revealed that Art1 contains an arrestin fold domain at the N-terminus, while the C-terminus contains two PY motifs that mediate interaction with Rsp5. Although it is understood that ARTs function to recruit ubiquitin ligase activity to specific cargo at the PM, little is known about how Art1 itself is regulated and how cargo specificity is achieved. Here we focus on dissecting the molecular mechanism of Art1 phospho-regulation and subcellular localization.

UBIQUITIN-MEDIATED TURNOVER OF PLASMA MEMBRANE PROTEINS

The abundance and localization of integral membrane proteins—including nutrient transporters, ion channels, and signaling receptors—play a critical role in the growth, differentiation, and survival of eukaryotic cells. The complex process of remodeling cell surface protein composition involves both biosynthetic addition of new integral membrane proteins (or cargoes) to the PM and removal of cargoes from the PM by endocytosis. A key regulator of the sorting, trafficking, and turnover of integral membrane proteins is ubiquitination.

Ubiquitin is a 76-amino acid peptide that can be conjugated to other proteins by the formation of an isopeptide bond between the COOH-terminal glycine carboxy group of ubiquitin and the ε-amino group of a lysine residue on the recipient protein (Komander, 2009; Ye and Rape, 2009). Ubiquitin conjugation, or ubiquitination, is the end result of three sequential enzymatic reactions catalyzed by a ubiquitin-activating enzyme (E1), a ubiquitin conjugating enzyme (E2), and a ubiquitin ligase (E3) (Deshaies and Joazeiro, 2009; Nagy and Dikic, 2009; Wenzel et al., 2010). A key feature of ubiquitination is that it is potentially recursive: Ubiquitin can modify itself on any one of its seven lysine residues (K6, K11, K27, K29, K33, K48, K63) or on its N terminus, leading to the formation of polyubiquitin chains that have different structures and properties depending on how the chains are assembled (Behrends and Harper, 2011; Komander, 2009).

E3 ubiquitin ligases mediate the addition of ubiquitin to substrates and thus determine the type and extent of ubiquitin modification. There are two major ubiquitin ligase families: (a) the RING (really interesting new gene) domain E3

ligases (616 in humans, 40 in yeast), which bind to E2-ubiquitin conjugates and substrates and provide optimal steric orientation for direct ubiquitin transfer to substrate (Deshaies and Joazeiro, 2009; Duda et al., 2011); and (*b*) the HECT (homologous to E6-AP C terminus) domain E3 ligases (28 in humans, 5 in yeast), which accept ubiquitin from E2 enzymes on catalytic cysteine residues and catalyze direct transfer of ubiquitin to substrates (Bernassola et al., 2008; Kee and Huibregtse, 2007; Ye and Rape, 2009). The activity of ubiquitin ligases can be antagonized by deubiquitinating enzymes, or DUBs. DUBs are proteases that catalyze the cleavage of ubiquitin-lysine isopeptide bonds. There are roughly 100 DUBs encoded in the human genome (less than 20 in yeast), which can be classified on the basis of five known DUB protein families: the Ubiquitin-Specific Protease (USP) family, the Ubiquitin C-Terminal Hydrolase (UCH) family, the Ovarian Tumor domain (OTU) family, the Machado-Josephin domain (MJD) family, and the JAMM (JAB1/MPN/MOV34) domain family (Komander et al., 2009). DUBs from the USP, UCH, OTU, and MJD families are cysteine proteases, whereas JAMM family DUBs are metalloproteases. The reversible nature of ubiquitination allows it to function as an important regulatory switch in the cell.

It is well established that protein K48-linked polyubiquitination of soluble, cytosolic proteins results in degradation by targeting to the proteasome and thus regulates protein stability (Komander, 2009; Xu et al., 2009). However, integral membrane proteins are not directly accessible to the proteasome, and thus, eukaryotic cells have evolved elaborate mechanisms to monitor, sort, and degrade them. These mechanisms rely on membrane trafficking events in the cell that are

often guided by ubiquitin modification of substrates (Figure 1.2A). There is an emerging consensus that, although K48-linked polyubiquitin chains function in proteasomal degradation, ubiquitin-mediated membrane trafficking events in the cell are largely governed by monoubiquitination and K63-linked polyubiquitination (Hoeller and Dikic, 2011; Lauwers et al., 2010). Taken together, ubiquitination plays an important role in the sorting, trafficking, and degradation of integral membrane proteins. Here, I place special emphasis on the role of ubiquitin in the quality control of integral membrane proteins at the PM (Figure 1.2B and Figure 1.3).

Ubiquitin-Mediated Endocytosis

Ubiquitin-mediated endocytosis first came into focus with studies in yeast demonstrating a ubiquitin requirement for endocytosis of various PM cargoes, including Ste6 (Kolling and Hollenberg, 1994), Ste2 (Hicke and Riezman, 1996; Jenness et al., 1997), Pdr5 (Egner and Kuchler, 1996), and Fur4 (Galan et al., 1996). Indeed, for many cargoes studied in yeast, ubiquitin modifications are both necessary and sufficient for endocytosis (Hicke and Riezman, 1996; Shih et al., 2000), although ubiquitin independent endocytosis of cargoes has also been described (Chen and Davis, 2002; Tan et al., 1996). The general consensus is that ubiquitin-mediated endocytosis is the dominant mechanism for internalization of most cargoes studied in yeast. However, in mammalian cells, the role of ubiquitin in endocytosis is somewhat more complicated. For many endocytic cargoes in mammalian cells, including receptor tyrosine kinases (RTKs) and GGPCRs, ubiquitin modification appears to be sufficient for endocytic uptake (Haglund et al., 2003; Sigismund et al., 2005). Strikingly, although many of these cargoes exhibit ligand

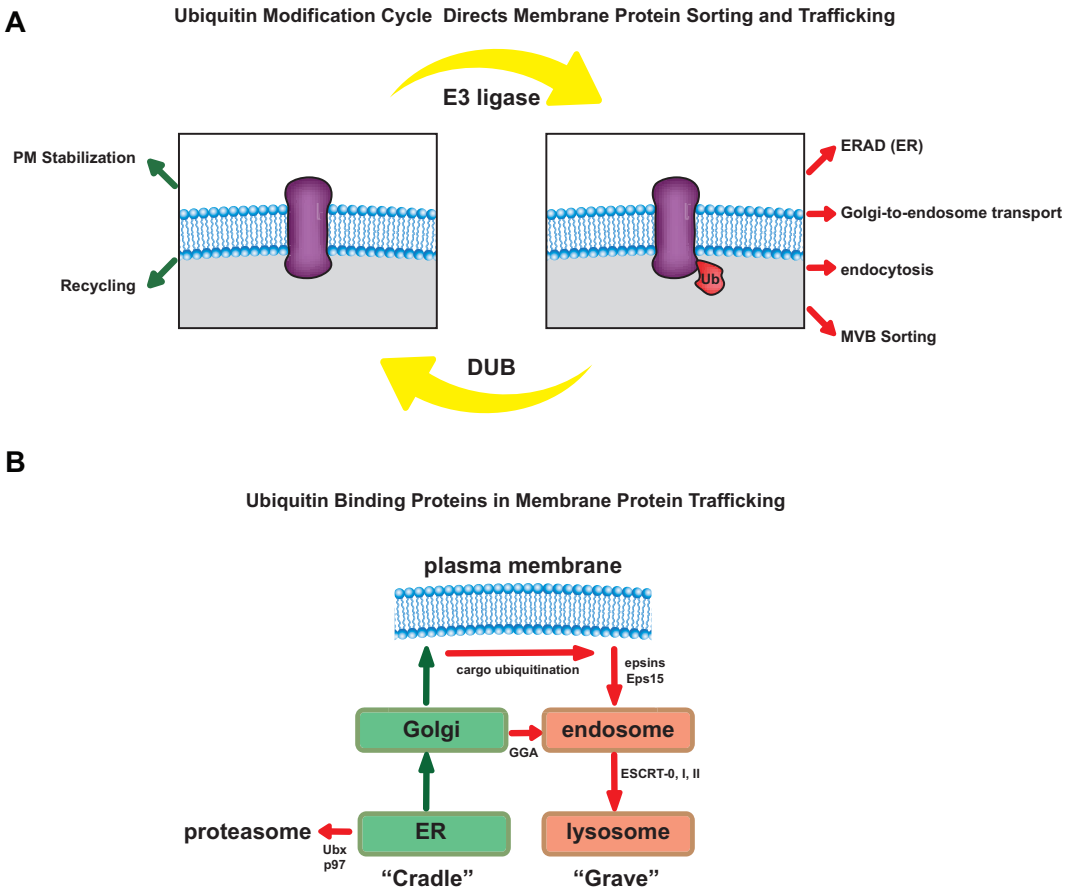
A
Ubiquitin Modification Cycle Directs Membrane Protein Sorting and Trafficking
E3 ligase
PM Stabilization
Recycling
Ub
ERAD (ER)
Golgi-to-endosome transport
endocytosis
MVB Sorting
DUB
B
Ubiquitin Binding Proteins in Membrane Protein Trafficking
plasma membrane
cargo ubiquitination
epsins
Eps15
Golgi
GGA
endosome
ESCRT-0, I, II
proteasome
Ubx
p97
ER
lysosome
“Cradle”
“Grave”

Figure 1-2

Figure 1.2. Common themes in ubiquitin-mediated membrane trafficking and turnover events. (A) The ubiquitin modification cycle of membrane protein sorting and trafficking. (B) Ubiquitin binding proteins in the membrane protein trafficking circuit. DUB, deubiquitinating enzyme; Eps15, epidermal growth factor receptor pathway 15; ER, endoplasmic reticulum; ERAD, endoplasmic reticulum–associated degradation; ESCRT, endosomal sorting complex required for transport; GGA, Golgi-localized, γ-ear-containing, ARF-binding protein; MVB, multivesicular body; PM, plasma membrane; Ubx, ubiquitin regulatory X domain-containing proteins; p97, an AAA ATPase that recognizes ubiquitinated substrates at the ER (via Ubx protein adaptors) and is thought to extract substrates from the ER membrane.

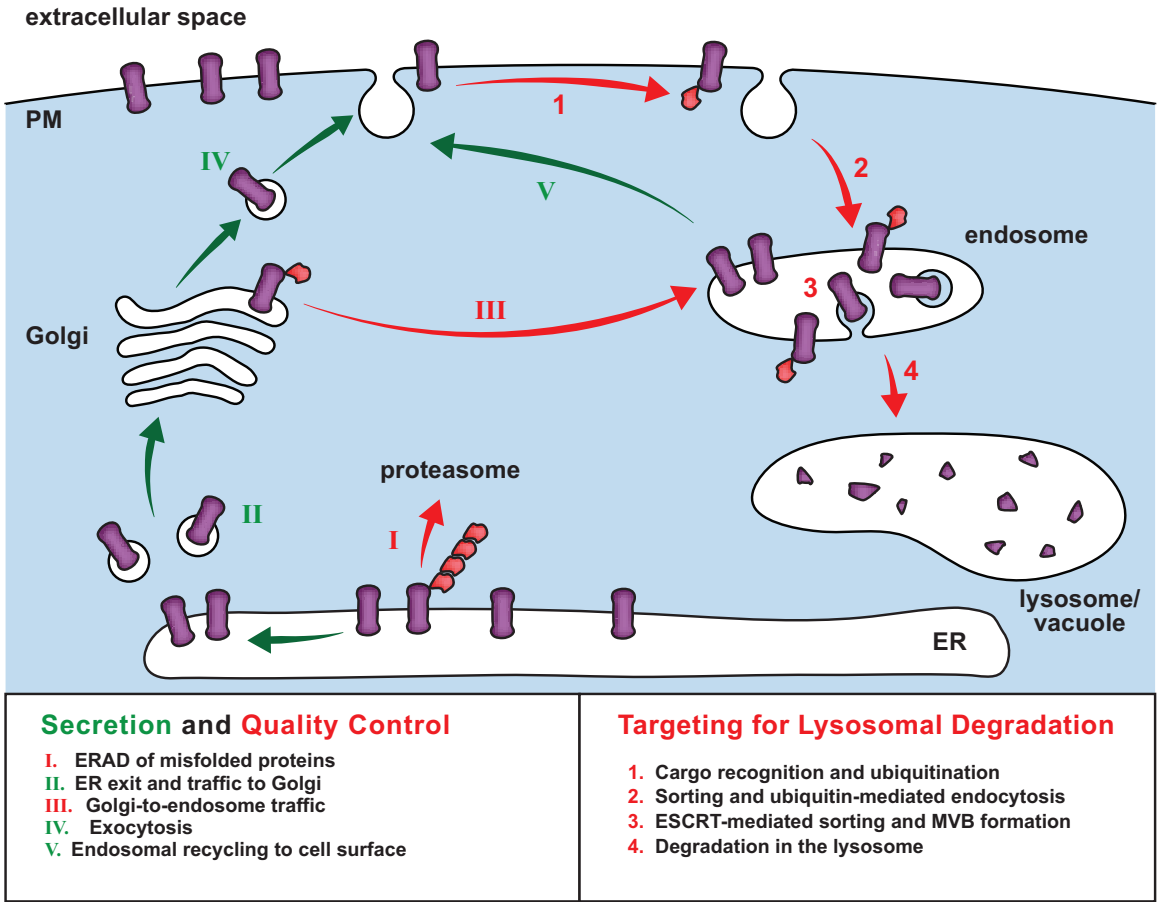
extracellular space
PM
1
2
IV
V
endosome
3
III
Golgi
4
proteasome
II
I
lysosome/
vacuole
ER
Secretion and Quality Control
I. ERAD of misfolded proteins
II. ER exit and traffic to Golgi
III. Golgi-to-endosome traffic
IV. Exocytosis
V. Endosomal recycling to cell surface
Targeting for Lysosomal Degradation
1. Cargo recognition and ubiquitination
2. Sorting and ubiquitin-mediated endocytosis
3. ESCRT-mediated sorting and MVB formation
4. Degradation in the lysosome

Figure 1-3

Figure 1.3. Ubiquitin-mediated membrane protein trafficking processes in the cell. ER, endoplasmic reticulum; ERAD, endoplasmic reticulum–associated degradation; ESCRT, endosomal sorting complex required for transport; MVB, multivesicular body; PM, plasma membrane.

dependent ubiquitin modification, they also exhibit ubiquitin-independent endocytosis. Thus, in mammalian cells, ubiquitination is often sufficient but not required for internalization by endocytosis. This is indicative of multiple redundant yet distinct mechanisms of endocytosis (Goh et al., 2010), which may coordinately influence the fate of internalized cargo on the endosome.

A fundamental question of ubiquitin-mediated endocytosis is how ubiquitin modified cargoes are recognized and sorted into endocytic vesicles. One prevailing hypothesis is that various UBDs located within the endocytic machinery may recruit ubiquitinated cargoes for internalization. For example, epsin family proteins (Ent1 and Ent2 in yeast) interact with clathrin, the AP-2 adaptor, and other endocytic proteins and have long been studied for their role in endocytosis. Epsins interact with ubiquitin via tandem ubiquitin-interacting motif (UIM) domains, which have been proposed to function in the sorting of ubiquitinated cargoes for endocytosis. Similarly, the eps15 and eps15R proteins (similar to yeast Ede1) interact with other endocytic proteins via N-terminal EH (Eps15 homology) domains and also interact with ubiquitin via C-terminal tandem UIM domains (Polo et al., 2002). In both yeast and mammals, epsins and Eps15 family members exhibit redundant functions for endocytosis (Shih et al., 2002; Sigismund et al., 2005) and have been shown to bind to ubiquitinated cargo (Kazazic et al., 2009; Sigismund et al., 2005).

Many UBD-containing proteins, including Eps15 proteins (Polo et al., 2002), are subject to coupled monoubiquitination (Hoeller and Dikic, 2011), fueling speculation that UBDs in epsins and Eps15 family proteins may function in the assembly of the endocytic protein interaction network. It is conceivable that

ubiquitin modification of endocytic proteins can "seed" the assembly of endocytic protein interaction networks. Perhaps the best evidence that ubiquitin modification regulates the function of endocytic proteins comes from the investigation of photoreceptor cell differentiation during compound eye development in *Drosophila*. One *Drosophila* mutant called *fat facets* exhibits excess photoreceptor cell differentiation, indicating that the protein encoded by *fat facets* (Faf) is a differentiation inhibitor. The Faf protein was shown to be a DUB (Huang et al., 1995) that deubiquitinates the protein encoded by a gene called *liquid facets* (*Lqf*), a *Drosophila* epsin family protein (Cadavid et al., 2000; Chen et al., 2002). Faf regulates the stability and abundance of Lqf (and perhaps other endocytic proteins) by antagonizing its ubiquitination and subsequent proteasomal degradation (Chen et al., 2002). Both Faf and Lqf are required for the endocytosis of the Notch ligand Delta (Overstreet et al., 2004), demonstrating how ubiquitination/deubiquitination dynamics of an endocytic protein is critical to cell differentiation and patterning during development.

In addition to epsins and Eps15 proteins, other endocytic proteins have been shown to bind ubiquitin, including Cin85 (yeast Sla1) (Stamenova et al., 2007), amphiphysin (Stamenova et al., 2007), and the yeast protein Lsb5 (Costa et al., 2005). The molecular function of these ubiquitin-binding activities is not clear, but the myriad of ubiquitin-binding elements within the endocytic machinery, possibly including UBDs that have not yet been described, suggests either significant redundancy or elaborate avidity affects, making it difficult to dissect precise biochemical events that govern ubiquitin-mediated endocytosis. Because the

affinity of interactions between individual UBDs and monoubiquitin is low, it is possible that efficiency of endocytic sorting might be determined by the number of ubiquitin modifications, the extent and linkage types of polyubiquitin chains, lateral interaction with other ubiquitinated cargoes at the PM, as well as orthogonal, ubiquitin-independent sorting signals. Thus, despite a clear regulatory role of ubiquitination in targeting cargo for endocytosis, it has been difficult to establish an exclusive role for ubiquitin in endocytosis for the following reasons: (1) In mammalian cells, there are different kinds of endocytosis, which have different sorting determinants and often act redundantly for internalization of specific cargo, although trafficking outcomes may be determined by the route of entry (i.e., lysosomal sorting versus recycling). (2) The endocytic protein interaction network contains many UBDs, which may act in a redundant manner or serve as avidity sensors to determine efficiency of sorting for endocytosis. (3) Some endocytic proteins are ubiquitinated, suggesting that some UBDs may mediate interactions within the endocytic protein network and that others may mediate recognition of ubiquitinated cargo. (4) PM cargoes participate in multiple interactions with other PM cargoes, suggesting that cargo homo- or heterooligomerization at the PM may allow nonubiquitinated cargo to piggyback during ubiquitin-mediated endocytosis.

Ubiquitin Editing at the Plasma Membrane and Endosome

The proteasome associates with both ubiquitin ligases and DUBs which edit ubiquitin chains on potential substrates, an effect that can either rescue a substrate or hasten its demise. As has been observed with the proteasome, the

ESCRT machinery associates with various E3 ubiquitin ligases and DUBs that can influence cargo fate on the endosome. In general, the association of E3 ubiquitin ligases with ESCRTs is thought to promote cargo sorting for lysosomal degradation (Bhandari et al., 2007; Malik and Marchese, 2010; Ren et al., 2007; Zhou et al., 2010), although there are some cases where such association negatively regulates ESCRT stability (Kim et al., 2007; Kim et al., 2006; McDonald and Martin-Serrano, 2008). In yeast, Rsp5 clearly localizes to endosomal structures (Katzmann et al., 2004; Wang et al., 2001) and has been shown to interact with a C-terminal PY motif in Hse1 (ESCRT-0), an interaction required for efficient sorting of some cargoes (Ren et al., 2007). Thus, even as cargoes are being sorted by ESCRTs, last-minute ubiquitin conjugation may influence sorting decisions.

Just as E3 ubiquitin ligases on the endosome can nudge cargo toward the grave, so can endosomal DUBs rescue cargo by removing ubiquitin, antagonizing their association with ESCRTs, and promoting their recycling back to the cell surface. For example, UCH-L3 is a DUB that promotes ENaC recycling to the cell surface by catalyzing its deubiquitination (Butterworth et al., 2007). The DUB Usp10 was shown to mediate the deubiquitination of cystic fibrosis transmembrane conductance regulator (CFTR) on endosomes and thus promote recycling to the surface (Bomberger et al., 2009). Two DUBs, Usp33 and Usp20, were recently shown to deubiquitinate the β_2-adrenergic receptor on endosomes and thus promote recycling to the cell surface (Berthouze et al., 2009). AMSH (associated molecule with the SH3 domain of STAM), a JAMM family DUB, was shown to interact with STAM (McCullough et al., 2004) and antagonize the lysosomal degradation of

the epidermal growth factor receptor (EGFR) (Kee et al., 2005; McCullough et al., 2006). In yeast, the UBP family DUB Ubp2 was shown to interact with Rsp5 (indirectly via the adaptor protein Rup1) and to associate with ESCRT-0 components on endosomes (Kee et al., 2005; Kee et al., 2006; Ren et al., 2007), although a role for Ubp2 in cargo recycling has not been rigorously demonstrated.

In addition to their role in rescuing ubiquitinated cargo from incorporation into ILVs, DUBs play a major role in recycling of ubiquitin from cargo prior to the ILV scission event. The recycling of ubiquitin from cargo significantly impacts ubiquitin homeostasis in the cell, a mutants defective for ubiquitin recycling exhibit MVB sorting defects (Amerik et al., 2006; Amerik et al., 2000; Swaminathan et al., 1999). This function has been well characterized for the yeast DUB Doa4 (Dupre and Haguenauer-Tsapis, 2001). Doa4 is recruited to Snf7, part of the ESCRT-III machinery, indirectly by its ability to bind the Snf7-interacting protein Bro1 (Luhtala and Odorizzi, 2004; Nikko et al., 2003; Odorizzi et al., 2003). In mammalian cells, recycling of ubiquitin from cargo may be mediated by UBPY, a UBP family DUB. Like Doa4, UBPY is required for efficient lysosomal degradation of trafficking cargo, and loss of UBPY function results in the accumulation of ubiquitinated proteins, particularly on endosomes (Mizuno et al., 2006; Row et al., 2006). Consistent with a function analogous to Doa4 in yeast, several reports have provided evidence that UBPY function is required for efficient lysosomal degradation of the EGFR (Alwan and van Leeuwen, 2007; Mizuno et al., 2006; Row et al., 2007; Row et al., 2006). Thus, both AMSH and UBPY may each contribute to both cargo stability and degradation by deubiquitinating cargo at different stages of ESCRT sorting.

THE ROLE OF UBIQUITIN IN CELL SURFACE REMODELING

Cells remodel protein composition at the PM to attenuate signaling responses, regulate nutrient uptake, and control ion flux across the PM. For single-celled eukaryotic organisms, such as yeast, surface remodeling plays an important role in nutrient homeostasis, stress responses, and pheromone signaling. In metazoans, surface remodeling plays a critical role in cell differentiation and fate decisions. A classic example involves T-cell maturation, which utilizes cell surface remodeling to convert thymocytes from double positive (CD4+8+) to single positive (CD4-8+ or CD4+8-) with only a single major histocompatibility complex coreceptor at the cell surface (Zamoyska and Lovatt, 2004). A key aspect of cell surface remodeling involves the targeting of specific proteins for endocytosis, and one such targeting determinant involves ubiquitin modification of trafficking cargo. Therefore, to understand how cells regulate PM protein composition, it is important to understand how specific PM proteins are targeted for ubiquitination and how these ubiquitinated cargoes are recognized, sorted into buds, and internalized by endocytosis.

Regulation of Signaling Receptors by Ubiquitin

One of the first PM cargoes demonstrated to undergo ubiquitin-mediated endocytosis was the yeast pheromone receptor Ste2, a GPCR (Hicke and Riezman, 1996). Ubiquitin modification is both necessary and sufficient for Ste2 endocytosis (Shih et al., 2000), leading to the hypothesis that endocytosis of GPCRs in mammalian cells would likewise be ubiquitin dependent. Given their pharmacological significance (Overington et al., 2006), mammalian GPCRs and the

mechanisms that mediate their downregulation have been studied extensively. Although several GPCRs studied in mammalian cells undergo ligand-dependent ubiquitination, these ubiquitination events are not required for internalization but are critical for MVB sorting on the endosome (Martin et al., 2003; Shenoy et al., 2001; Tanowitz and Von Zastrow, 2002).

Although GPCR ubiquitination is dispensable for endocytosis in mammalian cells, ubiquitin modification still plays an important role in the regulation of GPCR endocytosis. Following ligand binding, GPCRs activate associated heterotrimeric G proteins by promoting nucleotide exchange, leading to subunit release and dissociation. A ligand bound GPCR can subsequently be recognized by a GPCR kinase, which phosphorylates active GPCRs, causing them to recruit specialized adaptor proteins called β-arrestins. β-arrestins are multifunctional scaffold proteins that serve a variety of functions during receptor downregulation: They desensitize receptor signaling by preventing reassociation of G proteins with the GPCR; they promote GPCR endocytosis by binding to endocytosis proteins, including clathrin and AP-2; and they function as adaptors for E3 ubiquitin ligases. Interestingly, β-arrestins are ubiquitinated by the E3 ligase Mdm2, and this modification is critical for GPCR endocytosis (Shenoy et al., 2001). Furthermore, ubiquitination of β-arrestins enhances receptor interaction and thus promote endocytosis (Shenoy and Lefkowitz, 2003). Recently, the deubiquitinating enzyme Usp33 was shown to promote β-arrestin deubiquitination and to antagonize arrestin function (Berthouze et al., 2009). Thus, even though GPCR ubiquitination

itself is dispensable for endocytosis, β-arrestin ubiquitination is an important regulator of receptor internalization and downregulation.

It is worth noting that the paradigm of arrestin-mediated downregulation has recently expanded beyond GPCRs to many additional types of PM proteins (Lefkowitz et al., 2006; Simonin and Fuster, 2010). Furthermore, in addition to two β-arrestins and two visual arrestins, the human genome encodes at least five additional arrestin domain-containing (ARRDC) proteins. The human ARRDC family and the yeast family of ARTs exhibit striking similarity; both families contain N-terminal arrestin domains and multiple C-terminal PY motifs (Lin et al., 2008). Although the function of the ARRDC family of proteins is still under investigation, ARRDC3 was recently shown to function as an adaptor for the Nedd4 ubiquitin ligase and is required for the ubiquitination and endocytic downregulation of the β_2-adrenergic receptor (Nabhan et al., 2010). One recent study demonstrated that *Arrdc3* null mice exhibit resistance to obesity and increased energy expenditure, phenotypes that suggest an inability to downregulate β_2- adrenergic receptor signaling in adipose tissues (Patwari et al., 2011). Another recent study demonstrated that decreased ARRDC3 expression is associated with certain types of breast cancer and that ARRDC3 may suppress cancer progression by promoting the endocytic downregulation of β-4 integrin (Draheim et al., 2010). Thus, the growing family of arrestins and arrestin-related proteins may generally function as a family of ubiquitin ligase adaptors involved in the targeted ubiquitination and endocytic downregulation of GPCRs as well as other classes of PM cargo.

Attenuation of signaling processes from ligand-bound RTKs, like the EGFR, have been studied intensely because these signals facilitate cell growth and proliferation and can contribute to the onset of various cancers. A crucial determinant of the internalization of active RTKs is Cbl, a RING domain containing E3 ubiquitin ligase. There are three Cbl family RING E3 ligases encoded in the human genome—c-Cbl, Cbl-b, and Cbl-c. In the case of the EGFR, ligand binding promotes receptor dimerization and autophosphorylation, which result in the recruitment of the adaptor protein Grb2 complexed with Cbl. The RING domain of Cbl, in turn, can recruit an E2 enzyme and catalyze ubiquitin transfer to the EGFR. Although ubiquitin modification is sufficient to trigger EGFR endocytosis (Haglund et al., 2003; Huang et al., 2007) and the ubiquitinated EGFR interacts with epsin UIM domains (Kazazic et al., 2009), EGFR ubiquitination is not required for its internalization (Figure 1.4) (Haglund et al., 2003; Huang et al., 2007). The EGFR is subject to at least two modes of internalization: (*a*) ubiquitin-independent, clathrin-dependent endocytosis at low extracellular concentrations of the EGF and (*b*) ubiquitin-dependent, clathrin-independent internalization at high extracellular concentrations of the EGF (Chen and De Camilli, 2005; Sigismund et al., 2008; Sigismund et al., 2005). Although the mechanism of ubiquitin-dependent internalization has not been elucidated, it requires epsins and Eps15 family proteins (Sigismund et al., 2005), consistent with the possibility that UIM domains in these proteins may recognize and sort the ubiquitinated EGFR.

Importantly, interaction of the EGFR with Cbl is required for ubiquitin-independent endocytosis of the EGFR (Huang et al., 2007), suggesting that Cbl-

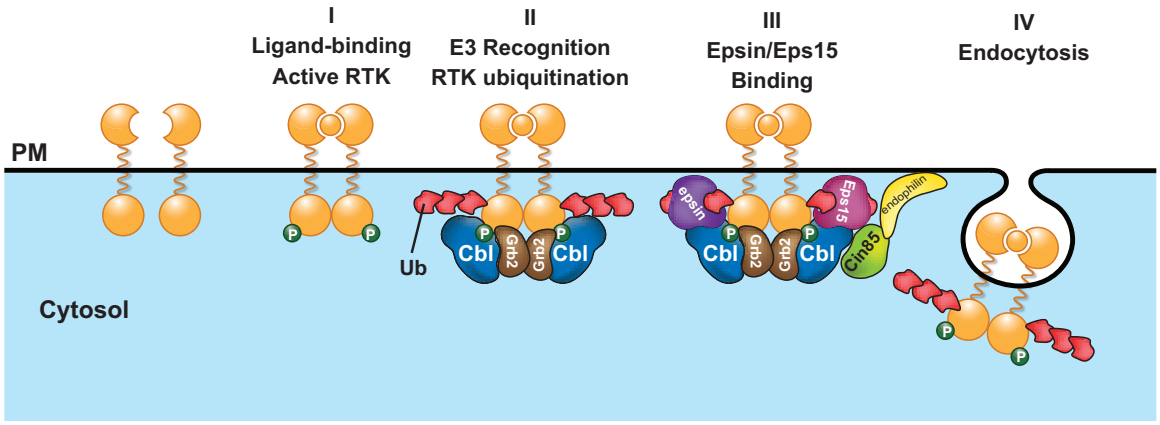
I
Ligand-binding
Active RTK
II
E3 Recognition
RTK ubiquitination
III
Epsin/Eps15
Binding
IV
Endocytosis
PM
Cytosol
Ub
Cbl
Grb2
Cbl
epsin
Eps15
endophilin
Cin85

Figure 1-4

Figure 1.4. Endocytosis of receptor tyrosine kinases (RTKs) can be ubiquitin-mediated but is not always ubiquitin-dependent. Cbl, a RING E3 ubiquitin ligase; Cin85, ubiquitin-binding endocytic adaptor protein; Eps15, epidermal growth factor receptor substrate 15; Grb2, growth factor receptor-bound protein 2; P, phosphate.

mediated EGFR internalization may not be related to receptor ubiquitination. Such a function may be related to Cbl-mediated recruitment of additional factors to active RTK signaling complexes, including Cin85 and endophilin, which are part of the endocytic protein interaction network. Furthermore, many such endocytic proteins, including Cin85, epsins, and Eps15 family proteins, are known to undergo coupled monoubiquitination (Bezsonova et al., 2008; Polo et al., 2002) and as such may be modified by Cbl. Thus, it is tempting to speculate that EGFR interaction with Cbl may trigger local assembly of endocytic machinery, although future work must determine how Cbl regulates interactions within the endocytic protein network.

Although ubiquitin-mediated endocytosis is often associated with attenuation of signaling processes, there are also examples where it is required to activate signaling receptors. Perhaps the best example of this involves the *Drosophila* Notch ligand Delta (Weinmaster and Fischer, 2011). Surface expression of Delta activates Notch signaling in adjacent cells, which triggers specific differentiation programs. The RING-type E3 ligase *neuralized* (*neur*) was found to promote Delta endocytosis in signal-sending cells but also to promote Notch signaling in signal-receiving cells. These observations are paradoxical: How is removal of a Notch ligand from the cell surface required for Notch activation in a neighboring cell? The precise mechanism is still under investigation, but recent studies have indicated that *neur*-mediated ubiquitination may trigger transcytosis of Delta from the basolateral membrane of the signal-sending cell to the apical membrane of the cell (Benhra et al., 2010), thus delivering the ligand to sites that can activate Notch on signal-receiving cells. This mode of Notch signal regulation is a common theme in vertebrate development

(Hansson et al., 2010; Koo et al., 2005a; Koo et al., 2005b), making this system an excellent example of how ubiquitin-mediated endocytosis can remodel the cell surface to drive cell differentiation.

Ubiquitin-Mediated Downregulation of Ion Channels

Regulation of the ENaC, a three-subunit complex at the PM, is critical for cellular ion homeostasis. ENaC undergoes ubiquitin-dependent endocytosis, which is mediated by its interaction with the E3 ubiquitin ligase Nedd4-2. Nedd4 family proteins are HECT-type E3 ubiquitin ligases with a distinct domain architecture: They contain an N terminal C2 domain, a series of two-to-four WW domains, and a C-terminal HECT ubiquitin ligase domain. WW domains typically mediate protein-protein interactions responsible for substrate targeting and are known to bind PY motifs, although some can also interact with phosphopeptides (Verdecia et al., 2000). The interaction of Nedd4-2 WW domains with C-terminal PY motifs in each of the ENaC subunits is required for ENaC ubiquitination and endocytosis. Ubiquitin-modified ENaC has been shown to undergo clathrin-mediated endocytosis, which requires the activity of epsins (Figure 1.5) (Wang et al., 2006). Regulatory factors can also influence Nedd4 function: The Sgk1 kinase was shown to phosphorylate Nedd4-2 and abrogate its interaction with ENaC by promoting its interaction with a 14-3-3 protein (Debonneville et al., 2001; Ichimura et al., 2005; Nagaki et al., 2006), whereas the AM sensor kinase was shown to destabilize ENaC at the cell surface by phosphorylating Nedd4-2 and enhancing its association with ENaC (Bhalla et al., 2006).

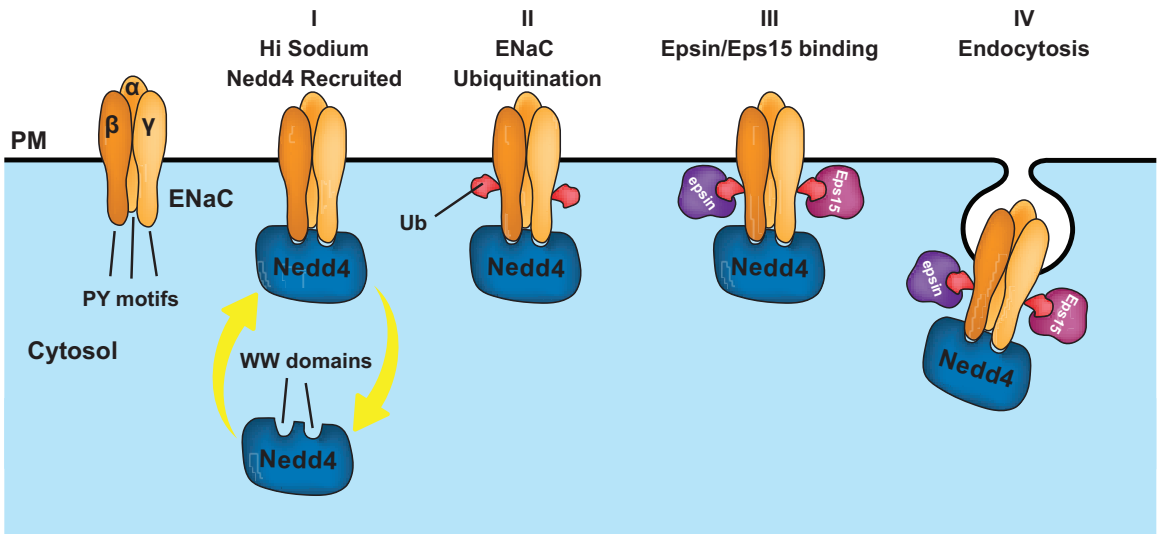
I
Hi Sodium
Nedd4 Recruited
II
ENaC
Ubiquitination
III
Epsin/Eps15 binding
IV
Endocytosis
PM
α
β
γ
ENaC
PY motifs
Cytosol
Nedd4
WW domains
Nedd4
Ub
Nedd4
epsin
Eps15
Nedd4
epsin
Eps15
Nedd4

Figure 1-5

Figure 1.5. Endocytic downregulation of ENaC is ubiquitin-dependent and is important for ion homeostasis in epithelial cells. Nedd4, HECT-type E3 ubiquitin ligase.

Aside from ENaC, Nedd4 family members have been implicated in the ubiquitin-mediated endocytosis of many other ion channels (He et al., 2008; Hryciw et al., 2004; Lin et al., 2011). Importantly, many ion channels linked to channelopathies including the cardiac voltage-gated sodium channel, $Na_v1.5$, and the potassium channels, KCNQ1 and hERG1, all encode PY motifs and may be regulated by Nedd4 family E3 ligases (Rougier et al., 2010). Additionally, connexin43, a gap junction protein that facilitates ion exchange between cells, contains a PY motif and has been shown to undergo Nedd4-dependent ubiquitination and endocytosis (Leithe and Rivedal, 2007). There are nine Nedd4 family ubiquitin ligases encoded in the human genome, and although not all have been characterized, several Nedd4 family members have been implicated in the ubiquitin-mediated endocytosis of various other PM cargoes, including amino acid transporters (Hatanaka et al., 2006; Vina-Vilaseca et al., 2011), RTKs (Arevalo et al., 2006; Li et al., 2009; Lin et al., 2010), and glucose transporters (Dieter et al., 2004). Thus, Nedd4 family E3 ligases may function generally to target a variety of PM cargoes for ubiquitin-mediated endocytosis, and their role is discussed throughout the remainder of this chapter.

Ubiquitin-Mediated Downregulation of Transporters

A clear example of ubiquitin-dependent endocytosis of a transporter in mammalian cells involves the dopamine transporter (DAT). DAT is a sodium chloride ion symporter responsible for dopamine reuptake at synapses, a process critical to control of dopamine signaling and thus synaptic function. DAT is ubiquitinated at the PM and internalized in a protein kinase C-dependent manner (Miranda and Sorkin, 2007). DAT ubiquitination requires the activity of Nedd4-2,

and internalization of DAT is clathrin dependent and requires epsins and Eps15 family proteins (Sorkina et al., 2006). Importantly, DAT endocytosis involves ubiquitin modification at three N-terminal lysine residues. Although DAT ubiquitination is dependent on the WW4 domain of Nedd4-2 (Vina-Vilaseca and Sorkin, 2010), it is unclear exactly how this interaction is mediated because DAT lacks a PY motif. Further studies are needed to determine (*a*) if this interaction is direct or adaptor driven and (*b*) how this interaction is regulated in a protein kinase C-dependent manner.

Unlike DAT, some transporters constitutively cycle between the PM and endosomes via a ubiquitin-independent recycling pathway. This allows nutrient receptors, such as the transferrin receptor (TfR) and the low-density lipoprotein receptor, to scavenge nutrients from the environment, deposit them in the lumen of the endosome, and then return to the surface to collect more nutrients. However, ubiquitination of these nutrient receptors is sufficient to divert such cargo away from the recycling pathway and instead target them for sorting into MVBs and lysosomal degradation. For example, instead of recycling back to the surface, the TfR fused to ubiquitin is targeted for lysosomal degradation (Raiborg et al., 2002). Furthermore, excess iron was shown to stimulate TfR ubiquitination and lysosomal degradation (Tachiyama et al., 2011), although the E3 ligase responsible is not known. Similarly, in cholesterol-replete conditions, the low-density lipoprotein receptor is ubiquitinated and targeted for lysosomal degradation. This is mediated by the RING E3 ligase, IDOL (Zhang et al., 2011), which is transcriptionally induced by a sterol-binding transcription factor (Zelcer et al., 2009). Thus, cells upregulate

ubiquitination of nutrient receptors, such as the TfR and low-density lipoprotein receptor, which are normally recycled, to reduce the cellular level of these receptors and thereby limit nutrient accumulation.

For most cargoes studied in yeast, the primary determinant of endocytosis appears to be ubiquitin modification, although other endocytic targeting signals have been described (Chen and Davis, 2002; Howard et al., 2002; Tan et al., 1996). Thus, cargo ubiquitination at the PM represents a critical point of regulation for internalization. The primary E3 ubiquitin ligase that mediates cargo ubiquitination and targeting for endocytosis is Rsp5, the lone Nedd4 family member encoded in the yeast genome. Because most yeast PM proteins do not contain PY motifs and thus cannot interact directly with Rsp5, this presents a conundrum: How does one ubiquitin ligase selectively regulate the abundance of perhaps hundreds of different proteins at the PM? The answer appears to lie in the existence of an elaborate network of adaptor proteins, each capable of targeting Rsp5 ubiquitin ligase activity to specific substrates at specific locations in the cell in a highly regulated manner. At the core of this adaptor network is a family of yeast ART proteins. There are 10 ARTs encoded in the yeast genome; each ART contains an N-terminal arrestin-like domain and multiple C-terminal PY motifs that interact with the WW domains of Rsp5. Like F-box proteins, which function in the recruitment of specific substrates to SCF ubiquitin ligase complexes, ARTs recruit Rsp5 ubiquitin ligase activity to specific proteins at the PM and thus play a critical role in regulating which PM proteins are selectively targeted for endocytosis. Other proteins, including Bul1, Bul2, Ear1, and Ssh4, also act as specificity adaptors for Rsp5. It has been proposed

that Bul1 and Bul2 may in fact be bona fide members of the ART protein family (Nikko and Pelham, 2009), although these proteins do not appear to contain significant primary sequence homology with ARTs. Despite their divergence, it is tempting to speculate that Bul1 and Bul2 could contain arrestin-like domains, but confirmation will require structural analysis of these proteins.

The mechanism of ART-mediated regulation of endocytosis was recently elucidated in two studies directed at understanding how PM proteins in yeast are ubiquitinated. *ART1* was identified in a chemical-genetic screen for mutants with defects in the endocytosis of Can1, the arginine transporter in yeast (Lin et al., 2008). Importantly, D*art1* cells are defective for endocytosis of a few specific cargoes, including Can1 and the methionine transporter, Mup1, but are not defective for endocytosis of most other cargoes (Lin et al., 2008). Art1 interacts with Rsp5 via two C-terminal PY motifs, an interaction required for cargo ubiquitination (Lin et al., 2008). Additionally, Art1 localizes to the PM and interacts with cargo, confirming its role as a ubiquitin ligase adaptor (Figure 1.6). Bioinformatic analysis identified additional ART proteins encoded in the yeast genome (Art1-Art10), each capable of binding to Rsp5. Endocytosis of the lysine transporter Lyp1 is dependent on Art2, and Can1- Lyp1 cargo chimera experiments revealed that ART specificity for these cargoes is mediated through the N-terminal cytosolic tail (Lin et al., 2008). A parallel study revealed that ART family proteins function redundantly in the ubiquitination and endocytosis of the yeast manganese transporter, Smf1. In this investigation, simultaneous deletion of seven ART family proteins, as well as the Rsp5-interacting protein, Bsd2, was required to block Smf1 ubiquitination and

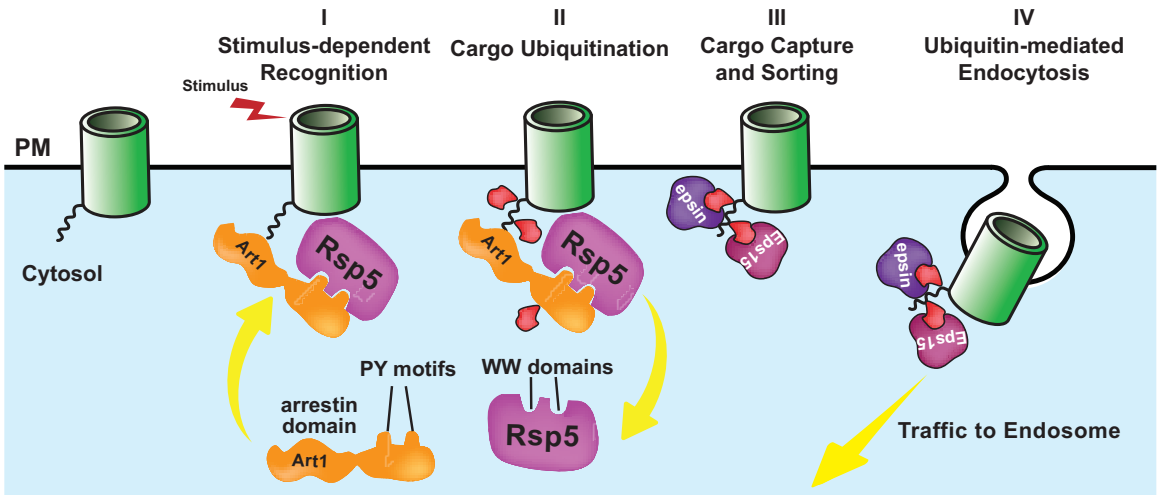
I
Stimulus-dependent
Recognition
II
Cargo Ubiquitination
III
Cargo Capture
and Sorting
IV
Ubiquitin-mediated
Endocytosis
Stimulus
PM
Cytosol
Art1
Rsp5
PY motifs
arrestin
domain
Art1
Art1
Rsp5
WW domains
Rsp5
epsin
Eps15
epsin
Eps15
Traffic to Endosome

Figure 1-6

Figure 1.6. Model of ART family protein function as Rsp5 adaptors in yeast. Yeast ARTs are adaptors for the ubiquitin E3 ligase, Rsp5, directing ubiquitin ligase activity to specific PM cargoes and targeting them for endocytosis. ART, arrestin-related trafficking adaptor

endocytosis (Nikko et al., 2008). This endocytic defect could be complemented by reintroduction of wild-type *ART2* but not by an allele of *art2* with point mutations in its C-terminal PY motifs (Nikko et al., 2008). Both of these studies contributed to a model of ARTs as Rsp5 adaptors that function in targeting PM proteins for endocytosis. Since then, other reports have described similar endocytic functions for other ART family proteins (Hatakeyama et al., 2010; Nikko and Pelham, 2009). It has also recently been reported that Art3 and Art6 may function in Golgi-to-endosome traffic, but it is unclear if this relates to their role as ubiquitin ligase adaptors (O'Donnell et al., 2010). This study is noteworthy because it suggests that ART proteins have nonendocytic trafficking functions, and it demonstrated that Art3 and Art6 interact with clathrin and AP-1. The later observation is reminiscent of β-arrestins in mammalian cells, which serve as endocytic adaptors by binding to clathrin and AP-2.

To drive Rsp5 specificity, ART family proteins must be capable of interacting with specific PM proteins in a regulated manner (Figure 1.7). ART-cargo interactions have been demonstrated (Hatakeyama et al., 2010; Lin et al., 2008; Nikko et al., 2008), and although the precise cargo-binding domain has not yet been mapped, the best candidate is the arrestin domain. More experimentation is required to map and characterize cargo specificity determinants within the ART family of proteins. Importantly, ART function is tightly regulated and often appears to be "activated" by specific stimuli. For example, stimulation of yeast cells with methionine activates Art1 to target the methionine transporter Mup1, resulting in rapid ubiquitination and endocytic downregulation (Lin et al., 2008). One major

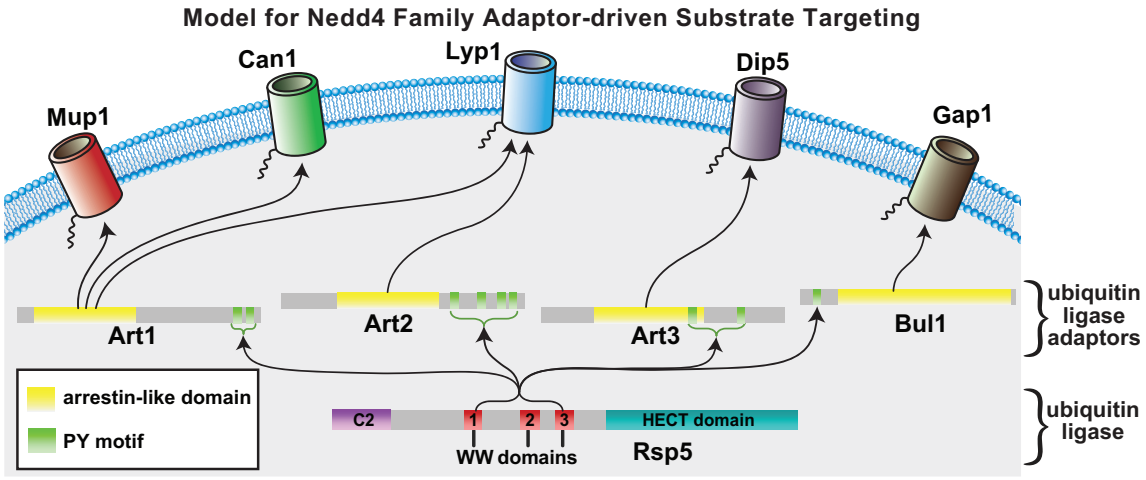
Model for Nedd4 Family Adaptor-driven Substrate Targeting
Mup1
Can1
Lyp1
Dip5
Gap1
Art1
Art2
Art3
Bul1
ubiquitin ligase adaptors
arrestin-like domain
PY motif
C2
1
2
3
HECT domain
WW domains
Rsp5
ubiquitin ligase

Figure 1-7

Figure 1.7. Model for adaptor-driven substrate targeting of the Rsp5 ubiquitin ligase in yeast. Structural modeling revealed that Art1 contains an arrestin fold domain at the N-terminus, while the C-terminus contains two PY motifs that mediate interaction with WW domains in Rsp5. ART, arrestin-related trafficking adaptor; Bul1, another known adaptor for Rsp5; Can1, yeast arginine transporter; C2, a domain that binds to calcium and lipids; Dip5, yeast dicarboxylic amino acid transporter; Gap1, yeast general amino acid transporter; Lyp1, yeast lysine transporter; Mup1, yeast methionine transporter; PM, plasma membrane.

mechanism of regulation may involve stimulus-induced cargo phosphorylation, as is the case with the recognition of GPCRs by β–arrestins in mammalian cells. Indeed, Smf1 phosphorylation correlates with increased Art2 binding, and substrate-induced phosphorylation of the dicarboxylic amino acid transporter, Dip5, triggers increased binding to Art3 (Hatakeyama et al., 2010), although the regulatory kinases and/or phosphatases in these cases are not known. It is also possible that substrate binding and transport might trigger conformational changes in cargo proteins that are recognized by ARTs. Recognition of either conformational changes or cargo phosphorylation represents a local regulatory mechanism that is based on sensing cargo activity.

An alternative regulatory mechanism for ART-cargo recognition may involve posttranslational modifications of the ART proteins themselves. Most ARTs appear to be ubiquitinated, and in the case of Art1, this is Rsp5 dependent (Lin et al., 2008). Art1 ubiquitination occurs on a single lysine residue (Hatakeyama et al., 2010; Hitchcock et al., 2003); mutation of this residue prevents ubiquitin modification and results in a loss-of-function phenotype (Lin et al., 2008). Such coupled ubiquitination events are not uncommon for ubiquitin ligase adaptors, and although its functional significance is clear, further experimentation is required to determine precisely how ubiquitin modification regulates Art1 function. ART proteins are extensively phosphorylated (Albuquerque et al., 2008) and are likely subject to phosphoregulation.

Although human homologs of ARTs are not obvious on the basis of their primary sequence, domain architecture suggests that yeast ARTs are similar to the

family of ARRDC proteins in mammalian cells (Lin et al., 2008; Nabhan et al., 2010). Like ARTs, ARRDC proteins have an N-terminal arrestin domain and C-terminal PY motifs, which have been shown to mediate interactions with Nedd4 family proteins (Nabhan et al., 2010). Thus, elucidating mechanisms of ART function in yeast may have important implications for understanding arrestin and ARRDC protein function in mammalian cells.

REFERENCES

Albuquerque, C.P., Smolka, M.B., Payne, S.H., Bafna, V., Eng, J., and Zhou, H. (2008). A multidimensional chromatography technology for in-depth phosphoproteome analysis. Mol Cell Proteomics *7*, 1389-1396.

Alwan, H.A., and van Leeuwen, J.E. (2007). UBPY-mediated epidermal growth factor receptor (EGFR) de-ubiquitination promotes EGFR degradation. J Biol Chem *282*, 1658-1669.

Amerik, A., Sindhi, N., and Hochstrasser, M. (2006). A conserved late endosome-targeting signal required for Doa4 deubiquitylating enzyme function. J Cell Biol *175*, 825-835.

Amerik, A.Y., Nowak, J., Swaminathan, S., and Hochstrasser, M. (2000). The Doa4 deubiquitinating enzyme is functionally linked to the vacuolar protein-sorting and endocytic pathways. Mol Biol Cell *11*, 3365-3380.

Arevalo, J.C., Waite, J., Rajagopal, R., Beyna, M., Chen, Z.Y., Lee, F.S., and Chao, M.V. (2006). Cell survival through Trk neurotrophin receptors is differentially regulated by ubiquitination. Neuron *50*, 549-559.

Aubry, L., Guetta, D., and Klein, G. (2009). The arrestin fold: variations on a theme. Curr Genomics *10*, 133-142.

Behrends, C., and Harper, J.W. (2011). Constructing and decoding unconventional ubiquitin chains. Nat Struct Mol Biol *18*, 520-528.

Benhra, N., Vignaux, F., Dussert, A., Schweisguth, F., and Le Borgne, R. (2010). Neuralized promotes basal to apical transcytosis of delta in epithelial cells. Mol Biol Cell *21*, 2078-2086.

Bernassola, F., Karin, M., Ciechanover, A., and Melino, G. (2008). The HECT family of E3 ubiquitin ligases: multiple players in cancer development. Cancer Cell *14*, 10-21.

Berthouze, M., Venkataramanan, V., Li, Y., and Shenoy, S.K. (2009). The deubiquitinases USP33 and USP20 coordinate beta2 adrenergic receptor recycling and resensitization. EMBO J *28*, 1684-1696.

Bezsonova, I., Bruce, M.C., Wiesner, S., Lin, H., Rotin, D., and Forman-Kay, J.D. (2008). Interactions between the three CIN85 SH3 domains and ubiquitin: implications for CIN85 ubiquitination. Biochemistry *47*, 8937-8949.

Bhalla, V., Oyster, N.M., Fitch, A.C., Wijngaarden, M.A., Neumann, D., Schlattner, U., Pearce, D., and Hallows, K.R. (2006). AMP-activated kinase inhibits the epithelial Na+ channel through functional regulation of the ubiquitin ligase Nedd4-2. J Biol Chem *281*, 26159-26169.

Bhandari, D., Trejo, J., Benovic, J.L., and Marchese, A. (2007). Arrestin-2 interacts with the ubiquitin-protein isopeptide ligase atrophin-interacting protein 4 and mediates endosomal sorting of the chemokine receptor CXCR4. J Biol Chem *282*, 36971-36979.

Bomberger, J.M., Barnaby, R.L., and Stanton, B.A. (2009). The deubiquitinating enzyme USP10 regulates the post-endocytic sorting of cystic fibrosis transmembrane conductance regulator in airway epithelial cells. J Biol Chem *284*, 18778-18789.

Bonifacino, J.S., and Weissman, A.M. (1998). Ubiquitin and the control of protein fate in the secretory and endocytic pathways. Annu Rev Cell Dev Biol *14*, 19-57.

Butterworth, M.B., Edinger, R.S., Ovaa, H., Burg, D., Johnson, J.P., and Frizzell, R.A. (2007). The deubiquitinating enzyme UCH-L3 regulates the apical membrane recycling of the epithelial sodium channel. J Biol Chem *282*, 37885-37893.

Cadavid, A.L., Ginzel, A., and Fischer, J.A. (2000). The function of the Drosophila fat facets deubiquitinating enzyme in limiting photoreceptor cell number is intimately associated with endocytosis. Development *127*, 1727-1736.

Chen, H., and De Camilli, P. (2005). The association of epsin with ubiquitinated cargo along the endocytic pathway is negatively regulated by its interaction with clathrin. Proc Natl Acad Sci U S A *102*, 2766-2771.

Chen, L., and Davis, N.G. (2002). Ubiquitin-independent entry into the yeast recycling pathway. Traffic *3*, 110-123.

Chen, X., Zhang, B., and Fischer, J.A. (2002). A specific protein substrate for a deubiquitinating enzyme: Liquid facets is the substrate of Fat facets. Genes Dev *16*, 289-294.

Collins, B.M., Norwood, S.J., Kerr, M.C., Mahony, D., Seaman, M.N., Teasdale, R.D., and Owen, D.J. (2008). Structure of Vps26B and mapping of its interaction with the retromer protein complex. Traffic *9*, 366-379.

Costa, R., Warren, D.T., and Ayscough, K.R. (2005). Lsb5p interacts with actin regulators Sla1p and Las17p, ubiquitin and Arf3p to couple actin dynamics to membrane trafficking processes. Biochem J *387*, 649-658.

Debonneville, C., Flores, S.Y., Kamynina, E., Plant, P.J., Tauxe, C., Thomas, M.A., Munster, C., Chraibi, A., Pratt, J.H., Horisberger, J.D.*, et al.* (2001). Phosphorylation of

Nedd4-2 by Sgk1 regulates epithelial Na(+) channel cell surface expression. EMBO J *20*, 7052-7059.

Deshaies, R.J., and Joazeiro, C.A. (2009). RING domain E3 ubiquitin ligases. Annu Rev Biochem *78*, 399-434.

Dieter, M., Palmada, M., Rajamanickam, J., Aydin, A., Busjahn, A., Boehmer, C., Luft, F.C., and Lang, F. (2004). Regulation of glucose transporter SGLT1 by ubiquitin ligase Nedd4-2 and kinases SGK1, SGK3, and PKB. Obes Res *12*, 862-870.

Draheim, K.M., Chen, H.B., Tao, Q., Moore, N., Roche, M., and Lyle, S. (2010). ARRDC3 suppresses breast cancer progression by negatively regulating integrin beta4. Oncogene *29*, 5032-5047.

Duda, D.M., Scott, D.C., Calabrese, M.F., Zimmerman, E.S., Zheng, N., and Schulman, B.A. (2011). Structural regulation of cullin-RING ubiquitin ligase complexes. Curr Opin Struct Biol *21*, 257-264.

Dupre, S., and Haguenauer-Tsapis, R. (2001). Deubiquitination step in the endocytic pathway of yeast plasma membrane proteins: crucial role of Doa4p ubiquitin isopeptidase. Mol Cell Biol *21*, 4482-4494.

Egner, R., and Kuchler, K. (1996). The yeast multidrug transporter Pdr5 of the plasma membrane is ubiquitinated prior to endocytosis and degradation in the vacuole. FEBS Lett *378*, 177-181.

Galan, J.M., Moreau, V., Andre, B., Volland, C., and Haguenauer-Tsapis, R. (1996). Ubiquitination mediated by the Npi1p/Rsp5p ubiquitin-protein ligase is required for endocytosis of the yeast uracil permease. J Biol Chem *271*, 10946-10952.

Goh, L.K., Huang, F., Kim, W., Gygi, S., and Sorkin, A. (2010). Multiple mechanisms collectively regulate clathrin-mediated endocytosis of the epidermal growth factor receptor. J Cell Biol *189*, 871-883.

Gurevich, V.V., and Gurevich, E.V. (2006). The structural basis of arrestin-mediated regulation of G-protein-coupled receptors. Pharmacol Ther *110*, 465-502.

Haglund, K., Sigismund, S., Polo, S., Szymkiewicz, I., Di Fiore, P.P., and Dikic, I. (2003). Multiple monoubiquitination of RTKs is sufficient for their endocytosis and degradation. Nat Cell Biol *5*, 461-466.

Hansson, E.M., Lanner, F., Das, D., Mutvei, A., Marklund, U., Ericson, J., Farnebo, F., Stumm, G., Stenmark, H., Andersson, E.R.*, et al.* (2010). Control of Notch-ligand endocytosis by ligand-receptor interaction. J Cell Sci *123*, 2931-2942.

Hatakeyama, R., Kamiya, M., Takahara, T., and Maeda, T. (2010). Endocytosis of the aspartic acid/glutamic acid transporter Dip5 is triggered by substrate-dependent recruitment of the Rsp5 ubiquitin ligase via the arrestin-like protein Aly2. Mol Cell Biol *30*, 5598-5607.

Hatanaka, T., Hatanaka, Y., and Setou, M. (2006). Regulation of amino acid transporter ATA2 by ubiquitin ligase Nedd4-2. J Biol Chem *281*, 35922-35930.

He, Y., Hryciw, D.H., Carroll, M.L., Myers, S.A., Whitbread, A.K., Kumar, S., Poronnik, P., and Hooper, J.D. (2008). The ubiquitin-protein ligase Nedd4-2 differentially interacts with and regulates members of the Tweety family of chloride ion channels. J Biol Chem *283*, 24000-24010.

Hicke, L., and Riezman, H. (1996). Ubiquitination of a yeast plasma membrane receptor signals its ligand-stimulated endocytosis. Cell *84*, 277-287.

Hitchcock, A.L., Auld, K., Gygi, S.P., and Silver, P.A. (2003). A subset of membrane-associated proteins is ubiquitinated in response to mutations in the endoplasmic reticulum degradation machinery. Proc Natl Acad Sci U S A *100*, 12735-12740.

Hoeller, D., and Dikic, I. (2011). Regulation of ubiquitin receptors by coupled monoubiquitination. Subcell Biochem *54*, 31-40.

Howard, J.P., Hutton, J.L., Olson, J.M., and Payne, G.S. (2002). Sla1p serves as the targeting signal recognition factor for NPFX(1,2)D-mediated endocytosis. J Cell Biol *157*, 315-326.

Hryciw, D.H., Ekberg, J., Lee, A., Lensink, I.L., Kumar, S., Guggino, W.B., Cook, D.I., Pollock, C.A., and Poronnik, P. (2004). Nedd4-2 functionally interacts with ClC-5: involvement in constitutive albumin endocytosis in proximal tubule cells. J Biol Chem *279*, 54996-55007.

Huang, F., Goh, L.K., and Sorkin, A. (2007). EGF receptor ubiquitination is not necessary for its internalization. Proc Natl Acad Sci U S A *104*, 16904-16909.

Huang, Y., Baker, R.T., and Fischer-Vize, J.A. (1995). Control of cell fate by a deubiquitinating enzyme encoded by the fat facets gene. Science *270*, 1828-1831.

Ichimura, T., Yamamura, H., Sasamoto, K., Tominaga, Y., Taoka, M., Kakiuchi, K., Shinkawa, T., Takahashi, N., Shimada, S., and Isobe, T. (2005). 14-3-3 proteins modulate the expression of epithelial Na+ channels by phosphorylation-dependent interaction with Nedd4-2 ubiquitin ligase. J Biol Chem *280*, 13187-13194.

Ing, B., Shteiman-Kotler, A., Castelli, M., Henry, P., Pak, Y., Stewart, B., Boulianne, G.L., and Rotin, D. (2007). Regulation of Commissureless by the ubiquitin ligase DNedd4

is required for neuromuscular synaptogenesis in Drosophila melanogaster. Mol Cell Biol *27*, 481-496.

Jenness, D.D., Li, Y., Tipper, C., and Spatrick, P. (1997). Elimination of defective alpha-factor pheromone receptors. Mol Cell Biol *17*, 6236-6245.

Katzmann, D.J., Sarkar, S., Chu, T., Audhya, A., and Emr, S.D. (2004). Multivesicular body sorting: ubiquitin ligase Rsp5 is required for the modification and sorting of carboxypeptidase S. Mol Biol Cell *15*, 468-480.

Kazazic, M., Bertelsen, V., Pedersen, K.W., Vuong, T.T., Grandal, M.V., Rodland, M.S., Traub, L.M., Stang, E., and Madshus, I.H. (2009). Epsin 1 is involved in recruitment of ubiquitinated EGF receptors into clathrin-coated pits. Traffic *10*, 235-245.

Kee, Y., and Huibregtse, J.M. (2007). Regulation of catalytic activities of HECT ubiquitin ligases. Biochem Biophys Res Commun *354*, 329-333.

Kee, Y., Lyon, N., and Huibregtse, J.M. (2005). The Rsp5 ubiquitin ligase is coupled to and antagonized by the Ubp2 deubiquitinating enzyme. EMBO J *24*, 2414-2424.

Kee, Y., Munoz, W., Lyon, N., and Huibregtse, J.M. (2006). The deubiquitinating enzyme Ubp2 modulates Rsp5-dependent Lys63-linked polyubiquitin conjugates in Saccharomyces cerevisiae. J Biol Chem *281*, 36724-36731.

Kendall, R.T., and Luttrell, L.M. (2009). Diversity in arrestin function. Cell Mol Life Sci *66*, 2953-2973.

Kim, B.Y., Olzmann, J.A., Barsh, G.S., Chin, L.S., and Li, L. (2007). Spongiform neurodegeneration-associated E3 ligase Mahogunin ubiquitylates TSG101 and regulates endosomal trafficking. Mol Biol Cell *18*, 1129-1142.

Kim, G.H., Park, E., Kong, Y.Y., and Han, J.K. (2006). Novel function of POSH, a JNK scaffold, as an E3 ubiquitin ligase for the Hrs stability on early endosomes. Cell Signal *18*, 553-563.

Kolling, R., and Hollenberg, C.P. (1994). The ABC-transporter Ste6 accumulates in the plasma membrane in a ubiquitinated form in endocytosis mutants. EMBO J *13*, 3261-3271.

Komander, D. (2009). The emerging complexity of protein ubiquitination. Biochem Soc Trans *37*, 937-953.

Komander, D., Clague, M.J., and Urbe, S. (2009). Breaking the chains: structure and function of the deubiquitinases. Nat Rev Mol Cell Biol *10*, 550-563.

Koo, B.K., Lim, H.S., Song, R., Yoon, M.J., Yoon, K.J., Moon, J.S., Kim, Y.W., Kwon, M.C., Yoo, K.W., Kong, M.P.*, et al.* (2005a). Mind bomb 1 is essential for generating functional Notch ligands to activate Notch. Development *132*, 3459-3470.

Koo, B.K., Yoon, K.J., Yoo, K.W., Lim, H.S., Song, R., So, J.H., Kim, C.H., and Kong, Y.Y. (2005b). Mind bomb-2 is an E3 ligase for Notch ligand. J Biol Chem *280*, 22335-22342.

Lauwers, E., Erpapazoglou, Z., Haguenauer-Tsapis, R., and Andre, B. (2010). The ubiquitin code of yeast permease trafficking. Trends Cell Biol *20*, 196-204.

Lefkowitz, R.J. (1998). G protein-coupled receptors. III. New roles for receptor kinases and beta-arrestins in receptor signaling and desensitization. J Biol Chem *273*, 18677-18680.

Lefkowitz, R.J., Rajagopal, K., and Whalen, E.J. (2006). New roles for beta-arrestins in cell signaling: not just for seven-transmembrane receptors. Mol Cell *24*, 643-652.

Leithe, E., and Rivedal, E. (2007). Ubiquitination of gap junction proteins. J Membr Biol *217*, 43-51.

Li, Y., Zhou, Z., Alimandi, M., and Chen, C. (2009). WW domain containing E3 ubiquitin protein ligase 1 targets the full-length ErbB4 for ubiquitin-mediated degradation in breast cancer. Oncogene *28*, 2948-2958.

Lin, A., Hou, Q., Jarzylo, L., Amato, S., Gilbert, J., Shang, F., and Man, H.Y. (2011). Nedd4-mediated AMPA receptor ubiquitination regulates receptor turnover and trafficking. J Neurochem *119*, 27-39.

Lin, C.H., MacGurn, J.A., Chu, T., Stefan, C.J., and Emr, S.D. (2008). Arrestin-related ubiquitin-ligase adaptors regulate endocytosis and protein turnover at the cell surface. Cell *135*, 714-725.

Lin, Q., Wang, J., Childress, C., Sudol, M., Carey, D.J., and Yang, W. (2010). HECT E3 ubiquitin ligase Nedd4-1 ubiquitinates ACK and regulates epidermal growth factor (EGF)-induced degradation of EGF receptor and ACK. Mol Cell Biol *30*, 1541-1554.

Luhtala, N., and Odorizzi, G. (2004). Bro1 coordinates deubiquitination in the multivesicular body pathway by recruiting Doa4 to endosomes. J Cell Biol *166*, 717-729.

Malik, R., and Marchese, A. (2010). Arrestin-2 interacts with the endosomal sorting complex required for transport machinery to modulate endosomal sorting of CXCR4. Mol Biol Cell *21*, 2529-2541.

Martin, N.P., Lefkowitz, R.J., and Shenoy, S.K. (2003). Regulation of V2 vasopressin receptor degradation by agonist-promoted ubiquitination. J Biol Chem *278*, 45954-45959.

McCullough, J., Clague, M.J., and Urbe, S. (2004). AMSH is an endosome-associated ubiquitin isopeptidase. J Cell Biol *166*, 487-492.

McCullough, J., Row, P.E., Lorenzo, O., Doherty, M., Beynon, R., Clague, M.J., and Urbe, S. (2006). Activation of the endosome-associated ubiquitin isopeptidase AMSH by STAM, a component of the multivesicular body-sorting machinery. Curr Biol *16*, 160-165.

McDonald, B., and Martin-Serrano, J. (2008). Regulation of Tsg101 expression by the steadiness box: a role of Tsg101-associated ligase. Mol Biol Cell *19*, 754-763.

Miranda, M., and Sorkin, A. (2007). Regulation of receptors and transporters by ubiquitination: new insights into surprisingly similar mechanisms. Mol Interv *7*, 157-167.

Mizuno, E., Kobayashi, K., Yamamoto, A., Kitamura, N., and Komada, M. (2006). A deubiquitinating enzyme UBPY regulates the level of protein ubiquitination on endosomes. Traffic *7*, 1017-1031.

Moore, C.A., Milano, S.K., and Benovic, J.L. (2007). Regulation of receptor trafficking by GRKs and arrestins. Annu Rev Physiol *69*, 451-482.

Nabhan, J.F., Pan, H., and Lu, Q. (2010). Arrestin domain-containing protein 3 recruits the NEDD4 E3 ligase to mediate ubiquitination of the beta2-adrenergic receptor. EMBO Rep *11*, 605-611.

Nagaki, K., Yamamura, H., Shimada, S., Saito, T., Hisanaga, S., Taoka, M., Isobe, T., and Ichimura, T. (2006). 14-3-3 Mediates phosphorylation-dependent inhibition of the interaction between the ubiquitin E3 ligase Nedd4-2 and epithelial Na+ channels. Biochemistry *45*, 6733-6740.

Nagy, V., and Dikic, I. (2009). Ubiquitin ligase complexes: from substrate selectivity to conjugational specificity. Biol Chem *391*, 163-169.

Nikko, E., Marini, A.M., and Andre, B. (2003). Permease recycling and ubiquitination status reveal a particular role for Bro1 in the multivesicular body pathway. J Biol Chem *278*, 50732-50743.

Nikko, E., and Pelham, H.R. (2009). Arrestin-mediated endocytosis of yeast plasma membrane transporters. Traffic *10*, 1856-1867.

Nikko, E., Sullivan, J.A., and Pelham, H.R. (2008). Arrestin-like proteins mediate ubiquitination and endocytosis of the yeast metal transporter Smf1. EMBO Rep *9*, 1216-1221.

O'Donnell, A.F., Apffel, A., Gardner, R.G., and Cyert, M.S. (2010). Alpha-arrestins Aly1 and Aly2 regulate intracellular trafficking in response to nutrient signaling. Mol Biol Cell *21*, 3552-3566.

Odorizzi, G., Katzmann, D.J., Babst, M., Audhya, A., and Emr, S.D. (2003). Bro1 is an endosome-associated protein that functions in the MVB pathway in Saccharomyces cerevisiae. J Cell Sci *116*, 1893-1903.

Overington, J.P., Al-Lazikani, B., and Hopkins, A.L. (2006). How many drug targets are there? Nat Rev Drug Discov *5*, 993-996.

Overstreet, E., Fitch, E., and Fischer, J.A. (2004). Fat facets and Liquid facets promote Delta endocytosis and Delta signaling in the signaling cells. Development *131*, 5355-5366.

Patwari, P., Emilsson, V., Schadt, E.E., Chutkow, W.A., Lee, S., Marsili, A., Zhang, Y., Dobrin, R., Cohen, D.E., Larsen, P.R., *et al.* (2011). The arrestin domain-containing 3 protein regulates body mass and energy expenditure. Cell Metab *14*, 671-683.

Polo, S., Sigismund, S., Faretta, M., Guidi, M., Capua, M.R., Bossi, G., Chen, H., De Camilli, P., and Di Fiore, P.P. (2002). A single motif responsible for ubiquitin recognition and monoubiquitination in endocytic proteins. Nature *416*, 451-455.

Raiborg, C., Bache, K.G., Gillooly, D.J., Madshus, I.H., Stang, E., and Stenmark, H. (2002). Hrs sorts ubiquitinated proteins into clathrin-coated microdomains of early endosomes. Nat Cell Biol *4*, 394-398.

Ren, J., Kee, Y., Huibregtse, J.M., and Piper, R.C. (2007). Hse1, a component of the yeast Hrs-STAM ubiquitin-sorting complex, associates with ubiquitin peptidases and a ligase to control sorting efficiency into multivesicular bodies. Mol Biol Cell *18*, 324-335.

Rougier, J.S., Albesa, M., and Abriel, H. (2010). Ubiquitylation and SUMOylation of cardiac ion channels. J Cardiovasc Pharmacol *56*, 22-28.

Row, P.E., Liu, H., Hayes, S., Welchman, R., Charalabous, P., Hofmann, K., Clague, M.J., Sanderson, C.M., and Urbe, S. (2007). The MIT domain of UBPY constitutes a CHMP binding and endosomal localization signal required for efficient epidermal growth factor receptor degradation. J Biol Chem *282*, 30929-30937.

Row, P.E., Prior, I.A., McCullough, J., Clague, M.J., and Urbe, S. (2006). The ubiquitin isopeptidase UBPY regulates endosomal ubiquitin dynamics and is essential for receptor down-regulation. J Biol Chem *281*, 12618-12624.

Shenoy, S.K., and Lefkowitz, R.J. (2003). Trafficking patterns of beta-arrestin and G protein-coupled receptors determined by the kinetics of beta-arrestin deubiquitination. J Biol Chem *278*, 14498-14506.

Shenoy, S.K., McDonald, P.H., Kohout, T.A., and Lefkowitz, R.J. (2001). Regulation of receptor fate by ubiquitination of activated beta 2-adrenergic receptor and beta-arrestin. Science *294*, 1307-1313.

Shih, S.C., Katzmann, D.J., Schnell, J.D., Sutanto, M., Emr, S.D., and Hicke, L. (2002). Epsins and Vps27p/Hrs contain ubiquitin-binding domains that function in receptor endocytosis. Nat Cell Biol *4*, 389-393.

Shih, S.C., Sloper-Mould, K.E., and Hicke, L. (2000). Monoubiquitin carries a novel internalization signal that is appended to activated receptors. EMBO J *19*, 187-198.

Sigismund, S., Argenzio, E., Tosoni, D., Cavallaro, E., Polo, S., and Di Fiore, P.P. (2008). Clathrin-mediated internalization is essential for sustained EGFR signaling but dispensable for degradation. Dev Cell *15*, 209-219.

Sigismund, S., Woelk, T., Puri, C., Maspero, E., Tacchetti, C., Transidico, P., Di Fiore, P.P., and Polo, S. (2005). Clathrin-independent endocytosis of ubiquitinated cargos. Proc Natl Acad Sci U S A *102*, 2760-2765.

Simonin, A., and Fuster, D. (2010). Nedd4-1 and beta-arrestin-1 are key regulators of Na+/H+ exchanger 1 ubiquitylation, endocytosis, and function. J Biol Chem *285*, 38293-38303.

Sorkina, T., Miranda, M., Dionne, K.R., Hoover, B.R., Zahniser, N.R., and Sorkin, A. (2006). RNA interference screen reveals an essential role of Nedd4-2 in dopamine transporter ubiquitination and endocytosis. J Neurosci *26*, 8195-8205.

Stamenova, S.D., French, M.E., He, Y., Francis, S.A., Kramer, Z.B., and Hicke, L. (2007). Ubiquitin binds to and regulates a subset of SH3 domains. Mol Cell *25*, 273-284.

Swaminathan, S., Amerik, A.Y., and Hochstrasser, M. (1999). The Doa4 deubiquitinating enzyme is required for ubiquitin homeostasis in yeast. Mol Biol Cell *10*, 2583-2594.

Tachiyama, R., Ishikawa, D., Matsumoto, M., Nakayama, K.I., Yoshimori, T., Yokota, S., Himeno, M., Tanaka, Y., and Fujita, H. (2011). Proteome of ubiquitin/MVB pathway: possible involvement of iron-induced ubiquitylation of transferrin receptor in lysosomal degradation. Genes Cells *16*, 448-466.

Tan, P.K., Howard, J.P., and Payne, G.S. (1996). The sequence NPFXD defines a new class of endocytosis signal in Saccharomyces cerevisiae. J Cell Biol *135*, 1789-1800.

Tanowitz, M., and Von Zastrow, M. (2002). Ubiquitination-independent trafficking of G protein-coupled receptors to lysosomes. J Biol Chem *277*, 50219-50222.

Verdecia, M.A., Bowman, M.E., Lu, K.P., Hunter, T., and Noel, J.P. (2000). Structural basis for phosphoserine-proline recognition by group IV WW domains. Nat Struct Biol *7*, 639-643.

Vina-Vilaseca, A., Bender-Sigel, J., Sorkina, T., Closs, E.I., and Sorkin, A. (2011). Protein kinase C-dependent ubiquitination and clathrin-mediated endocytosis of the cationic amino acid transporter CAT-1. J Biol Chem *286*, 8697-8706.

Vina-Vilaseca, A., and Sorkin, A. (2010). Lysine 63-linked polyubiquitination of the dopamine transporter requires WW3 and WW4 domains of Nedd4-2 and UBE2D ubiquitin-conjugating enzymes. J Biol Chem *285*, 7645-7656.

Wang, G., McCaffery, J.M., Wendland, B., Dupre, S., Haguenauer-Tsapis, R., and Huibregtse, J.M. (2001). Localization of the Rsp5p ubiquitin-protein ligase at multiple sites within the endocytic pathway. Mol Cell Biol *21*, 3564-3575.

Wang, H., Traub, L.M., Weixel, K.M., Hawryluk, M.J., Shah, N., Edinger, R.S., Perry, C.J., Kester, L., Butterworth, M.B., Peters, K.W.*, et al.* (2006). Clathrin-mediated endocytosis of the epithelial sodium channel. Role of epsin. J Biol Chem *281*, 14129-14135.

Warnock, D.G. (2001). Liddle syndrome: genetics and mechanisms of Na+ channel defects. Am J Med Sci *322*, 302-307.

Weinmaster, G., and Fischer, J.A. (2011). Notch ligand ubiquitylation: what is it good for? Dev Cell *21*, 134-144.

Wenzel, D.M., Stoll, K.E., and Klevit, R.E. (2010). E2s: structurally economical and functionally replete. Biochem J *433*, 31-42.

Xu, P., Duong, D.M., Seyfried, N.T., Cheng, D., Xie, Y., Robert, J., Rush, J., Hochstrasser, M., Finley, D., and Peng, J. (2009). Quantitative proteomics reveals the function of unconventional ubiquitin chains in proteasomal degradation. Cell *137*, 133-145.

Ye, Y., and Rape, M. (2009). Building ubiquitin chains: E2 enzymes at work. Nat Rev Mol Cell Biol *10*, 755-764.

Zamoyska, R., and Lovatt, M. (2004). Signalling in T-lymphocyte development: integration of signalling pathways is the key. Curr Opin Immunol *16*, 191-196.

Zelcer, N., Hong, C., Boyadjian, R., and Tontonoz, P. (2009). LXR regulates cholesterol uptake through Idol-dependent ubiquitination of the LDL receptor. Science *325*, 100-104.

Zhang, L., Fairall, L., Goult, B.T., Calkin, A.C., Hong, C., Millard, C.J., Tontonoz, P., and Schwabe, J.W. (2011). The IDOL-UBE2D complex mediates sterol-dependent degradation of the LDL receptor. Genes Dev *25*, 1262-1274.

Zhou, R., Kabra, R., Olson, D.R., Piper, R.C., and Snyder, P.M. (2010). Hrs controls sorting of the epithelial Na+ channel between endosomal degradation and recycling pathways. J Biol Chem *285*, 30523-30530.

Chapter 2

TORC1 Regulates Endocytosis via Npr1-mediated Phosphoinhibition of a Ubiquitin Ligase Adaptor

INTRODUCTION

Decisions of cell growth and differentiation are made by complex signaling networks that integrate various environmental and nutritional inputs and respond by coordinating diverse cellular processes towards a specific outcome. One example involves the target of rapamycin complex 1, or TORC1, a highly conserved multi-protein kinase complex that senses various cellular and environmental cues including nutrient availability, energy status, and growth signals and responds by coordinating activities associated with cell growth and proliferation. In general, signals that promote TORC1 kinase activity also promote cell growth and proliferation, while signals that inhibit TORC1 kinase activity tend to induce a starvation response. For example, TORC1 kinase phosphorylates both ribosomal S6 kinases and inhibitory eIF4E binding proteins, activities which promote translation initiation (Holz et al., 2005a, b). The TORC1 kinase also phosphorylates Atg13, preventing its association with Atg1 and thereby inhibiting the initiation of autophagy (Kamada et al., 2010), a conserved protein degradation pathway crucial to the starvation response in eukaryotic cells. Thus, TORC1 signaling coordinates cell growth by simultaneously promoting protein synthesis and inhibiting autophagy, while loss of TORC1 signaling triggers the onset of the starvation response by decreasing protein synthesis and inducing autophagy.

Some of the factors that regulate TORC1 signaling have been studied in detail. One important upstream activator of TORC1 signaling is Rheb, a lysosome-localized small GTPase that is antagonized by the GAP activity of TSC1-TSC2 heterodimers (Inoki et al., 2003). TSC2 is a key point of signal integration for TORC1 signaling: growth factors can stimulate TORC1 signaling via Akt/PKB-mediated inhibition of TSC2 (Inoki et al., 2002; Manning et al., 2002), while energy starvation can inhibit TORC1 signaling via AMPK-dependent phosphoactivation of TSC2 (Inoki et al., 2003). TORC1 signaling also responds to protein misfolding and quality control by sensing the availability of molecular chaperones, allowing the cell to regulate growth in response to protein folding stress (Qian et al., 2010). By mechanisms that are not completely understood, TORC1 also senses and responds to amino acid availability. This mode of TORC1 regulation involves the activity of four Rag GTPases which regulate amino acid-dependent localization of TORC1 to the lysosome, thus promoting interaction with and activation by Rheb (Sancak et al., 2010). Despite numerous reports elucidating the nutritional and environmental cues that influence TORC1 signaling and its downstream effector responses, a mechanistic understanding of how TORC1 integrates multiple signals to coordinate a holistic growth strategy for the cell remains to be elucidated.

Another way that eukaryotic cells regulate growth and proliferation in response to environmental changes is by regulating the activity and abundance of specific proteins at the cell surface. This is largely achieved via endocytic downregulation, which involves the endocytosis of cell surface proteins followed by delivery to the lysosome (or vacuole) where degradation occurs. Such endocytic

downregulation is critical to human health and disease. For example, failure to attenuate growth factor signaling from ligand-bound EGF receptor by endocytic downregulation can result in the aberrant proliferation of cells and cause cancer. To prevent hyperproliferation, the ubiquitin ligase Cbl and the adaptor protein Grb2 mediate the ubiquitination of stimulated EGFR molecules at the cell surface, targeting them for endocytosis and subsequent lysosomal degradation (Miranda and Sorkin, 2007). This example highlights the key role that endocytic downregulation plays in growth signal attenuation. While endocytic downregulation has been extensively studied as a mechanism for attenuation of signaling processes, less is known about how cells regulate surface protein abundance in response to changes in nutrient availability or cellular stress. Understanding how cells regulate the abundance and activity of cell surface proteins in response to changes in environment and nutritient availability is key to deciphering cellular strategies for adaptive growth.

In this study, we report that TORC1 signaling controls nutrient uptake by targeting the ubiquitin-mediated endocytosis of specific amino acid transporters. The mechanism involves a negative kinase signaling cascade in which TORC1 kinase inhibits the *n*itrogen *p*ermease *r*eactivator 1 (Npr1) kinase, which in turn inhibits a ubiquitin ligase adaptor. This ubiquitin ligase adaptor, the arrestin-related protein Art1, was previously shown to recruit Rsp5, the yeast homolog of Nedd4, to specific proteins at the plasma membrane (PM) in order to target them for endocytosis (Lin et al., 2008). We show that the TORC1-Npr1 negative kinase signaling cascade regulates Art1 translocation to the PM by N-terminal phosphorylation. Our results

demonstrate that a key effector pathway of TORC1 signaling coordinates the targeting of a ubiquitin ligase in order to regulate the endocytosis and vacuolar trafficking of specific nutrient transporters at the plasma membrane. Furthermore, these findings reveal that TORC1 controls amino acid uptake by tuning the abundance of transporters at the cell surface and that coordination of endocytosis with other cellular processes such as transcription, translation, and autophagy is critical for the ability of cells to adapt to changes in nutrient availability.

MATERIAL AND METHODS

Plasmids, Strains and Yeast Plating Assays

All plasmids and yeast strains used in this study are listed in Table S1 and Table S2, respectively. Canavanine plating assays were performed as previously described (Lin et al., 2008). Briefly, yeast cultures grown overnight in YPD were normalized to 1 OD/mL, serially diluted and plated onto SCD plates using a pin-frogger. The following concentrations of canavanine were tested in each experiment: 0 μg/mL, 1.0 μg/mL, 2.0 μg/mL, and 4.0 μg/mL.

Microscopy

All microscopy was performed using an Olympus IX71 microscopy equipped with FITC and rhodamine filters. Deconvolution and image analysis was performed using Softworx software (Applied Precision). For cargo trafficking assays, strains expressing chromosomally-tagged Vph1-mCherry were used to label the vacuolar membrane. In most experiments, cells were either mock-treated or treated with cycloheximide (CHX) (50 μg/mL) and/or rapamycin (RAP) (200 ng/mL) for 1.5 hours prior to imaging cells. Vacuolar trafficking of cargo was quantified by measuring fluorescence intensity of cargo signal (GFP) in the vacuole normalized to signal at the PM. For Art1-GFP and Npr1-GFP localization experiments, cells were stimulated with CHX, RAP, or both for 10 minutes prior to imaging. Art1 PM translocation was quantified.

Amino Acid Uptake Assays

To measure amino acid (arginine) uptake, yeast cells were grown to mid-log phase in SCD media and then labeled by addition of 5 μCi [^{3}H] arginine (Perkin Elmer).

Samples were collected at indicated timepoints by addition of ice-cold stopping solution (20mM NaN_3, 20mM NaF). Cells were pelleted, and the amount of [^{3}H] arginine remaining in the supernatant was measured using a Beckman Coutner LS 6500 scintillation counter.

Npr1 *in vitro* kinase assay

Recombinant Art1-6xHis-FLAG was incubated with yeast purified wild type or kinase dead GST-Npr1 for 30 minutes at 30°C in kinase buffer (50mM Tris pH7.5, 20mM $MgCl_2$, 1mM DTT, 25 μM [γ-^{32}P]-ATP (Perkin Elmer)). (See Supplemental Materials for detailed protein purification protocols). Subsequently, Art1-6xHis-FLAG was purified by incubating with M2 Flag beads for 1 hour at 4 °C. Beads were washed in TBS (50mM Tris pH7.5 and 150mM NaCl) and eluted in elution buffer (TBS with 5 mg/ml 3X FLAG Peptide (Sigma-Aldrich)). Protein samples were resolved by SDS-PAGE. Gels were both subjected to Western blot and dried for autoradiographing with Kodak BioMax MS film (Sigma-Aldrich)).

SILAC and Quantitative Mass Spectrometry

All quantitative mass spectrometry analysis was performed using SILAC labelling of yeast strains auxotrophic for lysine and arginine. Cells were grown to mid-log phase in the presence of either heavy or light isotopes (lysine and arginine) and affinity purification was performed as described in Supplemental Methods. Heavy and light purified samples were mixed and digested with 1μg of trypsin for 2 hours at 37˚C. For phosphoprofiling experiments, phosphopeptides were purified using IMAC chromatography as previously described (Albuquerque et al., 2008). Purified peptides were dried, reconstituted in 0.1% trifluoroacetic acid, and analysed by LC-

MS/MS using an Orbitrap XL mass spectrometer. Database search and SILAC quantitation was performed using Sorcerer software.

Quantitative Immunoblot Analysis

Quantitative fluorescence imaging of Western blots was performed using an Odyssey infrared imaging system (LI-COR Biosciences) as illustrated in Figure 2.5D. Antibodies used in this study include: α-FLAG (M2, Sigma); α-HA (12CA5, Roche).

^{32}P Labelling for Analysis of Protein Phosphorylation in Yeast

To measure ^{32}P incorporation into Art1, 5 ODs of yeast cells expressing Art1 fused to a C-terminal 3xFLAG-6XHis tandem tag were labelled with 0.8 mCi of ^{32}P-Na orthophosphate (Perkin Elmer) for two hours at 26˚C. Cells were then subject to treatment for 10 minutes with cycloheximide (50 μg/mL) or mock treatment, followed by precipitation of the cells in 10% trichloracetic acid (TCA). TCA pellets were then solubilised in cracking buffer (8M urea + 1% SDS in 50mM Tris) and diluted in lysis buffer (1X PBS + 1% Triton X-100 + protease inhibitors + phosphatase inhibitors) and bound to M2 affinity gel. After washing the beads, the sample was eluted with 3x-FLAG peptide (150 ng/μL) in phosphate buffer (50mM Na-phosphate, pH 8.0, 300mM NaCl, 0.1% Tween-20). The sample was further purified by binding to TALON Dynabeads (Invitrogen), washing with phosphate buffer, and eluting with 150 mM imidazole in phosphate buffer. This sample was then resolved by SDS-PAGE and analysed by Western Blot and by Phosphorimager (Molecular Dynamics). ^{32}P incorporation was imaged using a Typhoon scanner and quantified using Image J software.

Affinity Purification of Yeast Proteins

For purification of affinity-tagged yeast proteins, yeast cells were grown to mid-log phase, pelleted, washed with TE and then frozen as a dry pellet. Cell lysates were prepared by bead-beating for 30 minutes in lysis buffer (50mM Tris, 0.2% NP-40, 0.4% Triton X-100, 150mM NaCl, 5mM EDTA, 2X Complete EDTA-Free protease inhibitor tablets (Roche), 1X PhosStop (Roche), pH7.5). M2 flag beads (Sigma) were added to cleared yeast lysates and rotated for 1 hour at 4^0 C. Beads were washed three times in lysis buffer, then eluted in elution buffer (100mM Tris pH8.0, 1% SDS) at 95^0 C for 5 minutes. Eluates were reduced by addition of 10mM DTT and then alkylated by addition of iodoacetimide (20mM). For SILAC experiments, heavy and light samples were mixed, precipitated by adding (3:1) 50% acetone, 49.9% ethanol, and 0.1% acetic acid, resuspended (8M urea, 50mM Tris pH8.0), diluted 3:1 with water and digested with 1µg of trypsin overnight.

For purification of yeast Npr1 for *in vitro* kinase assays, GST-tagged Npr1 (wildtype or kinase dead) driven by the ADH1 promoter (pJAM608 and pJAM609) was transformed into *Δnpr1 cells* (JMY527). 300mLs cultures were grown to mid-log phase (OD_{600}=0.7) and treated with rapamycin for 15 minutes prior to harvest. Cells were washed in TE (10mM Tris pH7.5 and 0.5mM EDTA) and lysed by bead-beating in lysis buffer (50mM Tris pH7.5, 0.1% Triton X-100, 100mM NaCl, 1mM EDTA, 0.1% βME, 2XComplete EDTA-Free Protease Inhibitor tablets (Roche)). Glutathione Sepharose beads (GE Healthcare) were added to cleared yeast lysates and rotated for 1 hour at 4 °C. Beads were washed in wash buffer (50mM Tris pH7.5, 1% Triton X-100, 750mM NaCl, 1mM EDTA, 0.1% βME), then eluted in elution buffer (50mM Tris pH7.5, 1% Triton X-100, 750mM NaCl, 1mM EDTA, 0.1% βME, 10mM reduced

L-glutathione (Sigma-Aldrich)). Eluted GST-Npr1 was dialyzed in dialysis buffer (50mM Tris pH7.5, 20mM $MgCl_2$, 1mM DTT) at 4 °C, overnight.

Recombinant Protein Expression and Purification

Full length Art1-6xHis-FLAG (pJAM583) was transformed into Rosetta2 competent cells (EMD Chemicals USA). 1L cultures were grown to mid-log phase (OD_{600}=0.7) at 37°C. 1mM IPTG was added to bacteria cultures to induce protein expression at 16°C for 20 hours. Cells were lysed by sonication in PBS with protease inhibitors. TALON Metal Affinity Resin beads (Clontech) were added to cleared lysates and rotated for 1 hour at 4 °C. Beads were washed in PBS, and then eluted in elution buffer (PBS with 200mM imidazole).

RESULTS

TORC1 Regulates Endocytosis of Amino Acid Transporters

Previously we demonstrated that treatment of yeast cells with cycloheximide triggers the endocytosis and vacuolar trafficking of various plasma membrane proteins (Lin et al., 2008). We hypothesized that this might be part of a global cellular response to changes in nutrient availability, especially considering that cycloheximide has been shown to hyperactivate TORC1 signaling (Binda et al., 2009). We decided to test whether TORC1 signaling regulates the endocytosis, trafficking, or activity of cell surface proteins. First, we took advantage of the toxic arginine analog canavanine, which enters the cell through the arginine transporter Can1. Thus, sensitivity to canavanine is a function of the PM localization and activity of Can1. Previously, we used canavanine sensitivity to identify mutant strains defective for Can1 endocytosis (Lin et al., 2008). We observed that cells deleted for *TCO89*, a subunit of the yeast TORC1 signaling complex, exhibited canavanine hypersensitivity (Figure 2.1A) consistent with a potential defect in endocytosis. In contrast, mutants defective for TORC2, a related but distinct signaling complex that controls cell growth, survival and polarization, did not exhibit canavanine hypersensitivity (Figure 1A). These results suggested that TORC1 signaling may play a role in the endocytosis or the activity of Can1 at the cell surface.

To determine if TORC1 signaling is required for cycloheximide-triggered endocytosis, we examined Can1-GFP vacuolar trafficking in wildtype yeast cells treated with either cycloheximide or cycloheximide and rapamycin, a potent TORC1 inhibitor. Interestingly, rapamycin inhibited the endocytosis and vacuolar

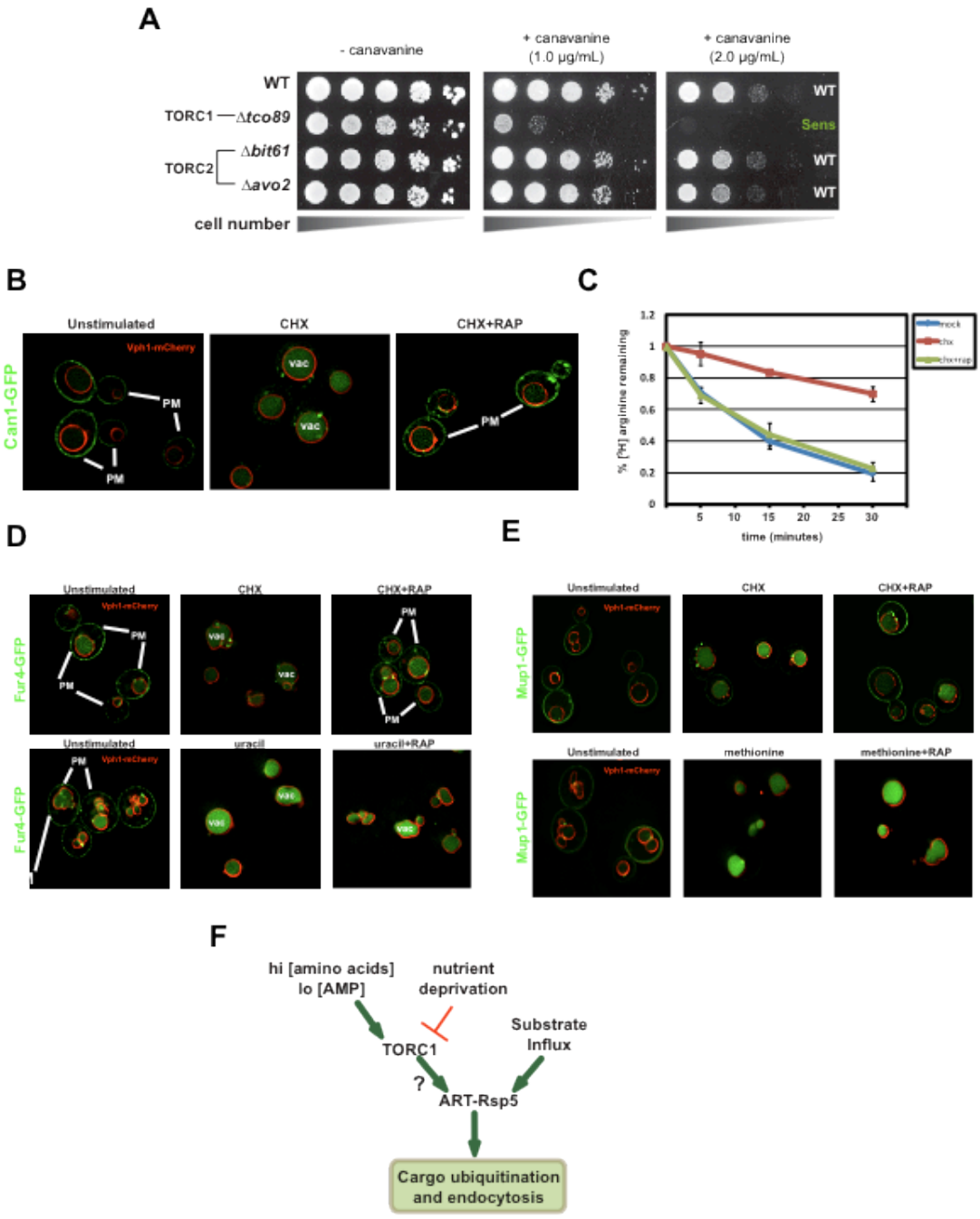
A
- canavanine
+ canavanine (1.0 µg/mL)
+ canavanine (2.0 µg/mL)
WT
TORC1 — Δtco89
TORC2 Δbit61
Δavo2
cell number
WT
Sens
WT
WT
B
Unstimulated
CHX
CHX+RAP
Can1-GFP
Vph1-mCherry
PM
vac
C
% [³H] arginine remaining
time (minutes)
D
Fur4-GFP
Unstimulated
CHX
CHX+RAP
uracil
uracil+RAP
E
Mup1-GFP
methionine
methionine+RAP
F
hi [amino acids]
lo [AMP]
nutrient deprivation
TORC1
Substrate Influx
?
ART-Rsp5
Cargo ubiquitination and endocytosis

Figure 2-1

Figure 2.1. TORC1 regulates the endocytosis of amino acid transporters. (A) Wildtype (background BY4741), TORC1, and TORC2 deficient yeast cells from the yeast deletion strain collection were scored for growth in the presence of canavanine. (B) Fluorescence distribution of Can1-GFP (green) was analyzed in wildtype yeast cells expressing the vacuolar marker Vph1-mCherry (red). Cells were either mock-treated ("unstimulated") or treated with cycloheximide ("CHX") or cycloheximide and rapamycin ("CHX+RAP") for 4 hours. Plasma membrane ("PM") and vacuole ("vac") localization are indicated. (C) The uptake of [^{3}H]arginine was measured in cells that were mock treated (blue), cycloheximide treated (red), or treated with cycloheximide and rapamycin (green). Error bars indicate standard deviation calculated from three replicate experiments. (D) Fluorescence distribution of Fur4-GFP (green) was analyzed in wildtype yeast cells expressing the vacuolar marker Vph1-mCherry (red). The affect of the following treatments were analyzed: mock-treated ("unstimulated"), cycloheximide-treated ("CHX"), cycloheximide- and rapamycin-treated ("CHX+RAP"), uracil-treated ("URA"), uracil- and rapamycin-treated ("URA+RAP"). All cells were imaged after 60 minutes of treatment. (E) Fluorescence distribution of Mup1-GFP (green) was analyzed in wildtype yeast cells expressing the vacuolar marker Vph1-mCherry (red). Cells were either mock-treated ("unstimulated") or treated with cycloheximide for 4 hours ("CHX"), cycloheximide and rapamycin ("CHX+RAP") for 4 hours, methionine for 60 minutes, or methionine and rapamycin for 60 minutes. (D) TORC1-regulated endocytosis may be mediated via the regulation of ART-Rsp5 ubiquitin ligase complexes.

trafficking of Can1-GFP in cycloheximide-treated cells (Figure 2.1B), suggesting a role for TORC1 in the endocytosis of Can1. Consistent with these results, we found that treatment of yeast cells with cycloheximide dramatically reduced arginine uptake, while simultaneous treatment with rapamycin abrogated this affect (Figure 2.1C). These results demonstrate that TORC1 signaling promotes the endocytic downregulation of the arginine transporter Can1.

Since many PM proteins undergo endocytosis and vacuolar trafficking in response to cycloheximide treatment, we tested additional cargo proteins and found that the cycloheximide-triggered endocytosis of the uracil transporter Fur4 and the methionine transporter Mup1 was abrogated in the presence of rapamycin (Figure 2.1D and 2.1E, respectively). Interestingly, rapamycin treatment did not affect the uracil-induced endocytosis of Fur4 (Figure 2.1D) or the methionine-induced endocytosis of Mup1 (Figure 2.1E), indicating that TORC1 signaling is not required for substrate-triggered endocytosis. Instead, these results suggest that TORC1 signaling promotes the endocytosis of multiple cell surface proteins as a general mechanism to limit protein abundance at the PM. Given our previous findings that cycloheximide-induced endocytosis of Can1 depends on the arrestin-like adaptor protein Art1 (Lin et al., 2008), which targets the Rsp5 ubiquitin ligase to specific cargoes at the PM, we hypothesized that TORC1 control of ubiquitin-mediated endocytosis may occur via regulation of Art1 function (Figure 2.1F). We set out to elucidate the molecular mechanisms that govern TORC1-mediated endocytosis.

The TORC1 Effector Kinase Npr1 Negatively Regulates Endocytosis

To determine how TORC1 regulates endocytosis, we scored the canavanine growth phenotypes of yeast deletion strains lacking different candidate effector kinases downstream of TORC1. We hypothesized that yeast cells deleted for TORC1-activated effector pathways that mediate Can1 endocytosis would exhibit hypersensitivity to canavanine. Although we did not observe any significant canavanine hypersensitive phenotypes among these deletion strains (Figure 2.2A, middle panel), we did observe a striking canavanine resistance phenotype in *Δnpr1* cells (Figure 2.2A, right panel). Npr1 is a protein kinase known to be phosphorylated and inhibited in a TORC1-dependent manner by a mechanism that likely involves both direct phosphorylation (Breitkreutz et al., 2010) and indirect control by regulation of a phosphatase that dephosphorylates and activates Npr1 (Figure 2.2B) (Bonenfant et al., 2003). We found that complementation of the canavanine resistance phenotype of *Δnpr1* cells required the Npr1 kinase activity (Figure 2.2C), suggesting that the Npr1 kinase negatively regulates Can1 endocytosis. We also observed that the canavanine resistance phenotype in *Δnpr1* cells required intact endocytic machinery (Figure 2.2D), suggesting that this phenotype is linked to endocytosis and not a Golgi-to-endosome shunt. To explore this further, we examined the steady state localization of Can1-GFP in wildtype and *Δnpr1* cells and found that deletion of the Npr1 kinase resulted in constitutive endocytosis and vacuolar trafficking of Can1-GFP (Figure 2.2E). Additional analysis revealed a similar role for Npr1 in the negative regulation of Fur4 and Lyp1 endocytosis (Figures 2.2F and 2.2G), while Mup1-GFP was unaffected in *Δnpr1* cells

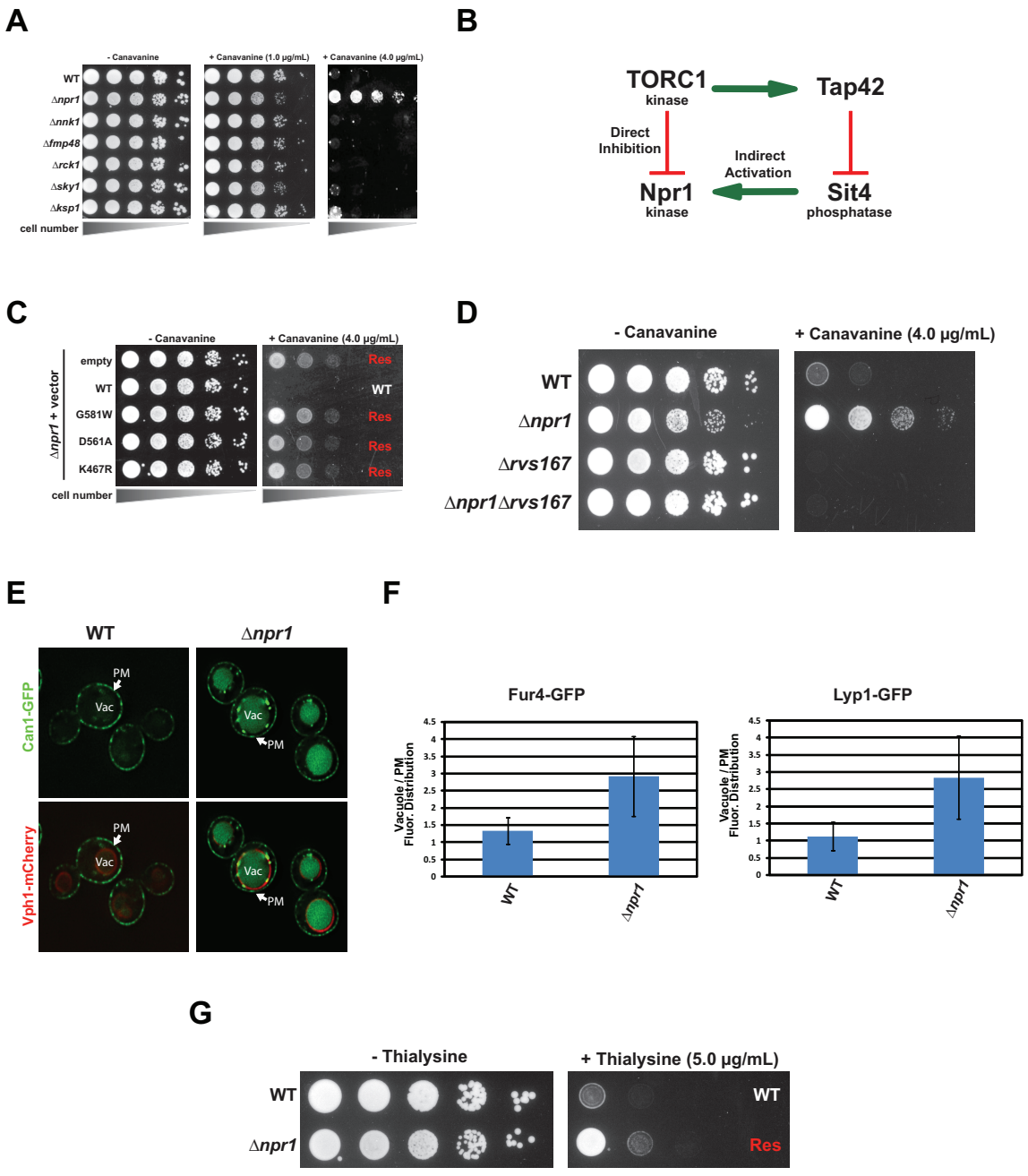
A
- Canavanine
+ Canavanine (1.0 µg/mL)
+ Canavanine (4.0 µg/mL)
WT
Δnpr1
Δnnk1
Δfmp48
Δrck1
Δsky1
Δksp1
cell number
B
TORC1
kinase
Tap42
Direct
Inhibition
Indirect
Activation
Npr1
kinase
Sit4
phosphatase
C
- Canavanine
+ Canavanine (4.0 µg/mL)
Δnpr1 + vector
empty
WT
G581W
D561A
K467R
Res
WT
Res
Res
Res
cell number
D
- Canavanine
+ Canavanine (4.0 µg/mL)
WT
Δnpr1
Δrvs167
Δnpr1Δrvs167
E
WT
Δnpr1
Can1-GFP
Vph1-mCherry
PM
Vac
F
Fur4-GFP
Lyp1-GFP
Vacuole / PM
Fluor. Distribution
WT
Δnpr1
G
- Thialysine
+ Thialysine (5.0 µg/mL)
WT
Δnpr1
WT
Res

Figure 2-2

Figure 2.2. The TORC1 effector Npr1 negatively regulates endocytosis (A) Wildtype (background BY4741) yeast cells and yeast cells defective for effector pathways downstream of TORC1 were scored for growth in the presence of canavanine. (B) Model for TORC1-mediated phosphoregulation of Npr1, based on previous studies (Breitkreutz et al., 2010; Gander et al., 2008; Jacinto et al., 2001). (C) Complementation of the canavanine resistance phenotype exhibited by *Δnpr1* yeast cells was tested using vectors expressing *NPR1* alleles under the control of its native promoter. Tested alleles included wildtype (WT) NPR1, a kinase activation loop mutant (*npr1-G581W*), a catalytic site mutant (*npr1-D561A*), and an ATP-binding pocket mutant (*npr1-K467R*). (D) Genetic interaction analysis of *NPR1* with *RVS167* (yeast homolog of amphiphysin), a protein required for efficient endocytosis. (E) Fluorescence microscopy analysis of Can1-GFP (green) in unstimulated wildtype and Δ*npr1* yeast cells. Vph1-mCherry (red) was used to label vacuoles. Plasma membrane (PM) and vacuole (Vac) are indicated. Quantitative analysis of Fur4-GFP and Lyp1-GFP (F) distribution in yeast cells. Fluorescence intensity of PM and vacuole was averaged over a population of cells (n>50) for each genotype. (G) Wildtype and Δ*npr1* yeast cells (BY4741) were grown in the absence or presence of thialysine, a toxic analog of lysine, to assess Lyp1 activity at the cell surface.

(Figure 2.3A). Npr1-related kinases such as Hrk1 (26.4% identical) and Prr2 (34.5% identical) do not exhibit growth phenotypes in the presence of canavanine (Figure 2.3B), highlighting the specialized role of Npr1 as a negative regulator of endocytosis.

To confirm the relationship between Npr1 and TORC1 kinases, we analyzed the canavanine growth phenotype of *Δtco89Δnpr1* double mutant cells and determined that they exhibited a canavanine resistance similar to *Δnpr1* cells (Figure 2.3C). The observation that canavanine hypersensitivity of *Δtco89* cells is dependent on the presence of Npr1 indicates that TORC1 controls endocytosis via negative regulation of the Npr1 kinase. To confirm that Npr1 activity negatively regulates endocytosis, we analyzed the affect of titrating Npr1 expression in wildtype yeast cells. We found that increased expression of the Npr1 kinase translated to a corresponding increase in canavanine sensitivity (Figure 2.3D), demonstrating that increased levels of Npr1 protein result in hyper-stabilization of Can1 at the plasma membrane.

Npr1 Regulates Art1 Activity Via Phosphoinhibition

To decipher the mechanism by which Npr1 negatively regulates endocytosis, we used *s*table *i*sotope *l*abeling of *a*mino acids in *c*ulture (SILAC) followed by phosphopeptide enrichment and quantitative mass spectrometry analysis to identify candidate substrates of the Npr1 kinase in an unbiased fashion. Since rapamycin is known to stimulate Npr1 kinase activity via inhibition of TORC1 (Gander et al., 2008), we compared the phosphoproteome of wildtype yeast cells

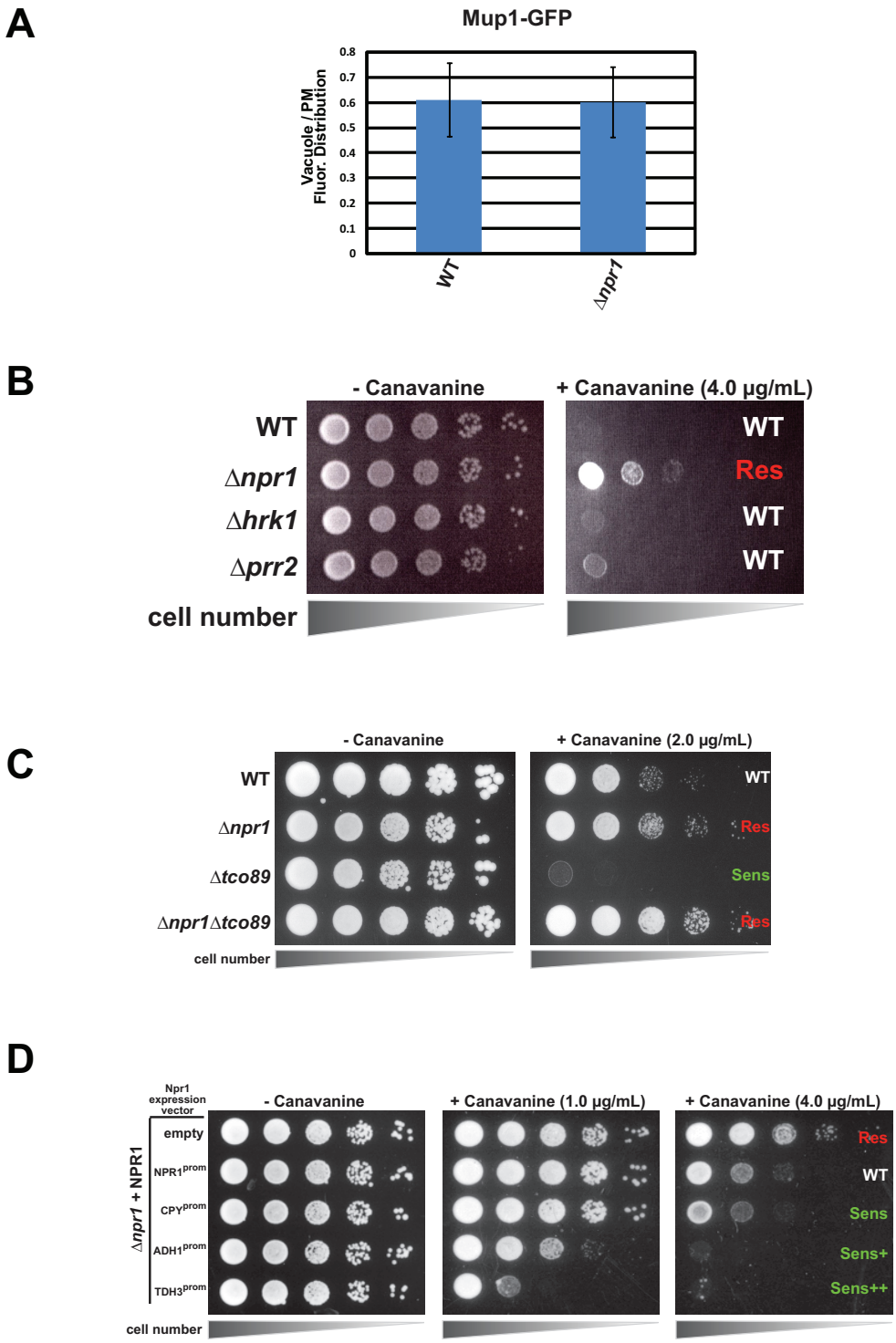
A
Mup1-GFP
Vacuole / PM Fluor. Distribution
0.8
0.7
0.6
0.5
0.4
0.3
0.2
0.1
0
WT
Δnpr1
B
- Canavanine
+ Canavanine (4.0 µg/mL)
WT
Δnpr1
Δhrk1
Δprr2
cell number
WT
Res
WT
WT
C
- Canavanine
+ Canavanine (2.0 µg/mL)
WT
Δnpr1
Δtco89
Δnpr1Δtco89
cell number
WT
Res
Sens
Res
D
Npr1 expression vector
- Canavanine
+ Canavanine (1.0 µg/mL)
+ Canavanine (4.0 µg/mL)
Δnpr1 + NPR1
empty
NPR1prom
CPYprom
ADH1prom
TDH3prom
cell number
Res
WT
Sens
Sens+
Sens++

Figure 2-3

Figure 2.3. Npr1 kinase negatively regulates endocytosis (A) Quantitative analysis of Mup1-GFP distribution in yeast cells. Fluorescence intensity of PM and vacuole was averaged over a population of cells (n>50) for each genotype. (B) Wildtype, Δ*npr1*, Δ*hrk1*, and Δ*prr2* yeast cells (SEY6210) were analyzed for their ability to grow in the presence of canavanine. (C) Growth of wildtype (BY4741), Δ*npr1*, Δ*tco89*, and Δ*npr1*Δ*tco89* yeast cells in the presence of canavanine was compared. (D) Expression of wildtype Npr1 was titrated using the following series of promoters: pNpr1 (endogenous), pCPY, pADH, and pTDH3. The affects of Npr1 titration on Can1 trafficking were determined by assaying growth in the presence of canavanine.

treated with rapamycin to that of *Δnpr1* cells treated with rapamycin in order to identify modifications that are dependent on Npr1 kinase activity (Table 1). Using this approach we identified several candidate Npr1 substrates, including several proteins with established roles in membrane traffic and nutrient transport. One of the candidates identified by this approach was Art1, which is required for cycloheximide-induced ubiquitination and endocytosis of Can1 (Figure 2.1F)(Lin et al., 2008). The identification of Art1 as a candidate substrate of Npr1 suggested that Npr1 may negatively regulate endocytosis via phosphoregulation of Art1. Genetic interaction analysis revealed that the canavanine resistance phenotype of *Δnpr1* cells is dependent upon the presence of Art1 (Figure 2.4A), suggesting that Npr1 negatively regulates endocytosis via inhibition of Art1. Furthermore, the constitutive endocytosis and vacuolar trafficking of Can1-GFP observed in *Δnpr1* cells was suppressed in *Δnpr1Δart1* double mutant cells (Figure 2.4B and 2.4C), indicating that the aberrant endocytosis of Can1-GFP observed in *Δnpr1* cells is mediated by Art1.

Based on these results, we hypothesized that the TORC1-Npr1 negative kinase signaling cascade regulates Art1 activation by phosphoinhibition (Figure 2.4D). A key prediction of this hypothesis is that loss of Npr1 kinase activity would alter the phospho-status of the Art1 protein. Consistent with this hypothesis, we found that Art1 recovered from *Δnpr1* cells exhibited a >50% decrease in the amount of phosphate incorporation relative to wildtype cells (Figure 2.4E). Furthermore, we found that the Art1 protein recovered from wildtype cells exists in two distinct forms, resolved as a doublet by SDS-PAGE (Figure 2.4F, lane 1).

Table 1: The Npr1 phosphoproteome reveals Art1 as a downstream effector

Category	Protein	Description	Xpress Ratios
Control	Npr1	Protein Kinase	107
Trafficking	Art1	Rsp5 ubiquitin ligase adaptor	27, 11
	SEC7	Arf GEF	27, 24
	TRS120	TRAPP complex component	121, 60
	LSP1	Eisosome component	79
Integral membrane proteins and transporters	VCX1	ion antiporter	117, 46, 17
	AGP1	amino acid transporter	98
	ITR1	inositol transporter	10
	GNP1	amino acid transporter	21, 10
Actin and polarization	RHO1	GTPase	215
	BEM3	RhoGAP	12
Lipid synthesis and binding	NUS1	prenyltransferase	10
	PIB2	PI3P binding protein	36
	ORM1	lipid homeostasis	39, 28, 12
Metabolic enzymes	IPP1	pyrophosphatase	88
Mito. import	TOM22	mitochondrial protein import	27
Function unknown	YLR257W	function unknown	62, 46, 32, 12

Table 1. The Npr1 phosphoproteome reveals Art1 as a downstream effector. Wildtype cells (labeled with heavy isotopes) and Δ*npr1* cells (labeled with light isotopes) were treated with rapamycin for 15 minutes and the phosphoproteome of each was quantitatively assessed using SILAC. A total of 3652 phosphopeptides were identified in this experiment. Xpress ratio indicates the fold enrichment in wildtype cells compared to Δ*npr1* cells. This table shows proteins containing phosphopeptides that exhibited at least a 10-fold increase in wildtype cells relative to Δ*npr1* cells.

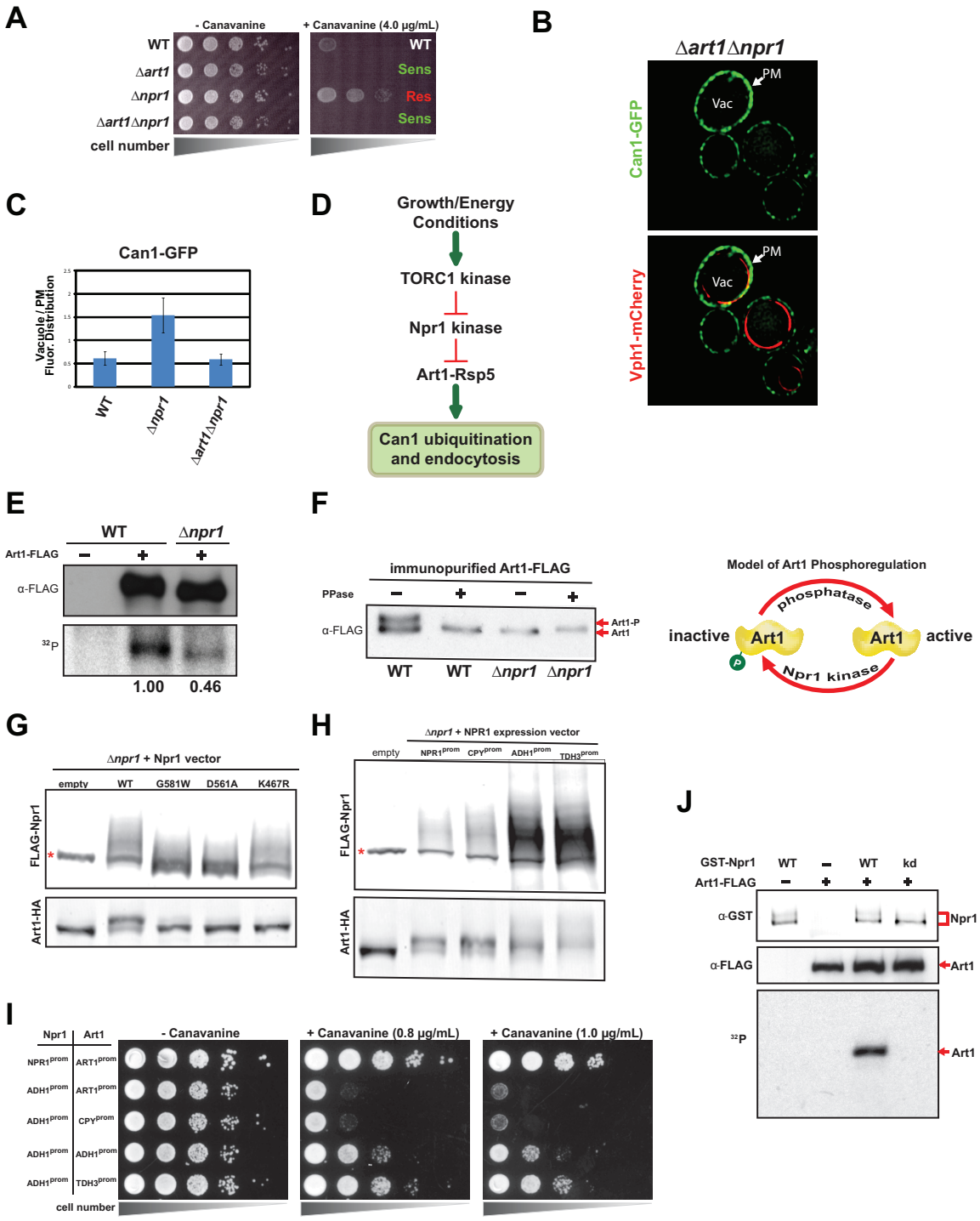
A
- Canavanine
+ Canavanine (4.0 µg/mL)
WT
Δart1
Δnpr1
Δart1Δnpr1
cell number
WT
Sens
Res
Sens
B
Δart1Δnpr1
Can1-GFP
Vph1-mCherry
PM
Vac
C
Can1-GFP
Vacuole / PM Fluor. Distribution
WT
Δnpr1
Δart1Δnpr1
D
Growth/Energy Conditions
TORC1 kinase
Npr1 kinase
Art1-Rsp5
Can1 ubiquitination and endocytosis
E
WT
Δnpr1
Art1-FLAG
α-FLAG
32P
1.00
0.46
F
immunopurified Art1-FLAG
PPase
α-FLAG
Art1-P
Art1
WT
WT
Δnpr1
Δnpr1
Model of Art1 Phosphoregulation
phosphatase
inactive
Art1
Art1
active
Npr1 kinase
G
Δnpr1 + Npr1 vector
empty
WT
G581W
D561A
K467R
FLAG-Npr1
Art1-HA
H
Δnpr1 + NPR1 expression vector
empty
NPR1prom
CPYprom
ADH1prom
TDH3prom
FLAG-Npr1
Art1-HA
I
Npr1
Art1
NPR1prom
ADH1prom
ADH1prom
ADH1prom
ADH1prom
ART1prom
ART1prom
CPYprom
ADH1prom
TDH3prom
cell number
- Canavanine
+ Canavanine (0.8 µg/mL)
+ Canavanine (1.0 µg/mL)
J
GST-Npr1
WT
WT
kd
Art1-FLAG
α-GST
α-FLAG
32P
Npr1
Art1
Art1

Figure 2-4

Figure 2.4. Npr1 regulates Art1 activity via phosphoinhibition (A) Canavanine sensitivity/resistance phenotypes were determined for wildtype (WT), Δ*art1*, Δ*npr1*, Δ*art1*Δ*npr1* cells. (B) Fluorescence microscopy analysis of Can1-GFP (green) in unstimulated Δ*art1*Δ*npr1* yeast cells. Vph1-mCherry (red) was used to label vacuoles. (C) Quantitative analysis of Can1-GFP distribution in cells from (B) and Figure 2C. Fluorescence intensity of PM and vacuole was averaged over a population of cells (n>50) for each genotype. (D) Based on genetic interaction data, we devised a model pathway for the TORC1-Npr1 negative signaling cascade that results in phosphoregulation of Art1. This pathway controls the cycling of Art1 between a phosphorylated inactive state and a dephosphorylated active state. (E) Art1 was affinity purified from unstimulated wildtype and *Δnpr1* yeast cells labeled with ^{32}P. Top panel depicts Western blot of total Art1 protein recovered, while bottom panel shows ^{32}P incorporation into Art1. Quantitation was performed by scanning Phosphorimager (bottom labels). (F) Art1 was affinity purified from wildtype or Δ*npr1* yeast cells and subject to phosphatase treatment or mock treatment. Affinity purified Art1 from wildtype cells can be resolved as two distinct bands, indicated by red arrows on the right. (G) Western blot analysis of Npr1 expression levels (top panel) and Art1 phosphorylation patterns (bottom panel). Red asterisk indicates a non-specific band. (H) Expression of wildtype Npr1 was titrated. Npr1 expression (top panel) and Art1 phosphorylation patterns (bottom panel) were analyzed by Western blot. (I) In a yeast strain overexpressing Npr1 from the ADH1 promoter, Art1 expression was titrated up. The resulting yeast cells were analyzed for the ability to grow in the presence of canavanine. (J)

Phosphorylation of recombinant Art1 was reconstituted using wildtype (WT) but not kinase dead (kd) Npr1 purified from yeast.

Following phosphatase treatment, the Art1 doublet collapses to a single band (Figure 2.4F, lane 2), indicating that the lower mobility form of Art1 is phosphorylated. Interestingly, Art1 protein recovered from *Δnpr1* cells did not exhibit the phospho-shift observed in wildtype cells (Figure 2.4F, lanes 3-4). Art1 phosphorylation was complemented by expression of wildtype Npr1 but not kinase-dead mutant alleles (Figure 2.4G). Furthermore, increasing Npr1 expression led to corresponding increases in Art1 phosphorylation (Figure 2.4H and 2.4I). Finally, we were able to demonstrate that Art1 is a substrate for active Npr1 kinase but not a kinase dead mutant *in vitro* (Figure 2.4J), providing evidence for direct phosphorylation. In summary, these results suggest that Npr1 negatively regulates endocytosis by phosphorylating Art1, a ubiquitin ligase adaptor.

TORC1 Signaling Tunes Art1 Activity By Modulating Phosphoinhibition

To test whether TORC1 activity mediates Art1 dephosphorylation, we examined radioactive phosphate incorporation into Art1 under conditions of TORC1 hyperactivation. We found that hyperactivation of TORC1 signaling by treatment of yeast cells with cycloheximide resulted in a >60% decrease in Art1 phosphorylation (Figure 2.5A). Based on our data, we propose a TORC1-Npr1 negative kinase signaling cascade that activates Art1 via sequential repression (Figure 2.5B). In this model, inhibition of TORC1 signaling (by starvation conditions or treatment of cells with rapamycin) triggers Npr1 activation by dephosphorylation. The increased Npr1 kinase activity leads to inhibition of Art1, which decreases endocytosis and stabilizes Can1 at the PM (Figure 2.5C lane 1, 4D and 2.5D). When TORC1 activity is

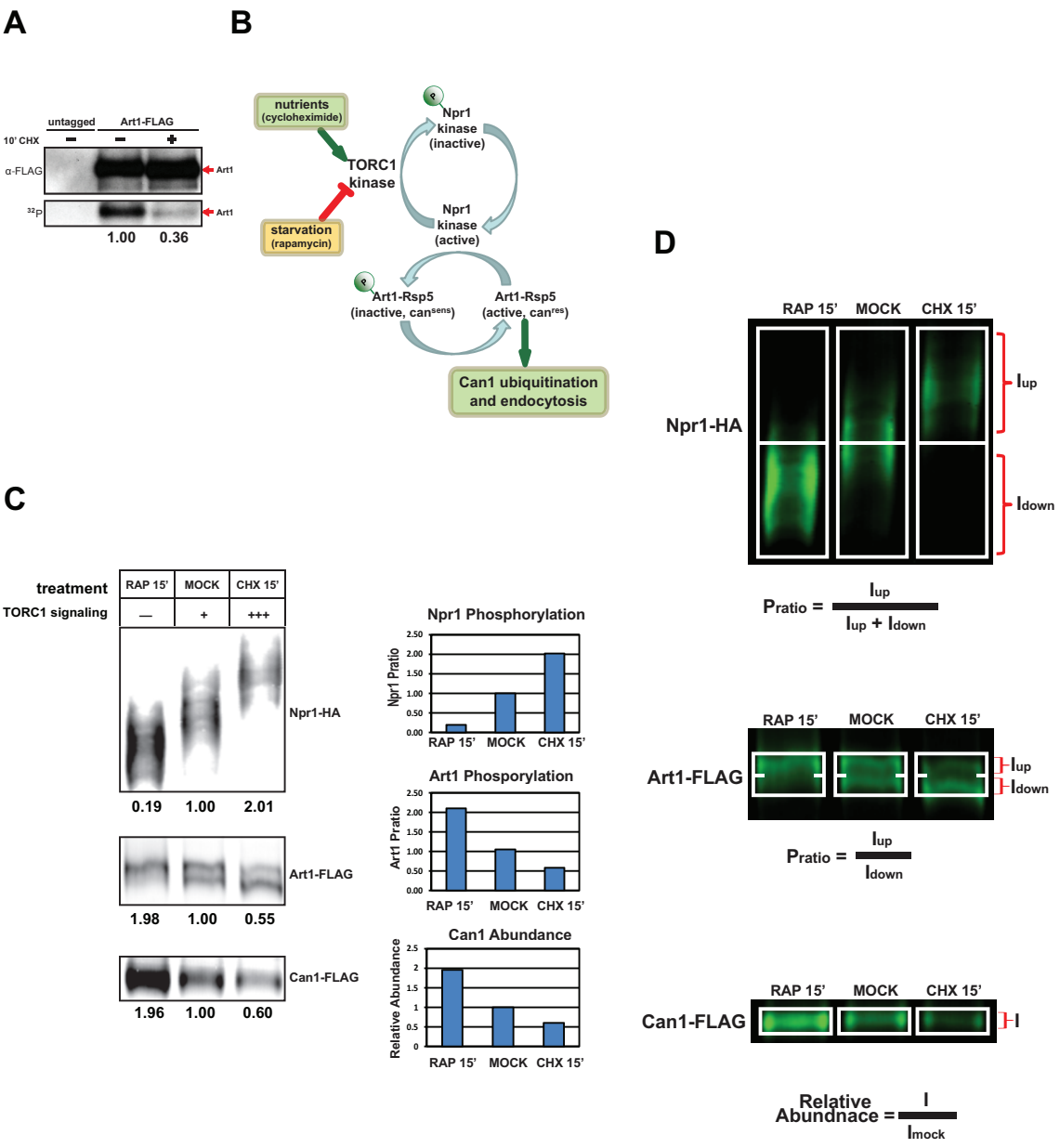
A
untagged
Art1-FLAG
10' CHX
α-FLAG
Art1
32P
Art1
1.00
0.36
B
nutrients
(cycloheximide)
TORC1
kinase
starvation
(rapamycin)
Npr1
kinase
(inactive)
Npr1
kinase
(active)
Art1-Rsp5
(inactive, can^sens)
Art1-Rsp5
(active, can^res)
Can1 ubiquitination
and endocytosis
C
treatment
TORC1 signaling
RAP 15'
MOCK
CHX 15'
—
+
+++
Npr1-HA
0.19
1.00
2.01
Art1-FLAG
1.98
1.00
0.55
Can1-FLAG
1.96
1.00
0.60
Npr1 Phosphorylation
Npr1 Pratio
Art1 Phosporylation
Art1 Pratio
Can1 Abundance
Relative Abundance
RAP 15'
MOCK
CHX 15'
D
RAP 15'
MOCK
CHX 15'
Npr1-HA
Iup
Idown
Pratio = Iup / (Iup + Idown)
Art1-FLAG
Pratio = Iup / Idown
Can1-FLAG
I
Relative Abundnace = I / Imock

Figure 2-5

Figure 2.5. TORC1 tunes Art1 activity by modulating phosphorylation (A) Art1 recovered from wildtype yeast cells labeled with ^{32}P and subject to cycloheximide stimulation or mock treatment. Top panel depicts Western blot of total Art1 protein recovered, while bottom panel shows ^{32}P incorporation into Art1. Quantitation was performed by scanning Phosphorimager (bottom labels). (B) Model for TORC1 activation of Art1-mediated endocytosis of Can1 by a sequential repression mechanism. (C) Wildtype yeast cells were treated with rapamycin (200ng/mL), cycloheximide (50 µg/mL), or mock treated (DMSO) for 15 minutes and analyzed for Npr1 phosphoshift (top panel), Art1 phosphoshift (middle panel), and Can1 abundance (lower panel). Values indicate Npr1 Pratio (below top panel), Art1 Pratio (below middle panel), and Can1 relative abundance (below bottom panel) all normalized to the mock condition. Indicators of TORC1 signaling activity (-, +, +++) are based on previous reports that RAP inhibits TORC1 signaling and CHX activates TORC1 signaling, both relative to mock treatment. Quantitation of data is shown on the right panel. Quantitation of immunoblots using fluorescence scanning was performed as in (D) as illustrated.

high (in nutrient-replete conditions or by treatment of cells with cycloheximide), Npr1 is hyperphosphorylated and its kinase activity is inhibited. This state favors Art1 dephosphorylation, which leads to increased Can1 endocytosis and vacuolar degradation (Figure 2.5C lane 3, 4D and 2.5D). During normal log phase growth conditions, TORC1 signals at an intermediate level, maintaining both Art1 and Npr1 in a meta-phosphorylated state (Figure 2.5C lane 2, 4D and 2.5D). This system endows TORC1 with fine control over the endocytic equilibrium of Can1, effectively tuning nutrient transport over a wide range of conditions. This signaling pathway responds to perturbations in TORC1 signaling within minutes (Figure 2.6A, 2.6B and unpublished results) and the response to both cycloheximide and rapamycin is dependent on TORC1 but not TORC2 (data not shown). Consistent with these results, the ability of cycloheximide to activate Art1 by inhibiting Npr1 is blocked by simultaneous treatment with rapamycin (Figure 2.6C). We also found that regulation of Can1 endocytosis by TORC1 translates to corresponding affects on arginine uptake: TORC1 signaling increased Can1 endocytosis and thus blocked arginine uptake, while TORC1 inhibition stabilized Can1 at the PM and thus increased the rate of arginine uptake (Figure 2.6D). These data support a model whereby TORC1 regulates endocytosis via a negative kinase cascade that tunes Art1 activity by phosphoinhibition.

To further explore the basis for TORC1 regulation of endocytosis, we examined Art1 phosphorylation across a variety of media conditions and cellular stresses. Similar to our results with rapamycin treatment, we found that shifting

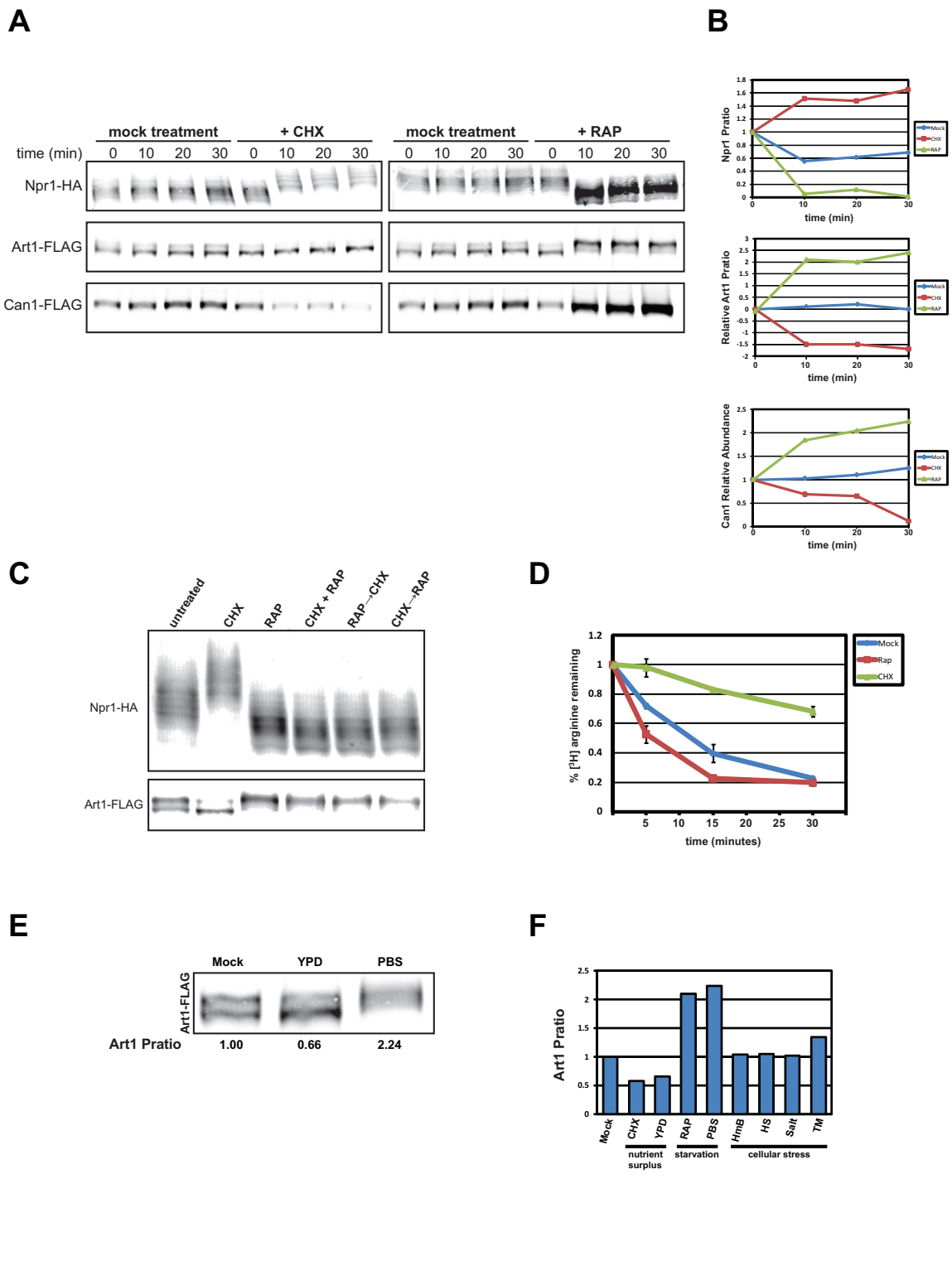
A
mock treatment
+ CHX
mock treatment
+ RAP
time (min)
0 10 20 30 0 10 20 30 0 10 20 30 0 10 20 30
Npr1-HA
Art1-FLAG
Can1-FLAG
B
Npr1 Pratio
Relative Art1 Pratio
Can1 Relative Abundance
time (min)
Mock
CHX
RAP
C
untreated
CHX
RAP
CHX + RAP
RAP→CHX
CHX→RAP
Npr1-HA
Art1-FLAG
D
% [3H] arginine remaining
time (minutes)
Mock
Rap
CHX
E
Mock
YPD
PBS
Art1-FLAG
Art1 Pratio
1.00
0.66
2.24
F
Art1 Pratio
Mock
CHX
YPD
RAP
PBS
HmB
HS
Salt
TM
nutrient surplus
starvation
cellular stress

Figure 2-6

Figure 2.6. Nutrient availability regulates Art1 activity by modulating phosphorylation (A) Timecourse analysis of the TORC1-Npr1 signaling response was quantified (B) using fluorescence scanning. (C) The signaling response from (Figure 2.5C) was analyzed in response to either co-treatment with or different orders of addition of cycloheximide and rapamycin. (D) Wildtype yeast cells were treated with either cycloheximide or rapamycin for 15 minutes and uptake of radioactive arginine was measured at the indicated timepoints. (E) The phospho-status of Art1 was analyzed in response to changes nutrient availability, including a shift from minimal media to YPD for 2 hours (nutrient surplus) or a shift from minimal media to PBS for 12 hours (starvation). (F) Quantitation of the Art1 phosphorylation ratio (Pratio) for the results in (E) along with additional treatments including 200 µg/mL Hygromycin B for 15 minutes (HmB), heat shock at 37^0 for 30 minutes (HS), 0.4M NaCl for 30 minutes (Salt), or 4 µg/mL tunicamycin for 15 minutes (TM).

from minimal media to PBS, a physiological starvation condition, triggered Art1 hyperphosphorylation (Figure 2.6E lane 3). In contrast, shifting yeast cells from minimal media to nutrient rich YPD triggered Art1 dephosphorylation (Figure 2.6E lane 2). Interestingly, Art1 phospho-status was not sensitive to other cellular stresses tested (Figure 2.6F). In summary, our results indicate that TORC1 senses nutrient availability and responds by regulating endocytosis in order to tune the activity of amino acid transporters at the cell surface.

Inhibition of Art1 Is Mediated By N-terminal Phosphorylation

To better understand the mechanism of Art1 phosphoinhibition, we employed quantitative mass spectrometry methodologies to map specific phosphosites in Art1 that are dependent on the TORC1-Npr1 negative kinase signaling cascade. First, we trypsin digested affinity purified Art1 from wildtype cells, enriched for phosphopeptides using immobilized metal affinity chromatography (IMAC), and analyzed samples using LC-MS/MS. This analysis revealed many phosphorylated residues in Art1, including an N-terminal phosphocluster (between amino acids 79 and 124), a series of mostly proline-directed phosphosites at the C-terminus of Art1 (from amino acids 599 to 722), and a few phosphosites in the arrestin fold domain (Figure 2.7A). Next, we used SILAC to determine which sites were dependent on Npr1 activity (Figure 2.7B). We found that both the N-terminal phosphocluster and the proline-directed phosphocluster were dependent on the presence of Npr1 (Figure 2.7C). Similarly, both clusters increased significantly during rapamycin-induced Art1 hyperphosphorylation

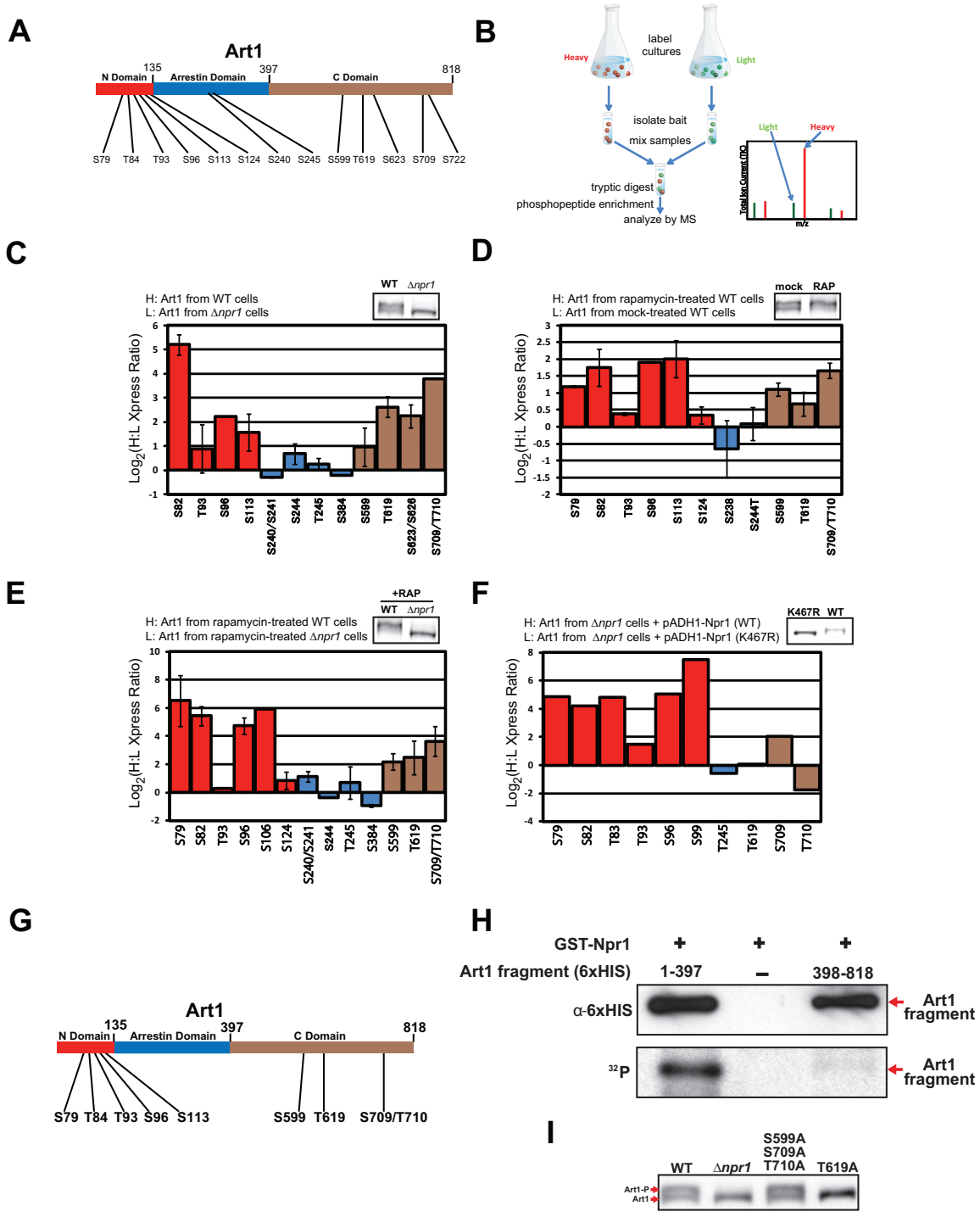
A
Art1
N Domain
135
Arrestin Domain
397
C Domain
818
S79 T84 T93 S96 S113 S124 S240 S245 S599 T619 S623 S709 S722
B
Heavy
label cultures
Light
isolate bait
mix samples
tryptic digest
phosphopeptide enrichment
analyze by MS
Light
Heavy
Total Ion Current (TIC)
m/z
C
H: Art1 from WT cells
L: Art1 from Δnpr1 cells
WT Δnpr1
Log2(H:L Xpress Ratio)
S82 T93 S96 S113 S240/S241 S244 T245 S384 S599 T619 S823/S826 S709/T710
D
H: Art1 from rapamycin-treated WT cells
L: Art1 from mock-treated WT cells
mock RAP
Log2(H:L Xpress Ratio)
S79 S82 T93 S96 S113 S124 S238 S244T S599 T619 S709/T710
E
+RAP
WT Δnpr1
H: Art1 from rapamycin-treated WT cells
L: Art1 from rapamycin-treated Δnpr1 cells
Log2(H:L Xpress Ratio)
S79 S82 T93 S96 S106 S124 S240/S241 S244 T245 S384 S599 T619 S709/T710
F
H: Art1 from Δnpr1 cells + pADH1-Npr1 (WT)
L: Art1 from Δnpr1 cells + pADH1-Npr1 (K467R)
K467R WT
Log2(H:L Xpress Ratio)
S79 S82 T83 T93 S96 S99 T245 T619 S709 T710
G
Art1
N Domain
135
Arrestin Domain
397
C Domain
818
S79 T84 T93 S96 S113
S599 T619 S709/T710
H
GST-Npr1 + + +
Art1 fragment (6xHIS) 1-397 – 398-818
α-6xHIS
Art1 fragment
32P
Art1 fragment
I
WT Δnpr1 S599A S709A T710A T619A
Art1-P
Art1

Figure 2-7

Figure 2.7. Inhibition of Art1 is mediated by N-terminal phosphorylation (A) Schematic dividing the Art1 protein into three regions: an N-terminal domain (red), the arrestin fold domain (blue), and a C-terminal domain (brown). Phosphorylation sites identified by mass spectrometry analysis are indicated. (B) Schematic demonstrating how SILAC followed by quantitative mass spectrometry analysis is used to measure changes at specific Art1 phosphosites. SILAC combined with quantitative mass spectrometry analysis was used to measure changes in phosphorylation at specific Art1 residues for pair wise comparisons of wildtype (WT) cells versus Δ*npr1* cells (C), rapamycin-treated WT cells versus mock-treated WT cells (D), rapamycin-treated WT cells versus rapamycin-treated Δ*npr1* cells (E), and Δ*npr1* cells overexpressing WT Npr1 versus Δ*npr1* cells overexpressing the kinase dead *npr1-K467R* allele (F). For each of C-F, bars are color-coded to reflect the position of the phosphosites in the Art1 protein. The y-axis values represent the Log_2 of the Xpress (H:L) ratio, a quantitative measure of isotopic representation. Western blots showing phosphoshifts as resolved by SDS-PAGE are shown in the upper right of each profiling experiment. Not all phosphopeptides were detected in every experiment, leading to variation in what can be scored for each condition. (G) Schematic of Art1 illustrating N-terminal and C-terminal (proline-directed) phosphorylation sites. (H) Npr1 *in vitro* kinase assays were performed by using recombinant purified Art1 fragments corresponding to the N-terminus (amino acids 1-397) or the C-terminus (amino acids 398-818). The two fragments exhibit the similar mobility by SDS-PAGE. Consistent with these results, we also determined by mass spectrometry that Npr1 phosphorylation of full length Art1 *in vitro* is directed

to the N-terminus, particularly S79 (data not shown). (I) Art1 from yeast cell extracts was analyzed by SDS-PAGE and Art1 point mutants were scored as either a doublet (wildtype) or singlet. Importantly, these results demonstrate that the bandshift is the result of phosphorylation at a C-terminal residue, T619, and that the mobility shift assay does not perfectly correlate with N-terminal phosphorylation of Art1. This is consistent with our results that loss of Npr1 *in vivo* causes a bandshift that cannot be reconstituted *in vitro*. T619 is a proline-directed phosphorylation site, and thus is not a substrate for Npr1 phosphorylation (Gander et al., 2009). However, phosphorylation at T619 is regulated by Npr1 (Figure 5C, 5D, and 5E). These results suggest that there is a second Art1 kinase which targets that C-terminus of Art1, and that these proline-directed phosphorylation events are somehow dependent on Npr1 kinase activity.

(Figure 2.7D). Interestingly, when we compared Art1 phosphopeptides from rapamycin-treated wildtype cells (hyperphosphorylated) and rapamycin-treated *Δnpr1* cells (hypophosphorylated), we observed a dramatic 30- to 60-fold difference in phosphorylation at the N-terminal phosphocluster and only modest (4- to 10-fold) increases for the proline-directed phosphocluster (Figure 2.7E). Furthermore, we found that overexpression of wildtype Npr1 resulted in similarly dramatic increases in phosphorylation at the N-terminal sites compared to overexpression of a kinase-dead variant (Figure 2.7F). Our quantitative mass spectrometry data strongly suggests that Npr1 promotes phosphorylation at the N-terminus of Art1 (especially Ser79, Ser82, Ser96 and Ser99). Our results suggest that Npr1 indirectly affects phosphorylation at C-terminal proline-directed sites in Art1 as previous studies have shown that a +1 proline is strongly disfavored by the Npr1 kinase (Gander et al., 2009) making these sites unlikely targets for direct regulation by Npr1. Indeed, using the *in vitro* kinase assay, Npr1 was capable of phosphorylating an N-terminal fragment of Art1, but not a C-terminal fragment that contains the proline-directed phosphorylation sites (Figure 2.7G and 2.7H). Importantly, we found that the Art1 bandshift observed by SDS-PAGE is dependent on the C-terminal proline-directed phosphorylation events, indicating it is the result of both Npr1 and yet another kinase (Figure 2.7I). Although *in vitro* phosphorylation of Art1 by Npr1 did not reconstitute the bandshift observed *in vivo* (Figure 2.7J), mass spectrometry analysis of Art1 phosphorylated by Npr1 *in vitro* identified the same N-terminal phosphorylation pattern (particularly at S79, data not shown) observed *in vivo*. Since Art1 C-terminal proline-directed phosphorylation events are in fact regulated

by Npr1 *in vivo* (Figure 2.7C, 2.7D, and 2.7E), our results suggest a possible interaction between N-terminal and C-terminal phosphorylation events, and further investigation will be required to determine the function of proline-directed phosphorylation at the C-terminus of Art1.

TORC1-dependent phosphoregulation of other ART family proteins was not evident by SDS-PAGE (Figure 2.8A), however quantitative mass spectrometry analysis revealed that other ART family proteins, most notably Art2 and Art3, may also be regulated by Npr1 (Figure 2.8B). These results suggest that TORC1 signaling does not regulate all ART family proteins, but rather appears to specifically regulate Art1 as well as perhaps Art2 and Art3. We also performed similar quantitative mass spectrometry analysis of Npr1 phosphorylation in response to changes in TORC1 signaling. We identified numerous Npr1 phosphosites primarily clustered at the N-terminus of the protein (Figure 2.8C). Consistent with our observations in Figure 4, this N-terminal phosphorylation of Npr1 is significantly reduced when TORC1 is inhibited (Figure 2.8D) and significantly increased when TORC1 is hyperactivated (Figure 2.8E). These results are consistent with previously reported mass spectrometry analysis of Npr1 phosphorylation (Gander et al., 2008). Given the large number of N-terminal phosphorylation events that respond in this manner, we deleted the N-terminal phosphocluster of Npr1 (Δ40-360) and found that the truncated protein does not complement canavanine resistance or Art1 phosphorylation (Figure 2.8F and 2.8G). These results indicate that Npr1 undergoes N-terminal phosphoinhibition similar to Art1, but that this N-terminal region is

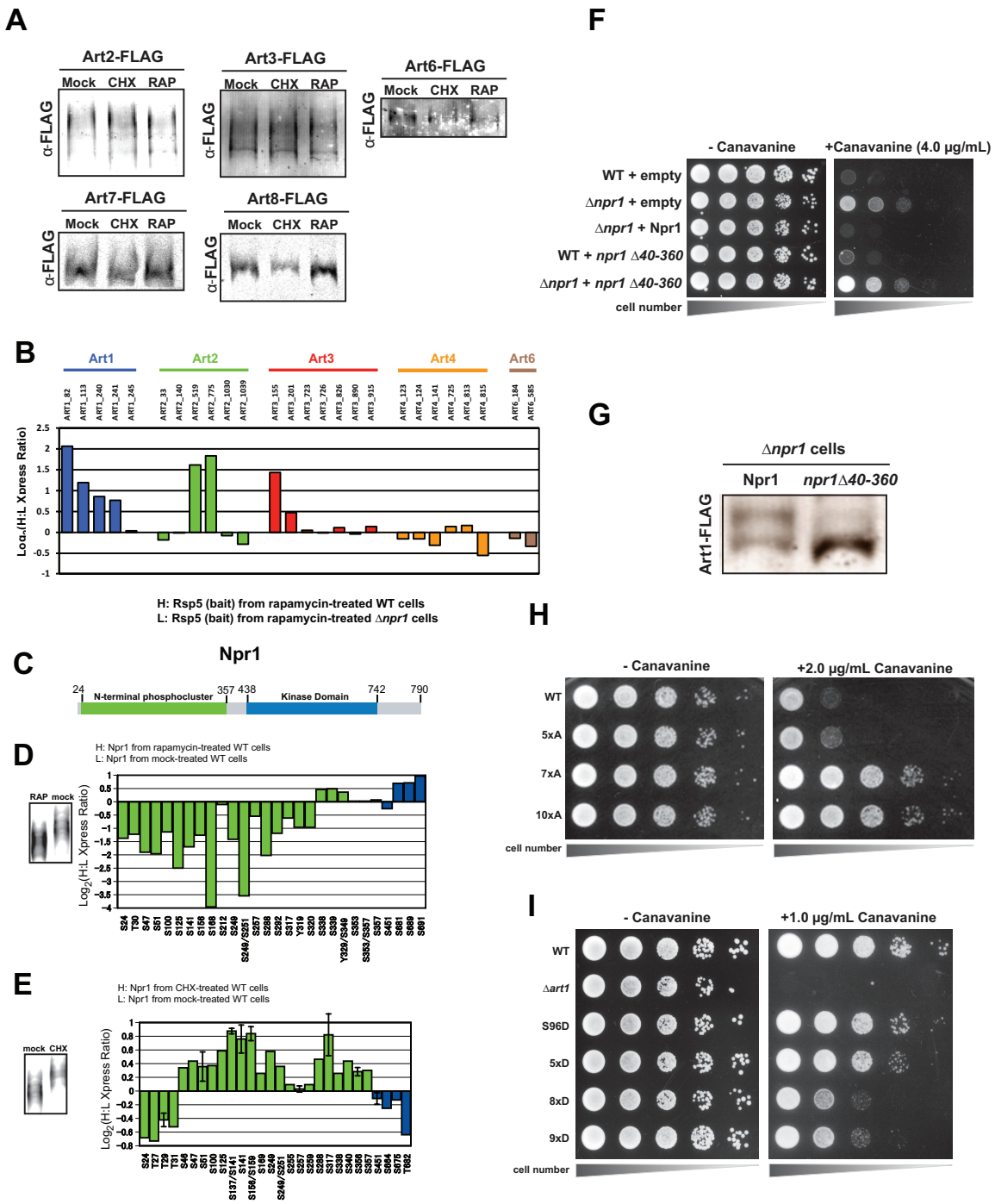
A
Art2-FLAG
Art3-FLAG
Art6-FLAG
Art7-FLAG
Art8-FLAG
Mock CHX RAP
α-FLAG
B
Art1
Art2
Art3
Art4
Art6
Log2(H:L Xpress Ratio)
H: Rsp5 (bait) from rapamycin-treated WT cells
L: Rsp5 (bait) from rapamycin-treated Δnpr1 cells
C
Npr1
24
N-terminal phosphocluster
357 438
Kinase Domain
742
790
D
H: Npr1 from rapamycin-treated WT cells
L: Npr1 from mock-treated WT cells
RAP mock
E
H: Npr1 from CHX-treated WT cells
L: Npr1 from mock-treated WT cells
mock CHX
F
- Canavanine
+Canavanine (4.0 μg/mL)
WT + empty
Δnpr1 + empty
Δnpr1 + Npr1
WT + npr1 Δ40-360
Δnpr1 + npr1 Δ40-360
cell number
G
Δnpr1 cells
Npr1
npr1Δ40-360
Art1-FLAG
H
- Canavanine
+2.0 μg/mL Canavanine
WT
5xA
7xA
10xA
cell number
I
- Canavanine
+1.0 μg/mL Canavanine
WT
Δart1
S96D
5xD
8xD
9xD
cell number

Figure 2-8

Figure 2.8. Phosphoregulation of ART family proteins and inhibition of Npr1 is mediated by N-terminal phosphorylation (A) Analysis of chromosomally expressed FLAG-tagged ART family proteins by SDS-PAGE. Expression of Art4, Art5, and Art9 were undetectable by Western blot. (B) Phosphoprofiling experiment similar to those in Figure 2.7C-F, except Rsp5 was used as the bait. This enabled the detection of phosphopeptides from many ART family proteins, which are known to interact with Rsp5. Analysis of experiments comparing mock-treated wildtype cells to rapamycin-treated wildtype cells, yielded similar results. (C) Schematic dividing the Npr1 protein into two regions: an N-terminal phosphocluster domain (green) and a C-terminal kinase domain (blue). SILAC combined with quantitative mass spectrometry analysis was used to measure changes in phosphorylation at specific Npr1 residues for pair wise comparisons of rapamycin-treated WT cells versus mock-treated WT cells (D) or mock-treated WT cells versus cycloheximide -treated WT cells (E). Bars are color-coded to reflect the position of the phosphosites in the Npr1 protein (as indicated in C). The y-axis values represent the Log_2 of the Xpress (H:L) ratio, a quantitative measure of isotopic representation. Western blots showing phosphoshifts as resolved by SDS-PAGE are shown in the upper right of each profiling experiment. (F) Functional analysis was performed using N-terminal truncation of Npr1 *(Δ40-360*) deleted for the key phosphocluster observed in D and E. (G) The N-terminal truncation of Npr1 *(Δ40-360*) was tested for the ability to complement Art1 phosphorylation. Alanine substitution mutant alleles (H) and phosphomimetic substitution alleles (I) of Art1 were analyzed for growth in the presence of canavanine. Labels correspond to the following substitution mutations.

5xA: S79, 82-85A. 7xA: S79, 82-85, 92, 93A. 10xA: S79, 82-85, 92, 93, 96, 99, 100A.

5xD: S79, 82-85D. 8xD: S79, 82-85, 92, 93, 96D. 9xD: S79, 82-85, 92, 93, 96, 113D.

essential for Npr1-mediated regulation of endocytosis.

To address the function of the Art1 N-terminal phosphocluster, we analyzed the effect of alanine (phospho-dead) or aspartic acid (phospho-mimetic) substitutions at these residues. Interestingly, we found that no single site substitution had a significant effect on Art1 function. However, we observed dramatic changes in Art1 function when multiple phosphosites were mutated. For example, multiple alanine substitutions at N-terminal phosphosites of Art1 led to a striking canavanine resistance phenotype (Figure 2.8H), similar to that observed with *Δnpr1* cells. Additionally, multiple aspartic acid substitutions at N-terminal phosphosites resulted in canavanine hypersensitivity (Figure 2.8I), indicating Art1 is stuck in an inhibited, phosphomimetic state. These results indicate that (1) Npr1 mediates the phosphorylation of a distinct cluster of residues at the N-terminus of Art1, (2) phosphorylation of these N-terminal residues inhibits Art1-mediated Can1 endocytosis, and (3) dephosphorylation of these residues results in activation of Art1-mediated Can1 endocytosis. Thus, the N-terminal phosphocluster of Art1 is a critical feature of the regulated endocytosis of Can1.

N-terminal Phosphorylation Antagonizes Art1 PM Recruitment

We next investigated how N-terminal phosphorylation of Art1 inhibits Can1 endocytosis. First, we considered the possibility that N-terminal phosphorylation could lower the affinity of Art1 for Rsp5, however our quantitative mass spectrometry results indicated that changes in Art1 phospho-status do not affect its interaction with Rsp5 (Figure 2.9A).

Previously, we showed that GFP-tagged Art1 in unstimulated wildtype cells localizes to the cytosol, Golgi and plasma membrane (Figure 2.9B, top panels) and cycloheximide-induced activation of endocytosis results in translocation of Art1 to the PM (Figure 2.9C, top panels) (Lin et al., 2008). Interestingly, we found that cycloheximide-induced PM recruitment of Art1 was blocked by addition of rapamycin (Figure 2.9C, bottom panels), and that wildtype cells treated with rapamycin exhibited less Art1-GFP at the plasma membrane compared to untreated cells (Figure 2.9B, bottom panels). Since these treatments "toggle" Art1 between phosphorylated and dephosphorylated states, the effect of rapamycin and cycloheximide on Art1 localization suggested that N-terminal phosphorylation may regulate Art1 recruitment to the plasma membrane.

To further explore this possibility, we mixed wildtype cells (marked with Sec7-Mars) and *Δnpr1* cells both expressing Art1-GFP. We treated this mixed culture with rapamycin, so that Art1 in wildtype cells would be hyperphosphorylated and Art1 in *Δnpr1* cells would be hypophosphorylated (Figure 2.9D inset). Interestingly, when we analyzed Art1-GFP distribution in the mixed culture, we found that hyperphosphorylated Art1 in the wildtype cells was localized primarily to the cytosol and Golgi, while hypophosphorylated Art1 in the *Δnpr1* cells accumulated extensively at the plasma membrane (Figure 2.9D and 2.9F). Furthermore, we found that alanine substitution at the N-terminal phosphosites resulted in increased PM recruitment even after treatment of cells with rapamycin (Figure 2.9E and 2.9F).

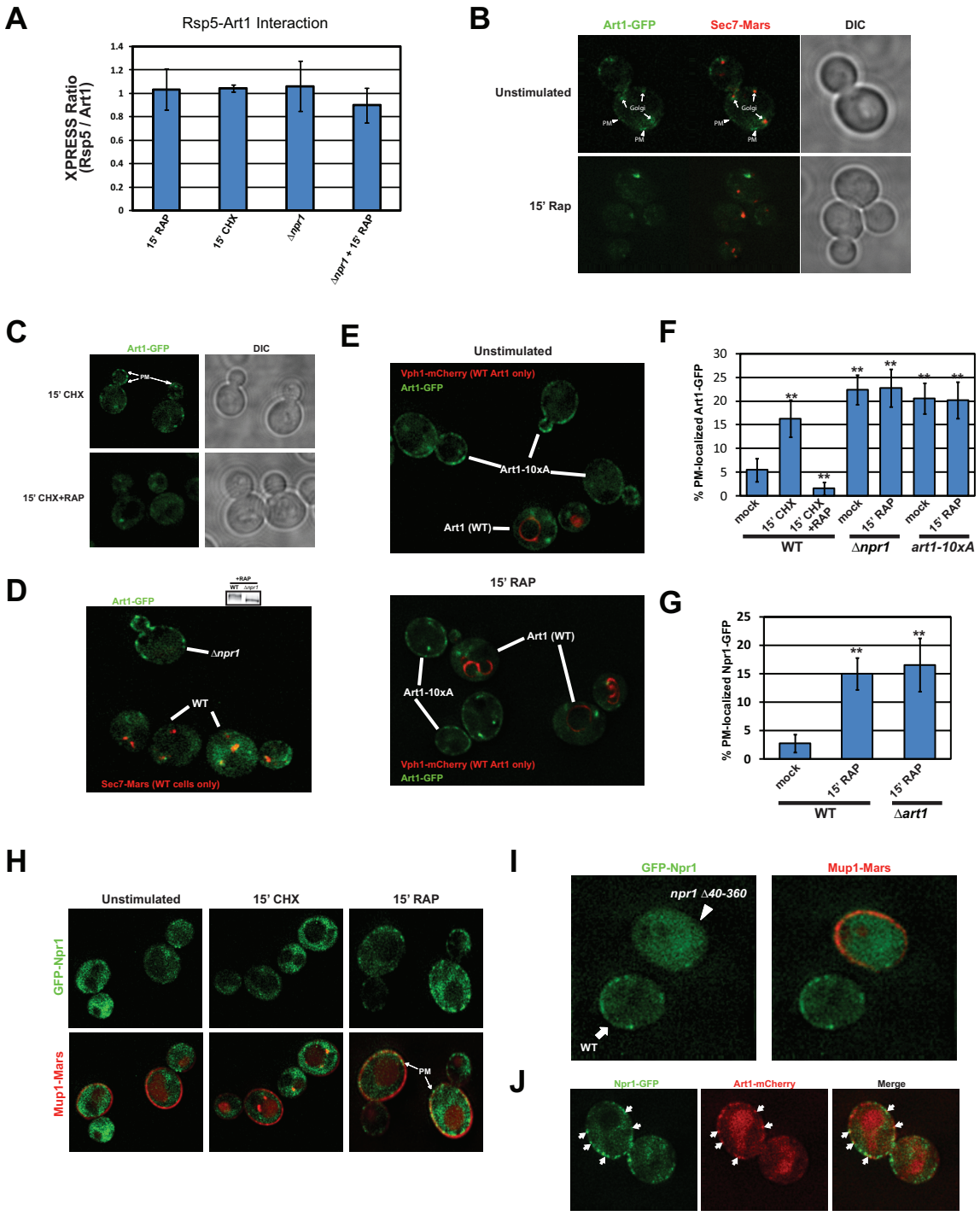
A
Rsp5-Art1 Interaction
XPRESS Ratio (Rsp5 / Art1)
15' RAP
15' CHX
Δnpr1
Δnpr1 + 15' RAP
B
Art1-GFP
Sec7-Mars
DIC
Unstimulated
15' Rap
C
Art1-GFP
DIC
15' CHX
15' CHX+RAP
D
Art1-GFP
Δnpr1
WT
Sec7-Mars (WT cells only)
E
Unstimulated
Vph1-mCherry (WT Art1 only)
Art1-GFP
Art1-10xA
Art1 (WT)
15' RAP
F
% PM-localized Art1-GFP
mock
15' CHX
15' CHX +RAP
15' RAP
WT
Δnpr1
art1-10xA
G
% PM-localized Npr1-GFP
WT
Δart1
H
Unstimulated
15' CHX
15' RAP
GFP-Npr1
Mup1-Mars
I
GFP-Npr1
Mup1-Mars
npr1 Δ40-360
WT
J
Npr1-GFP
Art1-mCherry
Merge

Figure 2-9

Figure 2.9. Art1 phosphorylation inhibits PM recruitment (A) Quantitative mass spectrometry (SILAC) was used to monitor changes in the interaction of Art1 with Rsp5 in *Δnpr1* mutant cells (compared to wildtype cells) or in response to treatment with rapamycin (200ng/mL for 15 minutes) or cycloheximide (50 μg/mL for 15 minutes) compared to mock treatment. XPRESS ratio represents the average H:L ratio of Rsp5 peptides, normalized to the average H:L ratio of Art1 peptides within each experiment. (B) Wildtype yeast cells expressing Art1-GFP (green) and Sec7-Mars (red) were analyzed by fluorescence microscopy. (C) Subcellular localization of Art1-GFP (green) was determined using fluorescence microscopy imaging of wildtype yeast cells. Cells were either treated with cycloheximide ("CHX") or co-treated with cycloheximide and rapamycin ("CHX+RAP"). (D) Wildtype yeast cells (labeled with Sec7-Mars (red)) or Δ*npr1* cells expressing Art1-GFP were mixed and treated with rapamycin (200 ng/mL for 15 minutes) and Art1 subcellular localization was analyzed using fluorescence microscopy. The inset is a Western blot demonstrating the phospho-status of Art1 in each condition. (E) Wildtype yeast cells expressing wildtype Art1-GFP (labeled with Vph1-mCherry (red)) or the N-terminal alanine substitution mutant (art1-8xA) were analyzed by fluorescence microscopy following mock (top panel) or rapamycin (bottom panel) treatment. (F) Art1-GFP PM localization was quantified (n=40 cells). Results are normalized to the percent PM localized Art1 from wildtype cells treated with rapamycin, a condition where we do not see Art1 PM recruitment. (G) GFP-Npr1 (green) subcellular localization was analyzed by fluorescence microscopy following mock, cycloheximide, or rapamycin treatments in wildtype yeast cells expressing Mup1-

Mars (red) to label the PM. (H) Npr1 PM localization was quantified (n=40 cells). Results are normalized to the percent PM localized Npr1 from wildtype cells treated with cycloheximide, a condition where we do not see Npr1 PM recruitment. (I) Cells expressing wildtype GFP-Npr1 (green) or GFP-*npr1*Δ*40-360* (green) were mixed and treated with rapamycin (200ng/mL for 15 minutes) prior to imaging by fluorescence microscopy. Cells expressing GFP-*npr1*Δ*40-360* were also expressing Mup1-Mars (red), a plasma membrane marker. (J) Wildtype yeast cells expressing Npr1-GFP and Art1-mCherry were grown to mid-log phase in the presence of methionine and treated with rapamycin (200 ng/mL for 5 minutes). Both Npr1 and Art1 subcellular localization was determined using fluorescence microscopy imaging. ** indicated $P < 0.005$.

To determine where in the cell Npr1 might phosphorylate Art1, we analyzed the subcellular localization of GFP-Npr1 and found that in unstimulated or cycloheximide-treated cells Npr1 was exclusively cytosolic (Figure 2.9G, left and middle panels). In contrast, treatment of cells with rapamycin resulted in the PM recruitment of GFP-Npr1 (Figure 2.9G, right panels, 2.9H, and 2.9I). To test the possibility that Art1 and Npr1 interact on the plasma membrane, we performed fluorescence co-localization microscopy using Art1-mCherry and GFP-Npr1. Interestingly, when cells were treated with rapamycin to trigger Npr1 PM recruitment, we observed co-localization of GFP-Npr1 punctae with Art1-mCherry punctae at the plasma membrane (Figure 2.9J). Although the co-localization we observed was limited, this result is consistent with a transient association of Npr1 with Art1 at the plasma membrane, whereby phosphorylation of Art1 limits its PM association.

DISCUSSION

We have uncovered an effector pathway downstream of TORC1 that regulates the composition of proteins at the PM by controlling endocytosis. Specifically, we show that (i) TORC1 signaling regulates ubiquitin ligase targeting and endocytosis of nutrient transporters at the PM, (ii) the effector mechanism that regulates endocytosis involves a TORC1-Npr1 negative kinase signaling cascade that tunes the phosphoinhibition of the ubiquitin ligase adaptor Art1, and (iii) the inhibition of Art1 requires phosphorylation at an N-terminal cluster of residues that control Art1 translocation to the PM (Figure 2.10). These findings establish a unique effector branch of the TORC1 signaling pathway that allows the cell to coordinate the activity of nutrient transporters at the PM as part of a global cellular strategy to regulate cell growth (Figure 2.10).

A Global Strategy for Regulating Endocytosis

The role of TORC1 as a regulator of ubiquitin-mediated endocytosis is intriguing because it demonstrates how diverse environmental and nutritional cues such as amino acid availability, energy status, and protein folding stress can affect changes in the abundance of proteins at the cell surface. In contrast to this global mode of TORC1-mediated endocytosis, many well-studied systems of endocytic downregulation involve specific targeting mechanisms, exemplified by the endocytosis-mediated attenuation of activated cell surface receptors such as EGFR and GPCRs in mammalian cells. The results presented in this study demonstrate that nutrient transporters in yeast are subject to both global signals mediated by

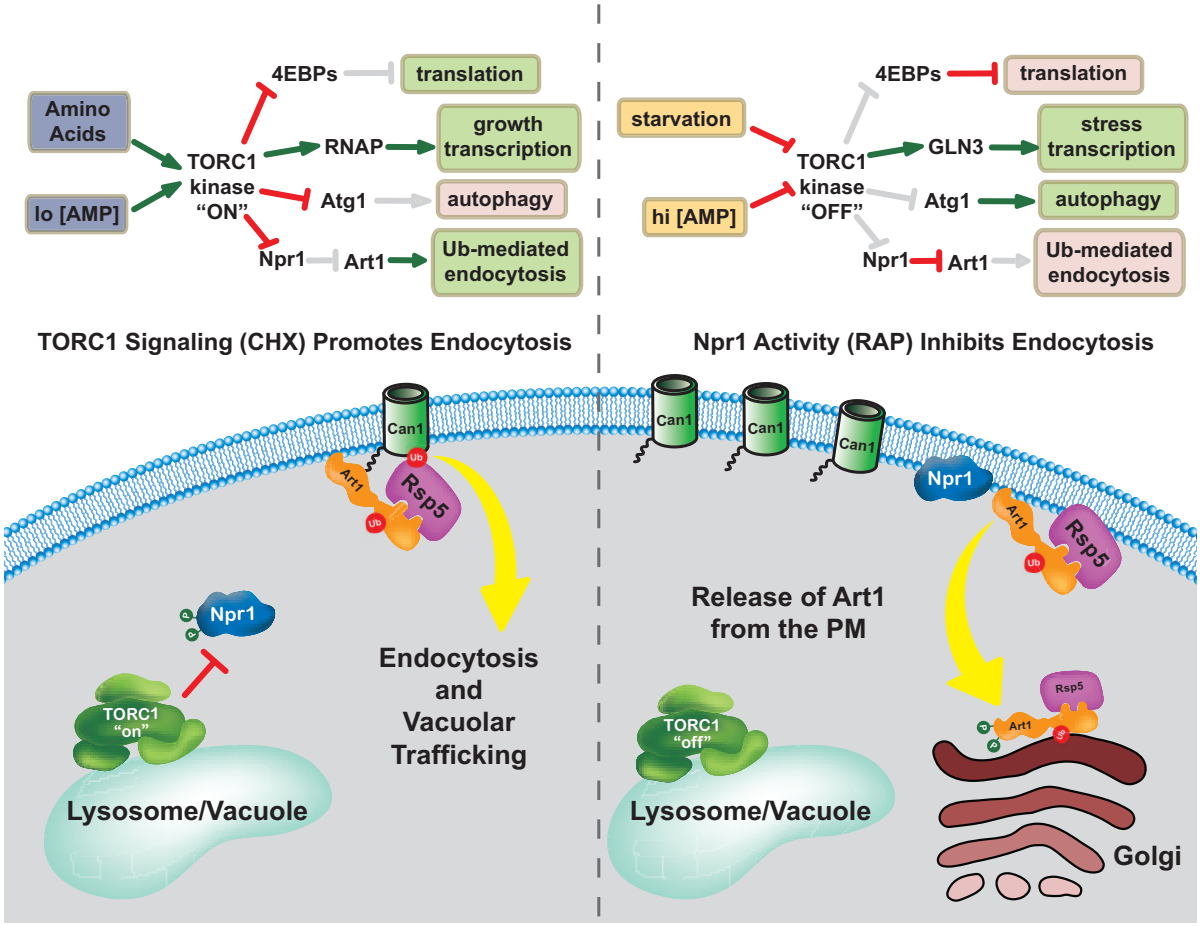
Amino Acids
lo [AMP]
TORC1 kinase "ON"
4EBPs
translation
RNAP
growth transcription
Atg1
autophagy
Npr1
Art1
Ub-mediated endocytosis
TORC1 Signaling (CHX) Promotes Endocytosis
starvation
hi [AMP]
TORC1 kinase "OFF"
4EBPs
translation
GLN3
stress transcription
Atg1
autophagy
Npr1
Art1
Ub-mediated endocytosis
Npr1 Activity (RAP) Inhibits Endocytosis
Can1
Art1
Rsp5
Ub
Npr1
TORC1 "on"
Lysosome/Vacuole
Endocytosis and Vacuolar Trafficking
Release of Art1 from the PM
TORC1 "off"
Lysosome/Vacuole
Golgi

Figure 2-10

Figure 2.10. A mechanism for TORC1 regulation of endocytosis. When TORC signaling is "on" (left panel), Npr1 is phosphoinhibited which promotes endocytosis of specific transporters by promoting Art1-Rsp5 translocation to the PM. When TORC1 signaling is "off" (right panel), as occurs during rapamycin treatment or starvation conditions, Npr1 is active and can phosphorylate Art1, an inhibited state that favors Golgi and cytosol localization. This novel effector mechanism allows TORC1 to modulate ubiquitin-mediated endocytosis and provides new insights into TORC1-mediated coordination of diverse cellular processes to achieve growth control (top diagrams). Gray arrows and bars indicate the release of a regulatory interaction due to upstream regulatory effects in the pathway.

TORC1 and specific signals that are substrate-dependent. Although these global and specific pathways operate independently in response to distinct cues (Figure 2.1D and S1), they converge on the same molecular mechanism of control by regulating the function of ubiquitin ligase adaptors (Figure 2.1F). This sort of signal integration allows TORC1 to bypass specific mechanisms of endocytic downregulation, adding a substrate-independent layer of endocytic control that is sensitive to the growth conditions of the cell.

Proteome-wide analysis of phosphorylation in yeast has demonstrated that ART family proteins are extensively phosphorylated (Albuquerque et al., 2008) and one recent study demonstrated that Npr1 can phosphorylate Art3 *in vitro*, although the functional significance of this modification remains unclear (O'Donnell et al., 2010). Interestingly, Art3 was recently shown to regulate the ubiquitination and endocytosis of the aspartic acid transporter Dip5 (Hatakeyama et al., 2010). We speculate that Npr1 could negatively regulate the endocytosis of Dip5 via phosphoinhibition of Art3, similar to its role as a negative regulator of Art1. Our phosphoprofiling experiments (Figure 2.7I) reveal that, while most ART phosphopeptides detected appeared to be Npr1-independent, Npr1-dependent phosphorylation events were detected in Art2 and Art3. Whether or not these phosphorylation events regulate endocytosis remains to be elucidated, but it seems likely given that both Art2 and Art3 have been shown to function in the endocytosis of specific cargoes (Hatakeyama et al., 2010; Lin et al., 2008). Furthermore, it is conceivable that other signaling pathways may similarly affect PM protein composition by regulating the activity of other ART family proteins.

A parallel strategy in mammalian cells might involve the family of uncharacterized arrestin-domain containing (ARRDC) proteins, which exhibit a domain structure similar to ART family proteins with N-terminal arrestin domains and C-terminal PY motifs. One mammalian ARRD family protein, ARRDC3, was recently shown to associate with the Nedd4 ubiquitin ligase and mediate the endocytic downregulation of β2-adrenergic receptor (Nabhan et al., 2010). It is tempting to speculate that mammalian ARRD family proteins may be subject to regulation by mTORC1 signaling, thus providing an mTORC1 effector branch analogous to the one presented in this study. Interestingly, mammalian β-arrestins are subject to a regulatory cycle that involves phosphoinhibition and activation by dephosphorylation (Lin et al., 2002), however further study will be required to determine the extent to which TORC1 signaling regulates the function of arrestin-related proteins in mammalian cells.

The Npr1 Kinase Links Nutrient Sensing to Endocytosis

Previous studies have suggested a role for Npr1 in the trafficking of amino acid transporters, however a consensus role for Npr1 has been elusive. For example, one study presents evidence that the Npr1 kinase promotes endocytosis of the tryptophan transporter TAT2 (Schmidt et al., 1998). In contrast, other studies have provided evidence that the Npr1 kinase functions to stabilize transporters at the plasma membrane (De Craene et al., 2001). Our analysis demonstrates that Npr1 stabilizes the arginine transporter Can1 at the plasma membrane by antagonizing the function of Art1. Interestingly, the phosphoproteomic data presented in this paper (Table 1) may actually reconcile the seemingly

contradictory reports regarding the role of Npr1 with respect to endocytosis. For example, although our results demonstrate that Npr1 negatively regulates endocytosis via phosphoinhibition of Art1, we also found several candidate Npr1 substrates that were plasma membrane-localized nutrient transporters. This result, combined with our observation that active Npr1 is recruited to the PM, suggests that Npr1 may phosphorylate both Art1 and transporters at the PM. The consequence of cargo phosphorylation is unclear but we speculate that this may either regulate transporter activity or promote endocytosis. Thus, a better understanding of Npr1-mediated phosphorylation of nutrient transporters at the PM may help to resolve some of the contradictory reports regarding the role of Npr1 as a regulator of endocytosis.

The Npr1 kinase represents an important mediator of TORC1 control of endocytosis in yeast, but the existence of an analogous pathway in mammalian cells is unclear. Although Npr1 has no obvious homolog in human cells, it is part of a large family of kinases that includes the glucose-sensing kinase Snf1, the yeast homolog of the mammalian AMP-activated kinase. We speculate that the family of AMPK/Snf1-related kinases in both yeast and mammals may have evolved as sensors of nutrient availability that regulate growth responses including endocytosis and membrane traffic. Consistent with our observation that part of this response may involve regulation of endocytosis, Snf1 was shown to phosphorylate the arrestin-related protein Art4 (Shinoda and Kikuchi, 2007) and related kinases Hal4 and Hal5 have been implicated in stabilizing potassium transporters at the plasma membrane by an unknown mechanism (Pérez-Valle et al., 2007). Although it

remains to be seen if mTORC1 regulates endocytosis in mammalian cells, we speculate that such regulation could involve effectors which include AMPK/Snf1-related kinases.

REFERENCES

Albuquerque, C., Smolka, M., Payne, S., Bafna, V., Eng, J., and Zhou, H. (2008). A multidimensional chromatography technology for in-depth phosphoproteome analysis. Mol Cell Proteomics *7*, 1389-1396.

Binda, M., Peli-Gulli, M.P., Bonfils, G., Panchaud, N., Urban, J., Sturgill, T.W., Loewith, R., and De Virgilio, C. (2009). The Vam6 GEF controls TORC1 by activating the EGO complex. Mol Cell *35*, 563-573.

Bonenfant, D., Schmelzle, T., Jacinto, E., Crespo, J.L., Mini, T., Hall, M.N., and Jenoe, P. (2003). Quantitation of changes in protein phosphorylation: a simple method based on stable isotope labeling and mass spectrometry. Proc Natl Acad Sci U S A *100*, 880-885.

Breitkreutz, A., Choi, H., Sharom, J., Boucher, L., Neduva, V., Larsen, B., Lin, Z., Breitkreutz, B., Stark, C., Liu, G.*, et al.* (2010). A global protein kinase and phosphatase interaction network in yeast. Science *328*, 1043-1046.

De Craene, J., Soetens, O., and Andre, B. (2001). The Npr1 kinase controls biosynthetic and endocytic sorting of the yeast Gap1 permease. J Biol Chem, 43939-43948.

Gander, S., Bonenfant, D., Altermatt, P., Martin, D., Hauri, S., Moes, S., Hall, M., and Jenoe, P. (2008). Identification of the rapamycin-sensitive phosphorylation sites within the Ser/Thr-rich domain of the yeast Npr1 protein kinase. Rapid Commun Mass Spectrom *22*, 3743-3753.

Gander, S., Martin, D., Hauri, S., Moes, S., Poletto, G., Pagano, M., Marin, O., Meggio, F., and Jenoe, P. (2009). A modified KESTREL search reveals a basophilic substrate

consensus for the Saccharomyces cerevisiae Npr1 protein kinase. J Proteome Res *8*, 5305-5316.

Hatakeyama, R., Kamiya, M., Takahara, T., and Maeda, T. (2010). Endocytosis of the aspartic acid/glutamic acid transporter Dip5 is triggered by substrate-dependent recruitment of the Rsp5 ubiquitin ligase via the arrestin-like protein Aly2. Mol Cell Biol.

Holz, M.K., Ballif, B.A., Gygi, S.P., and Blenis, J. (2005a). mTOR and S6K1 mediate assembly of the translation preinitiation complex through dynamic protein interchange and ordered phosphorylation events. Cell *123*, 569-580.

Holz, M.K., Ballif, B.A., Gygi, S.P., and Blenis, J. (2005b). mTOR and S6K1 mediate assembly of the translation preinitiation complex through dynamic protein interchange and ordered phosphorylation events. Cell *123*, 569-580.

Inoki, K., Li, Y., Zhu, T., Wu, J., and Guan, K.L. (2002). TSC2 is phosphorylated and inhibited by Akt and suppresses mTOR signalling. Nat Cell Biol *4*, 648-657.

Inoki, K., Zhu, T., and Guan, K.L. (2003). TSC2 mediates cellular energy response to control cell growth and survival. Cell *115*, 577-590.

Jacinto, E., Guo, B., Arndt, K.T., Schmelzle, T., and Hall, M.N. (2001). TIP41 interacts with TAP42 and negatively regulates the TOR signaling pathway. Mol Cell *8*, 1017-1026.

Kamada, Y., Yoshino, K., Kondo, C., Kawamata, T., Oshiro, N., Yonezawa, K., and Ohsumi, Y. (2010). Tor directly controls the Atg1 kinase complex to regulate autophagy. Mol Cell Biol *30*, 1049-1058.

Lin, C., MacGurn, J., Chu, T., Stefan, C., and Emr, S. (2008). Arrestin-related ubiquitin-ligase adaptors regulate endocytosis and protein turnover at the cell surface. Cell *135*, 714-725.

Lin, F., Chen, W., Shenoy, S., Cong, M., Exum, S., and Lefkowitz, R. (2002). Phosphorylation of beta-arrestin2 regulates its function in internalization of beta(2)-adrenergic receptors. Biochemistry *41*, 10692-10699.

Manning, B.D., Tee, A.R., Logsdon, M.N., Blenis, J., and Cantley, L.C. (2002). Identification of the tuberous sclerosis complex-2 tumor suppressor gene product tuberin as a target of the phosphoinositide 3-kinase/akt pathway. Mol Cell *10*, 151-162.

Miranda, M., and Sorkin, A. (2007). Regulation of receptors and transporters by ubiquitination: new insights into surprisingly similar mechanisms. Mol Interv *7*, 157-167.

Nabhan, J.F., Pan, H., and Lu, Q. (2010). Arrestin domain-containing protein 3 recruits the NEDD4 E3 ligase to mediate ubiquitination of the [beta]2-adrenergic receptor. EMBO Rep *11*, 605-611.

O'Donnell, A., Apffel, A., Gardner, R., and Cyert, M. (2010). Alpha-arrestins Aly1 and Aly2 regulate intracellular trafficking in response to nutrient signaling. Mol Biol Cell *21*, 3552-3566.

Qian, S.B., Zhang, X., Sun, J., Bennink, J.R., Yewdell, J.W., and Patterson, C. (2010). mTORC1 links protein quality and quantity control by sensing chaperone availability. J Biol Chem *285*, 27385-27395.

Sancak, Y., Bar-Peled, L., Zoncu, R., Markhard, A.L., Nada, S., and Sabatini, D.M. (2010). Ragulator-Rag complex targets mTORC1 to the lysosomal surface and is necessary for its activation by amino acids. Cell *141*, 290-303.

Schmidt, A., Beck, T., Koller, A., Kunz, J., and Hall, M.N. (1998). The TOR nutrient signalling pathway phosphorylates NPR1 and inhibits turnover of the tryptophan permease. EMBO J *17*, 6924-6931.

Shinoda, J., and Kikuchi, Y. (2007). Rod1, an arrestin-related protein, is phosphorylated by Snf1-kinase in Saccharomyces cerevisiae. Biochem Biophys Res Commun *364*, 258-263.

Chapter 3

Ppz Phosphatases Regulate Endocytosis via Dephosphorylation of a Ubiquitin Ligase Adaptor

INTRODUCTION

Post-translational modification of proteins provides an efficient mechanism for regulation of protein activity (Chen et al., 1994; Cohen, 1989; Stark, 1996). Just as important is the reversibility of post-translational modifications, which facilitates regulation of proteins via regulatory cycles. In chapter 2, we demonstrated how Art1 activity is phospho-inhibited by the Npr1 kinase, which itself is ultimately controlled by signaling through TORC1 kinase. These results provide a mechanism for phosphoinhibition of Art1 and they demonstrate that Art1 activation is associated with dephosphorylation (Figure 2.6 A and B), however they do not address the mechanism of Art1 activation by dephosphorylation. Recently, it was reported that the activity of Art4/Rod1, another Rsp5 E3 ubiquitin ligase adaptor, can be mediated through a phospho-regulatory cycle (Becuwe et al., 2012). The Glc7/Reg1 phosphatase reverses the AMPK Snf1 kinase-mediated phospho-inhibition of Art4, triggering the endocytosis of a monocarboxylate transporter Jen1. Understanding Art1 activation will require the identification of the Art1 phosphatase(s) and dissection of their role in the Art1 phosphorylation cycle.

It has been reported that several phosphatases play important roles in regulating ubiquitination and endocytosis (Becuwe et al., 2012; Goebel-Goody et al., 2011; Smillie and Cousin, 2012). Here, we performed a phosphatase canavanine screen to identify potential Art1 phosphatases. The dephosphorylation of Art1

might through (1) a non-specific phosphatase activity (ie, massive redundancy) or (2) a specific phosphatase. For (1), we may not be able to identify any single phosphatase mutant showing a canavanine phenotype. However, for (2), several phosphatase mutants may show a canavanine phenotype. They include phosphatases that have been implicated in regulating endocytosis or phosphatases that localize at PM and/or Golgi, where Art1 localizes. As discussed in Chapter 2, the phosphatases in the TORC1 pathway upstream of Npr1 are also the phosphatases that regulate Art1 phosphorylation and activity. By doing this screen, we identified several phosphatases that might be involved in regulating of cargo endocytosis.

In this chapter, I will report two major findings of that contribute to our understanding of how cargo at the PM are targeted for ubiquitination and endocytosis: 1) Ppz phosphatases positively regulate ubiquitination and endocytosis of different cargoes in response to various stimulations; 2) The likely mechanism of this regulation involves dephosphorylation of Art1, an Rsp5 adaptor.

MATERIAL AND METHODS

Plasmids, Strains and Screening for Canavanine Phenotypes

All plasmids and yeast strains used in this study are listed in Table S1 and Table S2, respectively. Canavanine plating assays were performed as previously described (Lin et al., 2008). Briefly, yeast mutant cultures grown overnight in YPD were normalized to 1 OD/mL, serially diluted and plated onto SCD plates using a pin-frogger. The following concentrations of canavanine were tested in each experiment: 0 μg/mL, 0.6 μg/mL, 0.8 μg/mL, 1.0 μg/mL, 2.0 μg/mL, 4.0 μg/mL and 6.0 μg/mL.

Yeast Thialysine Plating Assays

Yeast cultures grown overnight in YPD were normalized to 1 OD/mL, serially diluted and plated onto SCD plates using a pin-frogger. The following concentrations of thialysine were tested in each experiment: 0 μg/mL, 1.0 μg/mL, 2.5 μg/mL, 5.0 μg/mL, and 10.0 μg/mL

Fluorescence Quenching Flow Cytometry Assays

This assay was modified from (Prosser et al.) by Nicholas Buchkovich. In brief, WT and mutant cells were grown at 26°C until midlog phase and stimulated by Methionine to trigger Mup1-pH endocytosis. The fluorescent intensity of each cell was measured by using flow cytometry every 3.5 minutes for 2.5 hours. The intensity gate for positive cells was set up according to the WT cells under unstimulated condition (around 99.5% of cells).

Mup1-HTF Ub Ladder Immunoblot

WT and mutant cells with chromosomal tagged Mup-HTF were grown at 26°C until midlog phase and treated with methionine. After stimulation for 0, 5, 10, and 20 minutes, cells were harvested and subjected to TCA precipitation. 0.1 OD of whole cell lysate in each sample was loaded to 10% SDS-PAGE and protein were imaged by Western blot by using α-FLAG (M2, Sigma) antibody.

Microscopy

All microscopy was performed using an Olympus IX71 microscopy equipped with FITC and rhodamine filters. Deconvolution and image analysis was performed using Softworx software (Applied Precision). For cargo trafficking assays, strains expressing chromosomally-tagged Vph1-mCherry were used to label the vacuolar membrane. Cells were grown at 26°C and either mock-treated or treated with cycloheximide (CHX) (50 μg/mL), and/or rapamycin (RAP) (200 ng/mL), and methionine prior to imaging cells. For screening potential endocytic phosphatase mutants, cells were grown at 30°C and without any stimulation prior to imaging cells. For Art1-GFP and Ppz1-MARS co-localization experiment, cells were stimulated with CHX for 30 minutes prior to imaging.

Additional related material and methods are the same as described in Chapter 2

RESULTS

Identification of Phosphatases that Regulate Trafficking of the Arginine Transporter Can1

Since the completion of the genome sequencing project of *Saccharomyces cerevisiae*, proteins in the budding yeast can be easily identified and grouped according to their enzymatic functions (Goffeau et al., 1996). Based on sequence analysis of the kinase and phosphatases catalytic domains, there are a total of 117 protein kinases and 32 protein phosphatases genes in the yeast genome (Sakumoto et al., 1999). Among these phospho-regulating proteins, there are 102 and 30 viable deletion kinase and phosphatase strains, respectively (Hirasaki et al., 2011; Sakumoto et al., 1999). To identify the potential phosphatases that regulate the endocytic pathway, we performed a canavanine screen for all the phosphatase null strains. According to our phospho-regulatory cycle proposed in Figure 2.4F, deletion of a *bona fide* Art1 phosphatase would exhibit a canavanine sensitive phenotype. Therefore, by taking a similar approach as our kinase screen, we took all the viable phosphatase disruptants from the BY4741 knockout collections and plated them on the canavanine plates to score for a canavanine sensitive phenotype. As Table 2 shows, 5 phosphatase deletion strains exhibited a canavanine sensitive phenotype while 6 disruptants exhibited a canavanine resistant phenotype. Of all the phosphatase mutants examined, Δ*ppz1* cells exhibited the most severe canavanine hypersensitivity, suggesting Ppz1 may play a role in Can1 endocytosis.

To further explore a possible role for these candidate phosphatases in

Table 2. Canavanine screen of budding yeast phosphatome. All the viable phosphatase mutants from the yeast deletion collection were plates on the canavanine plates (0, 0.6, 0.8, 1.0, 2.0, 4.0 and 6.0 μg/ml canavanine) to score Can1 endocytosis defect.

Ppase Family	Gene Name	Can. phenotype
PPP	PPH21	Can Res
	PPH22	Can Res
	PPG1	Can Sen
	PPQ1	Can Sen
	PPZ1	Can Sen
PPM	PTC1	Can Sen
	PTC4	Can Res
Protein Tyrosine	YVH1	Can Sen
	SIW14	Can Res
Others	OCA1	Can Res
	OCA2	Can Res

endocytosis, we examined Can1 trafficking in each phosphatase deletion strain exhibiting canavanine hypersensitivity. Can1-GFP was expressed in BY4741 WT cells as well as the phosphatase mutants and grown at 30°C instead of 26°C to increase the basal level of endocytosis. Cells were grown to midlog phase and imaged by fluorescence microscopy to score Can1 endocytosis and vacuolar trafficking (Figure 3.1A). In WT cells, some Can1 localized at PM, however, a significant fraction of the GFP signal localized to the vacuole, consistent with vacuolar trafficking and degradation in response to heat stress (Figure 3.1A, top left panel). Phosphatase mutants Δ*ppq1*, Δ*ptc1* and Δ*ppg1*, exhibited Can1 trafficking pattern indistinguishable from WT cells, suggesting these phosphatases are not required for Can1 endocytosis. Interestingly, Can1 endocytosis was blocked in two phosphatase mutants, Δ*ppz1* and Δ*yvh1* (Figure 3.1A, bottom middle and bottom right, respectively). However, unlike the strong PM localized Can1-GFP signal in Δ*ppz1* mutants, there were several early endosome-like Can1-GFP accumulation in Δ*yvh1* mutants, suggesting Yvh1 may function at early endosome maturation process rather than early endocytosis. This result is consistent with a possible role for the Ppz1 phosphatase as a positive regulator of Can1 endocytosis.

Ppz Phosphatases Positively Regulate Cargo Endocytosis

The PP1 family phosphatases Ppz1 and Ppz2 are two homologous Ser/Thr protein phosphatases (Sakumoto et al., 2002; Sakumoto et al., 1999). Deletion of PPZ1 gene causes temperature and caffeine sensitive phenotypes while deletion of PPZ2 gene alone has no significant phenotypes. However, the phenotypes can be

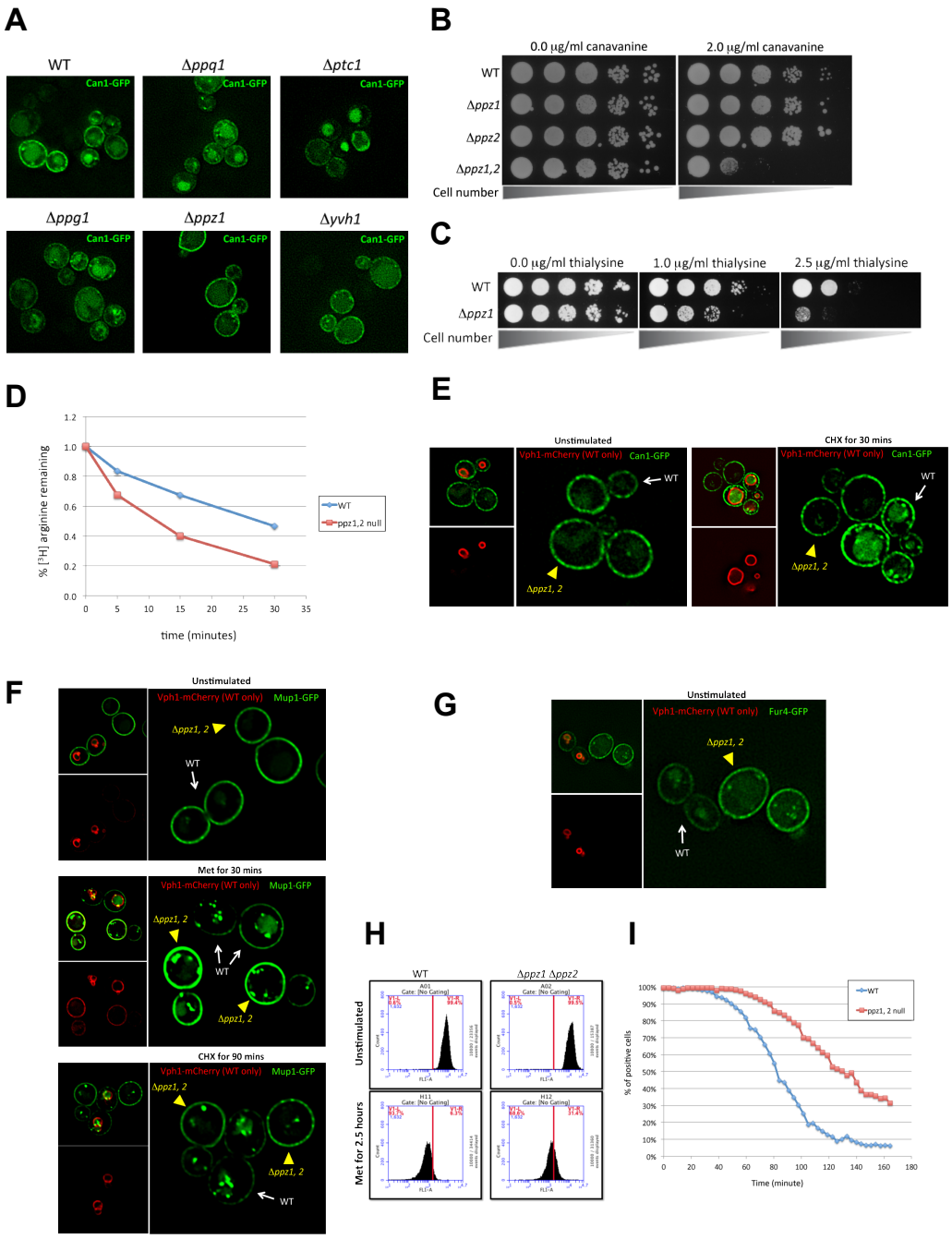
A
WT
Δppq1
Δptc1
Δppg1
Δppz1
Δyvh1
Can1-GFP
B
0.0 μg/ml canavanine
2.0 μg/ml canavanine
WT
Δppz1
Δppz2
Δppz1,2
Cell number
C
0.0 μg/ml thialysine
1.0 μg/ml thialysine
2.5 μg/ml thialysine
WT
Δppz1
Cell number
D
% [3H] arginine remaining
time (minutes)
WT
ppz1,2 null
E
Unstimulated
CHX for 30 mins
Vph1-mCherry (WT only)
Can1-GFP
WT
Δppz1, 2
F
Unstimulated
Met for 30 mins
CHX for 90 mins
Vph1-mCherry (WT only)
Mup1-GFP
Δppz1, 2
WT
G
Unstimulated
Vph1-mCherry (WT only)
Fur4-GFP
Δppz1, 2
WT
H
WT
Δppz1 Δppz2
Unstimulated
Met for 2.5 hours
I
% of positive cells
Time (minute)
WT
ppz1, 2 null

Figure 3-1

Figure 3.1. Ppz1 and Ppz2 phosphatases positively regulate endocytosis of different plasma membrane proteins (A) WT (background BY4741) cells, as well as potential endocytic phosphatase (Ppq1, Ptc1, Ppg1, Ppz1 and Yvh1) mutants from the yeast deletion collection were transformed by Can1-GFP to score for Can1 endocytosis defect. Cells were cultured at 30°C to increase the basal level of endocytosis and grown to midlog phase, and were subjected to microscopy imaging. (B) WT (background SEY6210) cells and Δ*ppz1*Δ*ppz2* double phosphatases knockouts were plated on canavanine plates to score for Can1 endocytosis defect. (C) WT (background BY4741) cells and Ppz1 phosphatase mutant from the yeast deletion collection were plated on thialysine plates to score for Lyp1 endocytosis defect. (D) WT (blue) and Δ*ppz1*Δ*ppz2* (red) cells were grown to midlog phase and subjected to [^{3}H] arginine. Samples were collected at 5, 15, and 30 minute time points. (E) Can1-GFP was imaged in WT cells (with chromosomal tagged Vph1-mCherry) and Δ*ppz1*Δ*ppz2* cells under unstimulated (left panel) and 30 minutes of cycloheximide (50 μg/ml) treatment (right panel) conditions. (F) Mup1-GFP was imaged in WT cells (with chromosomal tagged Vph1-mCherry) and Δ*ppz1*Δ*ppz2* cells under unstimulated (upper panel), 30 minutes of methionine treatment (middle panel) and 90 minutes of cycloheximide (50 μg/ml) treatment (lower panel) conditions. (G) Fur4-GFP was imaged in WT cells (with chromosomal tagged Vph1-mCherry) and Δ*ppz1*Δ*ppz2* cells under unstimulated condition. (H) Mup1-pHluorin was chromosomal tagged in both WT cells and Δ*ppz1*Δ*ppz2* mutants. After growing to midlog phase, WT cells and mutants were subjected to the flow cytometry and counted for fluorescent positive cells under unstimulated (upper panels) and

methionine stimulated (lower panels) conditions. (I) Cells from Figure 3.1(H) were stimulated by methionine and collected in every 3.5 minutes for a total of 2.5 hours. The percentage of fluorescent positive cells was counted by flow cytometry at every time point.

intensified by deleting both PPZ genes, suggesting a partial functional redundancy of these two phosphatases (Sakumoto et al., 2002). Ppz phosphatases have been reported to be negative regulators for the potassium transporters Trk1 and Trk2 (Merchan et al., 2010), which are regulators of salt tolerance and pH homeostasis in the cells (Mulet et al., 1999; Posas et al., 1995; Yenush et al., 2002). It has been shown that the Hal4 and Hal5 kinases, which have high sequence similarities to Npr1 kinase, activate Trk transporters by antagonizing Ppz phosphatases activity (Mulet et al., 1999). This data suggests that Npr1 and Ppz phosphatases may function together to control plasma membrane cargos activities via Art1, and/or other Ub ligase adaptors (other ARTs, Buls, etc.). Although Ppz phosphatases have been shown to regulate ion homeostasis and salt tolerance, identification of their downstream effectors and signaling pathways remains lacking.

To further characterize the trafficking function of Ppz1 phosphatase, we made a Δ*ppz1* strain in the SEY6210 background and tested for canavanine hypersensitivity. However, we did not observe a significant difference between WT cells and Δ*ppz1* single knockout mutants (Figure 3.1B, first two rows). Since functional redundancy between Ppz1 and Ppz2 phosphatases has been reported (Sakumoto et al., 2002), we tested whether the double knockout is sensitive to canavanine. As shown in Figure 3.1B, the Δ*ppz1*Δ*ppz2* mutant is hypersensitive to canavanine while neither single mutant shows a canavanine sensitive phenotype, suggesting functional redundancy between these two phosphatases in the SEY6210 background. To further analyze whether Ppz phosphatases regulate endocytosis of additional cargo molecules, we tested the endocytosis of the lysine permease Lyp1

in the Δ*ppz1* mutant by plating it together with the BY4741 WT cells in the presence of thialysine, a toxic lysine analog (Figure 3.1C). Similar to the canavanine plating results, the Δ*ppz1* mutant showed a thialysine hypersensitive phenotype, suggesting Ppz phosphatases are involved in regulating the endocytosis of Lyp1. We further confirmed our canavanine plating results by directly measuring Can1 amino acid transporting ability. By using an assay to quantify arginine uptake, we tested Can1 transport function in Ppz phosphatases mutant (Figure 3.1D). We found that arginine uptake is faster in Δ*ppz1*Δ*ppz2* double mutant cells compared to WT cells, consistent with Can1 accumulation at the PM in Δ*ppz1*Δ*ppz2* mutant cells.

To further explore the role of Ppz phosphatases in stimulus-triggered endocytosis, Can1-GFP was imaged in WT (chromosomal tagged with Vph1-mCherry) and Δ*ppz1*Δ*ppz2* cells following 30 minutes of cycloheximide (CHX) treatment (Figure 3.1E). Can1-GFP localized to the PM in both WT and Δ*ppz1*Δ*ppz2* cells in the absence of any stimulation. However, CHX stimulation triggers significant vacuolar Can1-GFPsignal in WT cells compared to mutants, suggesting Ppz phosphatases are required for stimuli-mediated Can1 endocytosis. In addition, methionine-stimulated Mup1 endocytosis was also defective in Δ*ppz1*Δ*ppz2* mutant cells (Figure 3.1F, top and middle panels). Moreover, the basal level of Fur4 endocytosis was blocked in Δ*ppz1* Δ*ppz2* mutant cells. These results suggest that Ppz phosphatases regulate the endocytosis of at least four different PM cargoes, including Can1, Lyp1, Mup1 and Fur4.

We wanted to determine if the trafficking defect in Δ*ppz1*Δ*ppz2* mutant cells is a block or a kinetic delay of cargo endocytosis. To distinguish between these

possibilities and to better understand the kinetics of cargo degradation in Ppz phosphatase mutant, we performed flow cytometry analysis of cells expressing Mup1 tagged with superecliptic pHluorin (Mup1-pH) to monitor cargo delivery to the vacuole, as measured by fluorescence quenching (Prosser et al.). Upon methionine stimulation, Mup1-pH traffics to the vacuole (pH ~6.2) where the fluorescence of superecliptic pHluorin is quenched. We grew WT and Δ*ppz1*Δ*ppz2* cells with chromosomal tagged Mup1-pH to midlog phase and subjected them to the flow cytometry to score for the fluorescent positive cells (Figure 3.1H). After 2.5 hours of methionine stimulation, only 6.3% of cells retain the fluorescent signal, while 31% of Δ*ppz1*Δ*ppz2* mutant cells were retained fluorescence. By collecting cell samples every 3.5 minutes post methionine stimulation, we found that the rate of Mup1-pH quenching is slower in the phosphatase mutant (Figure 3.1I). These results are consistent with the microscopy data and suggest that Ppz phosphatases regulate the endocytosis of several PM cargoes in response to different stimulation conditions.

Ppz phosphatases inhibitors Hal3 and Vhs3 Inhibit the Endocytosis of Different Plasma Membrane Amino Acid Transporters

Previous yeast genetic screens for genes involved in salt tolerance phenotypes identified both Ppz phosphatases as well as a complex of proteins (Hal3, Vhs3, and Cab3) that appears to negatively regulate Ppz phosphatase activity (de Nadal et al., 1998). Specifically, it has been reported that depletion of Ppz phosphatases resulted in increases salt tolerance, while depletion of Hal3 and Vhs3 results in decreased salt tolerance, suggesting that these proteins may antagonize Ppz phosphatases.

Recent work has demonstrated that Hal3 together with Vhs3 and Cab3 form a heteromeric complex (Ruiz et al., 2009). Hal3 binds to the C-terminal phosphatase catalytic domain of Ppz1 to inhibit its enzymatic activity (Munoz et al., 2004). Therefore, depletion of Hal3 or Vhs3 can be used to hyperactivate Ppz phosphatases (Hirasaki et al., 2011; Yenush et al., 2005). By using the canavanine plating assay in phosphatases inhibitors mutants, we tested whether hyper-activated Ppz1 and Ppz2 can trigger more Can1 endocytosis. As shown in Figure 3.2A, Δ*vhs3* and Δ*hal3* mutants showed a canavanine resistant phenotype, consistent with the previous studies that Vhs3 and Hal3 are negative regulators of Ppz phosphatases.

Based on our canavanine plating result of Δ*vhs3* and Δ*hal3* mutants, we hypothesized that Vhs3 and Hal3 are involved in the endocytic pathway as negative regulators of Ppz phosphatases. To test whether Vhs3 can regulate other cargo endocytosis, we plated Δ*vhs3* mutant together with the BY4741 WT cells on the thialysine plates. Consistent with the canavanine results, Δ*vhs3* mutant cells exhibited thialysine resistance (Figure 3.2B). Moreover, the endocytosis of Mup1 was examined by monitoring Mup1-GFP trafficking in cells lacking the inhibitory proteins. Mup1-GFP was imaged in the WT cells (chromosomal tagged with Vph1-mCheery) and both Δ*hal3* (Figure 3.2C) and Δ*vhs3* (Figure 3.2D) mutants under unstimulated condition. Mup1-GFP vacuolar localization was increased compared to the WT cells. Furthermore, the Mup1-GFP endocytosis was intensified in the Δ*vhs3*Δ*hal3* double disruptants (Figure 3.2E), which may indicate that both Hal3 and Vhs3 are important for Ppz phosphatases-mediated cargo endocytosis. Of note,

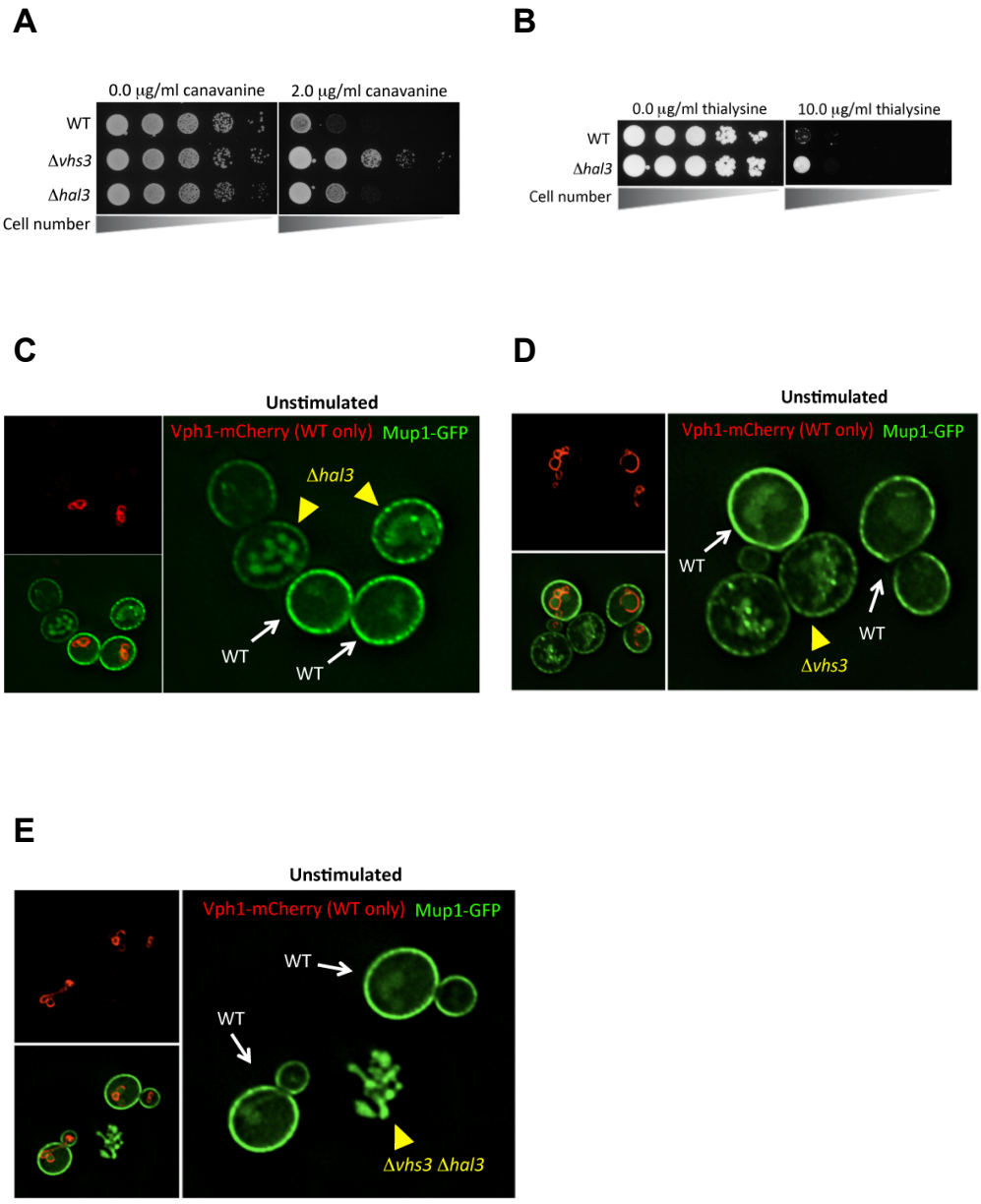
A
0.0 μg/ml canavanine
2.0 μg/ml canavanine
WT
Δvhs3
Δhal3
Cell number
B
0.0 μg/ml thialysine
10.0 μg/ml thialysine
WT
Δhal3
Cell number
C
Unstimulated
Vph1-mCherry (WT only) Mup1-GFP
Δhal3
WT
WT
D
Unstimulated
Vph1-mCherry (WT only) Mup1-GFP
WT
WT
Δvhs3
E
Unstimulated
Vph1-mCherry (WT only) Mup1-GFP
WT
WT
Δvhs3 Δhal3

Figure 3-2

Figure 3.2. Ppz1 and Ppz2 phosphatases inhibitors negatively regulate endocytosis of different plasma membrane proteins (A) WT (background SEY6210) cells and Ppz1 Ppz2 phosphatase inhibitor (Vsh3 and Hal3) mutants were plated on canavanine plates to score for Can1 endocytosis defect. (B) WT (background BY4741) cells and Ppz1 Ppz2 phosphatases inhibitor (Hal3) mutant from the yeast deletion collection were plated on thialysine plates to score for Lyp1 endocytosis defect. (C) Mup1-GFP was imaged in WT cells (with chromosomal tagged Vph1-mCherry) and Δ*hal3* cells under unstimulated condition. (D) Mup1-GFP was imaged in WT cells (with chromosomal tagged Vph1-mCherry) and Δ*vhs3* cells under unstimulated condition. (E) Mup1-GFP was imaged in WT cells (with chromosomal tagged Vph1-mCherry) and Δ*hal3* Δ*vhs3* cells under unstimulated condition.

the vacuole morphology is abnormal in Δ*vhs3*Δ*hal3* double disruptants. The increase in vacuolar Mup1-GFP signal could be a side effect of an unknown pathway. Further studies are required to address this issue.

Ppz Phosphatases Function in Regulating the Early Steps of Endocytic Pathway

To determine which step of the endocytic pathway is regulated by Ppz phosphatases, we tested each step of the endocytic pathway. First, vacuole morphology was analyzed in Ppz phosphatase mutants by using the FM4-64 staining (Figure 3.3A). There was no significant defect of vacuole morphology in Δ*ppz1*Δ*ppz2* mutants, which may suggest that endosomal sorting and vacuolar fusion are not affected. Second, by using GFP-CPS, we examined the MVB sorting in the Ppz phsophatases mutants. GFP-CPS was expressed and imaged in the WT cells (chromosomal tagged with Vph1-mCheery) and Δ*ppz1*Δ*ppz2* mutants under unstimulated condition (Figure 3.3B). In these cells, we did not observe E dot formation, a classic subcellular structure seen in the ESCRT mutants (Henne et al., 2011), suggesting Ppz phosphatases do not affect MVB sorting. Our data suggest that the Ppz phosphatases are not involved in regulating the late steps of endocytic pathway.

Next, we analyzed Mup1 degradation following methionine stimulation in the WT, Δ*ppz1*Δ*ppz2* and Δ*art1* mutant cells (Figure 3.3C). Importantly, degradation of Mup1 is blocked in Δ*ppz1*Δ*ppz2* and Δ*art1* mutant cells, consistent with the observed trafficking defect.

Finally, we wanted to determine if Ppz phosphatases play a role in cargo ubiquitination. Mup1-HTF was expressed and assayed by immunoblot in WT cells

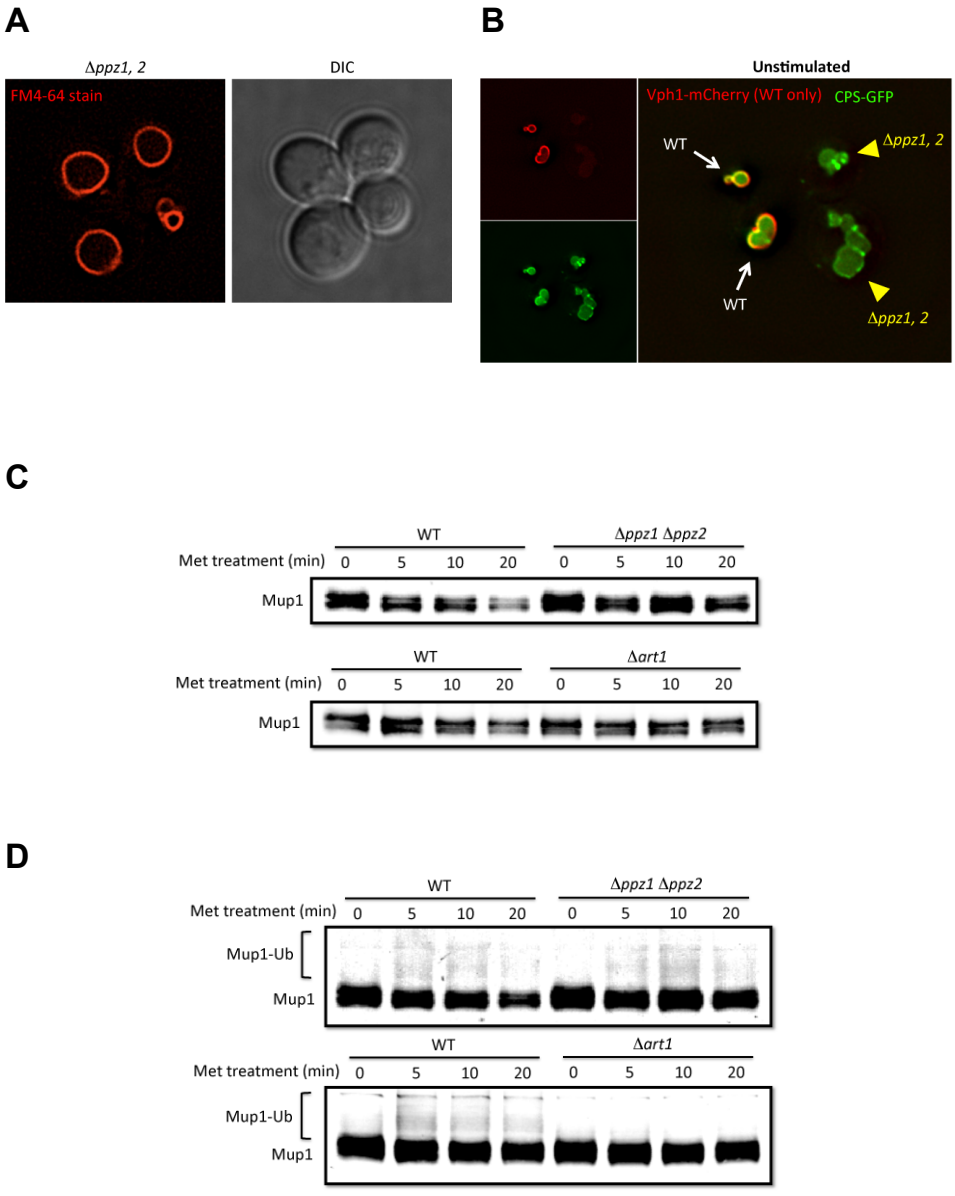
A
Δppz1, 2
DIC
FM4-64 stain
B
Unstimulated
Vph1-mCherry (WT only)
CPS-GFP
WT
Δppz1, 2
WT
Δppz1, 2
C
WT
Δppz1 Δppz2
Met treatment (min)
0
5
10
20
0
5
10
20
Mup1
WT
Δart1
Met treatment (min)
0
5
10
20
0
5
10
20
Mup1
D
WT
Δppz1 Δppz2
Met treatment (min)
0
5
10
20
0
5
10
20
Mup1-Ub
Mup1
WT
Δart1
Met treatment (min)
0
5
10
20
0
5
10
20
Mup1-Ub
Mup1

Figure 3-3

Figure 3.3. Ppz1 and Ppz2 phosphatases play roles in the early step of cargo endocytic pathway (A) Δ*ppz1*Δ*ppz2* cells were grown to midlog phase and subjected to vacuoles labeling by staining cells with FM4-64 for 1 hour. Vacuolar morphology was imaged by microscopy after staining and washing. (B) GFP-CPS vacuolar sorting was imaged in WT cells (with chromosomal tagged Vph1-mCherry) and Δ*ppz1*Δ*ppz2* cells under unstimulated condition. (C) Mup1-HTF degradation kinetics after methionine stimulation was measured by Western blot. WT, Δ*ppz1*Δ*ppz2* and Δ*art1* cells with chromosomal tagged Mup1-HTF were grown to midlog phase and subjected to methionine stimulation. Samples were collected at 0, 5, 10, and 20 minute time points. (D) Mup1-HTF ubiquitination kinetics after methionine stimulation was measured by Western blot. WT, Δ*ppz1*Δ*ppz2* and Δ*art1* cells with chromosomal tagged Mup1-HTF were grown to midlog phase and subjected to methionine stimulation. Samples were collected at 0, 5, 10, and 20 minute time points.

and Δ*ppz1*Δ*ppz2* and Δ*art1* (as negative controls) mutants in different time points after methionine stimulation (Figure 3.3D). Consistent with previous studies (Lin et al., 2008), Mup1-Ub is blocked in Δ*art1* mutant (Figure 3.3D, bottom panel). In Δ*ppz1*Δ*ppz2* mutant cells, Mup1ubiquitination following methionine stimulation was still observed, but ubiquitination appeared to be kinetically delayed (10 minutes) compared to WT cells (5 minutes). This data is consistent with our Mup-pH results in Figure 3.1I, which demonstrated a delay in Mup1 endocytosis. Taken together, these results suggest that Ppz phosphatases regulate early steps of the endocytic pathway, including cargo ubiquitination.

Ppz Phosphatases are Required for Art1-mediated Cargo Endocytosis

We hypothesized that Ppz phosphatases may function as upstream activators for Art1-mediated endocytosis. To test this hypothesis, we over-expressed Art1 in Δ*ppz1*Δ*ppz2* mutant cells to test the genetic interaction between them (Figure 3.4A). Overexpression of Art1 in WT cells confers a canavanine resistance phenotype compared to WT cells carrying an empty vector. However, Δ*ppz1*Δ*ppz2* mutant was canavanine hypersensitive even in the presence of Art1 overexpression, suggesting that Art1-mediated endocytosis of Can1 is dependent on the function of the Ppz phosphatases. To further examine whether Ppz phosphatases can regulate Art1 phosphorylation status, we measured Art1 mobilityshift by SDS-PAGE in Δ*ppz1*Δ*ppz2* mutant cells (Figure 3.4B). We did not observe a significant Art1 band-shift in Δ*ppz1*Δ*ppz2* mutant cells in the absence of stimulation, which is consistent with previous microscopy results (Figure 3.1E). In order to see the Art1 band-shift

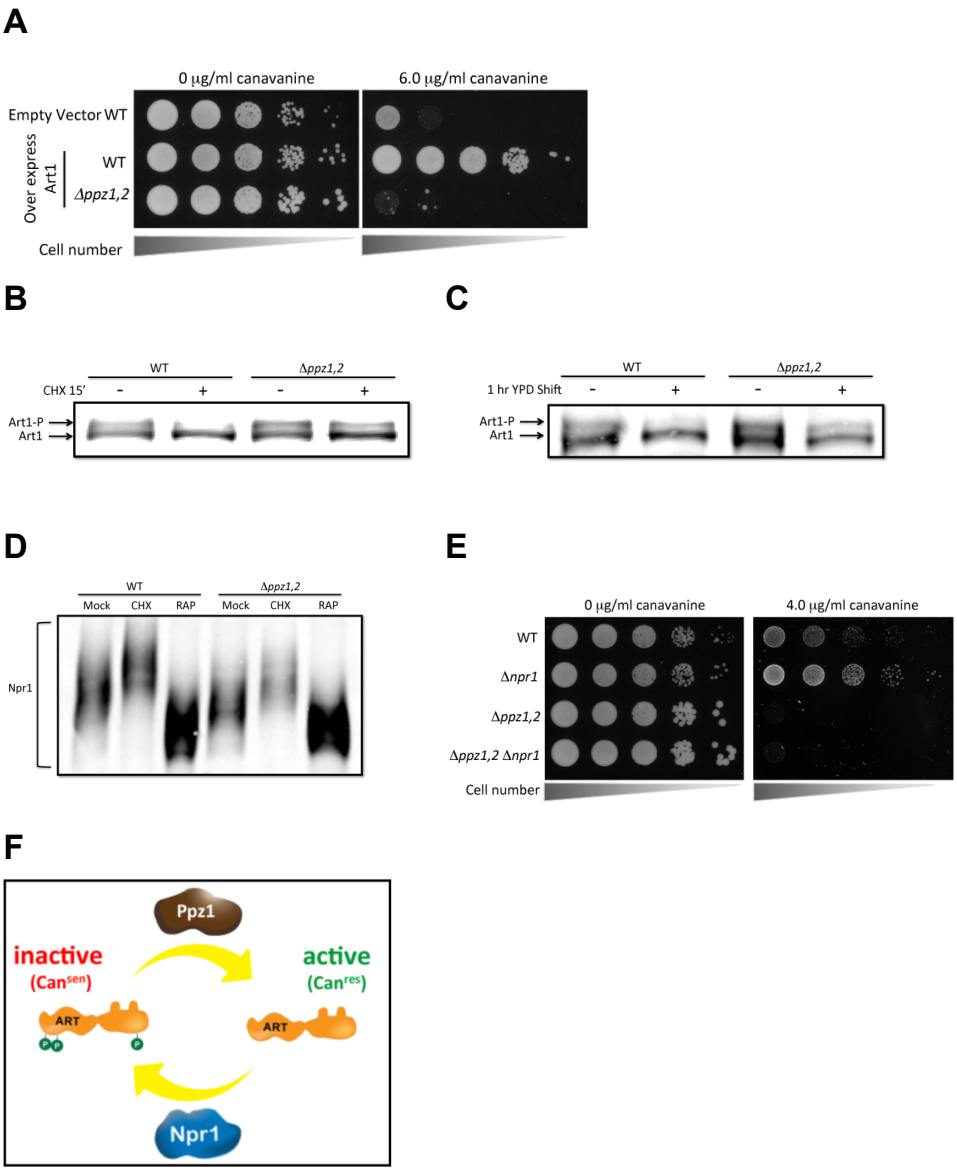
A
0 μg/ml canavanine
6.0 μg/ml canavanine
Empty Vector WT
Over express Art1
WT
Δppz1,2
Cell number
B
WT
Δppz1,2
CHX 15'
Art1-P
Art1
C
WT
Δppz1,2
1 hr YPD Shift
Art1-P
Art1
D
WT
Δppz1,2
Mock
CHX
RAP
Npr1
E
0 μg/ml canavanine
4.0 μg/ml canavanine
WT
Δnpr1
Δppz1,2
Δppz1,2 Δnpr1
Cell number
F
Ppz1
inactive
(Can^sen)
active
(Can^res)
ART
Npr1

Figure 3-4

Figure 3.4. Ppz1 and Ppz2 phosphatases are required for Art1-mediated Can1 endocytosis (A) WT cells expressing empty vector, as well as WT and Δ*ppz1*Δ*ppz2* cells carrying Art1 overexpression plasmids (driven by a TDH3 promoter) were plated on canavanine plates to score for the ability of Art1-mediated Can1 endocytosis. (B) WT and Δ*ppz1*Δ*ppz2* cells were transformed by Art1-HTF plasmids and treated with or without 50 μg/ml of cycloheximide for 15 minutes before collecting cell samples. Art1 band-shift was measured by Western blot in these samples. (C) WT and Δ*ppz1*Δ*ppz2* cells were transformed by Art1-HTF plasmids and treated with or without YPD shift for 1 hour before collecting cell samples. Art1 band-shift was measured by Western blot in these samples. (D) WT and Δ*ppz1*Δ*ppz2* cells were transformed by Npr1-HA plasmids and treated with or without 50 μg/ml of cycloheximide or 200 ng/ml rapamycin for 15 minutes before collecting cell samples. Npr1 band-shift was measured by Western blot in these samples. (E) Δ*ppz1*Δ*ppz2*Δ*npr1* cells were plated on canavanine plates with WT, Δ*npr1* and Δ*ppz1*Δ*ppz2* strains to test for genetic interactions between Npr1 and the Ppz1 Ppz2 phosphatases. (F) Model of Art1 phospho-regulation. Art1 is phosphorylated and inactivated by Npr1 kinase; Art1 is de-phosphorylated and activated by Ppz1 phosphatase.

that occurs during activation, we treated both WT cells and Δ*ppz1*Δ*ppz2* mutants with CHX to trigger the de-phosphorylation event of Art1. Interestingly, this Art1 dephosphorylation event is delayed in Δ*ppz1*Δ*ppz2* mutant cells. Similar results were observed following a shift to growth in YPD (Figure 3.4C). These results indicate that Ppz phosphatases regulate Art1 phosphorylation status during stimulation conditions.

It has been reported that deletion of Ppz1 causes a caffeine sensitive phenotypes (Hirasaki et al., 2011; Sakumoto et al., 2002) while deletion of Npr1 leads to a caffeine resistant phenotypes (data not shown). Two potential explanations for these observations include: 1) Ppz phosphatases function as the upstream regulators for Npr1 kinase; 2) Ppz phosphatases and Npr1 kinase function in two parallel, antagonistic pathways that both converge on the regulation of Art1. To test the first possibility, we determined whether Npr1 activity is mediated by Ppz phosphatases by looking at Npr1 band-shift under different treatments in Δ*ppz1*Δ*ppz2* mutant cells (Figure 3.4D). We did not observe any significant changes on Npr1 mobility by SDS-PAGE in Δ*ppz1*Δ*ppz2* mutant cells compared to WT cells, suggesting that Ppz phosphatases do not affect the phosphorylation of Npr1. To better understand the genetic interaction between Ppz phosphatases and Npr1 kinase, the Δ*npr1*Δ*ppz1*Δ*ppz2* triple knockout was constructed and tested for growth in the presence of canavanine (Figure 3.4E). The triple knockout showed a canavanine hypersensitive phenotype similar to that of Δ*ppz1*Δ*ppz2* mutant cells, suggesting that Ppz phosphatases are required for Art1 hyperactivation in a Δ*npr1*

mutant background. Our results suggest that Art1 phospho-regulatory cycle requires both Npr1 kinase and Ppz phosphatases (Figure 3.4F). However, we still do not know if Art1 is a direct substrate of Ppz1 or Ppz2 and further studies are required to dissect the mechanism of Ppz-mediated regulation of Art1 function.

Ppz Phosphatases Activate Art1 at the Plasma Membrane

The regulation of protein subcellular localization is one key feature to control enzyme activity towards its substrate. For example, Npr1 translocates to the PM to phosphoinhibit Art1 during RAP treatment (Figure 2.9H). At steady state, Ppz1-GFP is localized to the cytosol and the PM (Figure 3.5A, left panel) where it forms transient patches with half-life less than 3 seconds (data not shown). Since CHX treatment triggers Art1 activation, we tested whether CHX treatment can affect Ppz1 PM localization or dynamics. However, neither the PM/cytosol signal ratio (Figure 3.5A, middle panel) nor the Ppz1 patch half-life (data not shown) changed in response to CHX stimulation. We further tested whether RAP treatment can affect Ppz1 PM localization. However, the Ppz1 subcellular localization after RAP stimulation remained the same (Figure 3.5A, right panel). Together, these results suggest that Ppz1 associates with the PM but this localization pattern is not regulated in response to stimulation.

It has been shown that following CHX stimulation, Art1 is recruited to the PM and forms patches (Figure 2.9C). However, this PM recruitment is intact in Δ*ppz1* Δ*ppz2* mutants (data not shown), suggesting the Ppz phosphatases are not required for Art1 PM recruitment (Art1 PM translocation is the subject of Chapter 4). Since both Art1 and Ppz1 form patches at the PM, we tested whether these patches co-

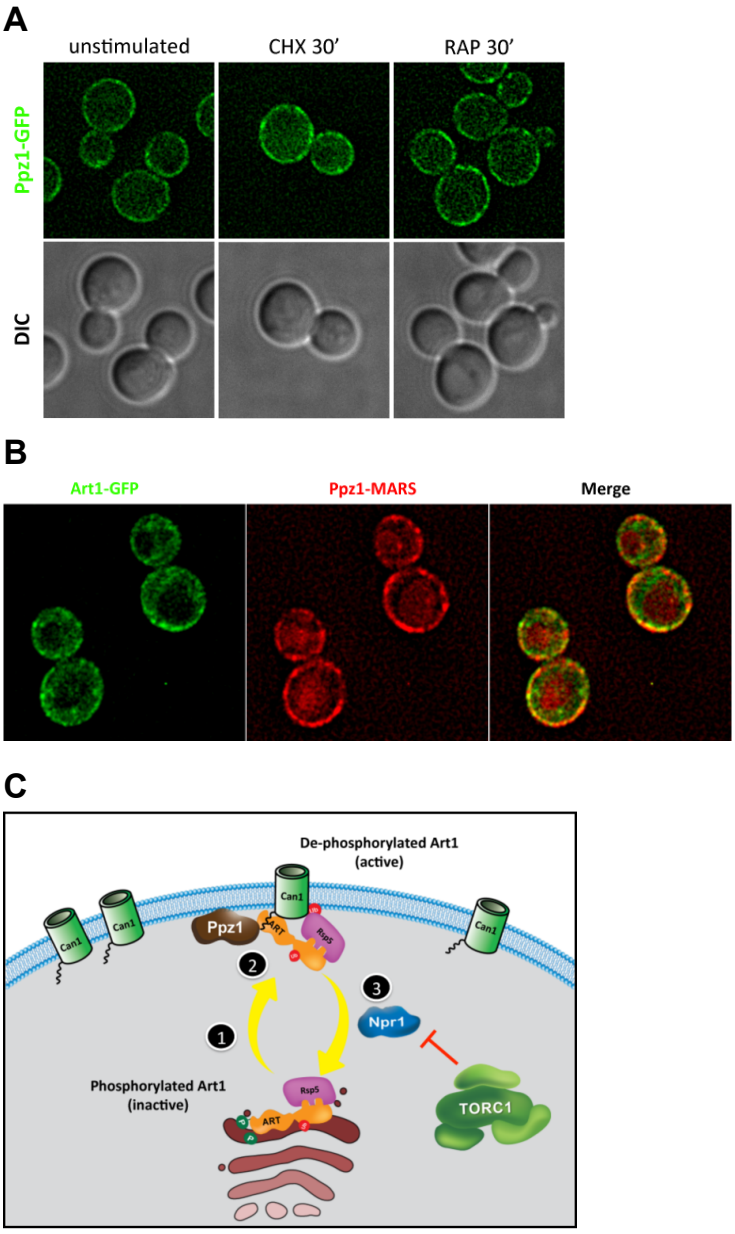
A
unstimulated
CHX 30'
RAP 30'
Ppz1-GFP
DIC
B
Art1-GFP
Ppz1-MARS
Merge
C
De-phosphorylated Art1
(active)
Can1
Ppz1
ART
Rsp5
Npr1
TORC1
Phosphorylated Art1
(inactive)
1
2
3

Figure 3-5

Figure 3.5. Ppz1 partially co-localized with Art1 at the plasma membrane (A) Ppz1-GFP was transformed to WT cells and subjected for microscopy image. Cells were grown to midlog phase and then treated with mock-treatment or 50 μg/ml of cycloheximide or 200 ng/ml rapamycin for 15 minutes before imaging. (B) WT cells expressing both Art1-GFP and Ppz1-MARS were grown to midlog phase and then treated with 50 μg/ml of cycloheximide for 15 minutes to trigger Art1 PM translocation. (C) A mechanism for Art1 phospho-regulation. (1) Following stimulation, the Art1-Rsp5 complex is recruited from the Golgi apparatus to the plasma membrane (the translocation mechanism is discussed in detail in chapter 4). (2) The PM localized Art1 is dephosphorylated and activated by Ppz1 and Ppz2 phosphatases. This Art1-Rsp5 complex further ubiquitinates and targets membrane cargoes for endocytosis. (3) In order to dampen this endocytic signal, the TORC1-Npr1 kinase cascade is activated to phosphorylate Art1. Phosphorylated Art1 then releases from the PM finishing this phospho-regulatory cycle.

localize in cells expressing Art1-GFP and Ppz1-MARS (Figure 3.5B). Following CHX treatment to trigger Art1 PM translocation, we detected partial co-localization of Art1 and Ppz1 at the PM, suggesting Ppz1 has the potential to activate Art1 at the PM. We also observed a Ppz1 mobility shift by SDS-PAGE following a YPD shift (data not shown), suggesting that post-translational modification may regulate Ppz1 activity. Taken together, these results indicate that unknown signaling pathways may regulate Ppz1 activity, which in turn can regulate Art1 activity. Further studies are required to dissect the molecular mechanism of Ppz-mediated regulation of Art1 activity.

DISCUSSION

We have uncovered a novel Ppz phosphatase-mediated Art1 dephosphorylation mechanism that regulates the endocytosis of several PM proteins. As shown in Figure 3.5C, we propose the following phospho-regulatory cycle for Art1: (1) following stimulation, Art1 is recruited to the PM where Ppz phosphatases reside, (2) Ppz phosphatases dephosphorylate and activate Art1 to trigger PM cargo endocytosis, and (3) recruitment of Npr1 causes Art1 phosphorylation and inhibition, which completes the Art1 phospho-regulatory cycle. These findings not only characterize the regulation of endocytosis by Ppz phosphatases but also establish the foundation for understanding the dephospho-activation mechanism of Art1 by the PP1 family Ppz phosphatases.

Identifying and Characterizing other Art1 Phosphatases

In our phosphatase canavanine screen, some mutants showed a canavanine resistant phenotype, which are interesting and may be involved in some novel endocytic regulatory pathways. Our primarily experimental design was to search for mutants with a canavanine sensitive phenotype. Future studies of these canavanine resistant phosphatase mutants may help us reveal new endocytosis regulators or pathways.

Based on the sequence alignment of yeast phosphatases, we found that the catalytic domains from the same phosphatase family are highly conserved. Given their homology, many phosphatases exhibit overlapping functions which leads to phenotypic redundancy (Arino, 2002; Sakumoto et al., 2002). In Figure 3.4B, we

observed the unphosphorylated form of Art1 in Δ*ppz1*Δ*ppz2* mutant in the steady state. Furthermore, many of the phenotypes observed in Δ*ppz1*Δ*ppz2* mutant cells appear to be related to kinetic delays, but not complete block, of endocytosis.(Figure 3.1I). These data suggest that there are phosphatases other than Ppz phosphatases which may be involved in Art1 dephosphorylation. In our phosphatase canavanine screen, we identified five phosphatases with a canavanine hypersensitive phenotype. Although Δ*ppz1* mutant showed the strongest phenotype in both canavanine plating and Can-GFP trafficking (Figure 3.1A) assays, we cannot not rule out the possibility that other phosphatases are also involved in regulating Art1 dephosphorylation. Moreover, one pitfall of our screen is that we cannot identify phosphatases that have redundant endocytic function. In order to identify all potential Art1 phosphatases, I propose to make different deletion combinations of these five potential phosphatases and score for canavanine sensitivity and Art1 phosphorylation. The other potential way to identify Art1 phosphatases is to do a phosphatase repressor screen in the Npr1 overexpressing strain to screen for any protein that suppresses Npr1 canavanine phenotype. Further characterization will be required to determine how these phosphatases regulate Art1 activity. For example, dissecting the regulatory mechanism will require precise mapping of phosphorylation sites in Art1 that are regulated by Ppz phosphatases.

Dissecting the Molecular Mechanism of Ppz Phosphatases-mediated Endocytosis

In Figure 3.4B, we demonstrated that Art1 dephosphorylation is delayed in Δ*ppz1*Δ*ppz2* mutant cells during CHX stimulation. This result indicates that Ppz

phosphatases are an upstream regulator of Art1 phosphorylation. However, the phosphorylation sites regulated by Ppz phosphatases are still not known. Based on our Art1 phosphoprofiling results showed in Chapter 2, Npr1 regulates the N-terminal sites of Art1, while the Art1 C-terminal proline-directed sites are regulated by another unknown kinase (discussed in Chapter 5). These are the potential sites for Ppz phosphatases to regulate. In order to dissect which terminal of Art1 do Ppz phosphatases regulate, we can use the same strategy shown in Figure 2.7C. I will perform quantitative phosphoprofiling analysis of Art1-FLAG expressed cells with or without Ppz phosphatases. In addition, we are also interested in identifying additional Ppz phosphatase substrates. To address this question, a Ppz1 phosphoproteome can be performed to identify proteins with increased phosphorylation in the absence of Ppz phosphatases. Taken together, these proteomic approaches will help us to better understand the molecular mechanism of Ppz phosphatases-mediated regulation of endocytosis.

Identifying and Characterizing the Ppz1 Protein Interaction Network

In the yeast genome, there are around 3 times more kinases than phosphatases (117:32). How phosphatases reverse the phosphorylation created by kinases in a specific manner, especially when most of the phosphatases share similar functions, is an important question. A general strategy for phosphatases to achieve substrate specificity is to recruit regulatory proteins. This strategy is especially common in the case of type 1 Ser/Thr phosphatase family (Bollen, 2001; Cohen, 2002). We have demonstrated that inhibitors of Ppz phosphatases also play a role in regulating endocytosis (Figure 3.2). However, we speculate that there may be other Ppz

phosphatase regulators that contribute to phosphatase activation or substrate recognition. In order to address this question, we hope to identify additional Ppz1 regulators by performing SILAC followed by quantitative mass spectrometry in cells with or without FLAG tagged Ppz1. This experiment may identify novelPpz1 interacting proteins and provide the framework for future investigation of Ppz phosphatase regulation and substrate targeting.

Determine the role of Ppz Phosphatases in the regulation of other Rsp5 Adaptors

It has been reported that different cargoes can be recognized and targeted for endocytosis by different ARTs during specific stimulation conditions (Lin et al., 2008; Nikko and Pelham, 2009). Heat stress-induced endocytosis of Mup1 is delayed in Ppz phosphatases (data not shown), which suggests that, in addition to Art1, Ppz phosphatases may regulate other ART family proteins. Moreover, our data suggests that Npr1 kinase may also regulate Art2, Art3, Art4 and Art6 (Figure 2.8B). To further characterize the other ARTs that Ppz phosphatases regulate, we can perform the SILAC followed by phospho-peptide purification and quantitative mass spectrometry in Rsp5-FLAG expressed cells with or without Ppz phosphatases. These results will be the foundation of understanding how Ppz phosphatases might control the abundance of cell surface proteins by regulating the broader network of ART family proteins.

REFERENCES

Arino, J. (2002). Novel protein phosphatases in yeast. Eur J Biochem *269*, 1072-1077.

Becuwe, M., Vieira, N., Lara, D., Gomes-Rezende, J., Soares-Cunha, C., Casal, M., Haguenauer-Tsapis, R., Vincent, O., Paiva, S., and Leon, S. (2012). A molecular switch on an arrestin-like protein relays glucose signaling to transporter endocytosis. J Cell Biol *196*, 247-259.

Bollen, M. (2001). Combinatorial control of protein phosphatase-1. Trends Biochem Sci *26*, 426-431.

Chen, X.H., Xiao, Z., and Fitzgerald-Hayes, M. (1994). SCM2, a tryptophan permease in Saccharomyces cerevisiae, is important for cell growth. Mol Gen Genet *244*, 260-268.

Cohen, P. (1989). The structure and regulation of protein phosphatases. Annu Rev Biochem *58*, 453-508.

Cohen, P.T. (2002). Protein phosphatase 1--targeted in many directions. J Cell Sci *115*, 241-256.

de Nadal, E., Clotet, J., Posas, F., Serrano, R., Gomez, N., and Arino, J. (1998). The yeast halotolerance determinant Hal3p is an inhibitory subunit of the Ppz1p Ser/Thr protein phosphatase. Proc Natl Acad Sci U S A *95*, 7357-7362.

Goebel-Goody, S.M., Baum, M., Paspalas, C.D., Fernandez, S.M., Carty, N.C., Kurup, P., and Lombroso, P.J. (2011). Therapeutic implications for striatal-enriched protein tyrosine phosphatase (STEP) in neuropsychiatric disorders. Pharmacol Rev *64*, 65-87.

Goffeau, A., Barrell, B.G., Bussey, H., Davis, R.W., Dujon, B., Feldmann, H., Galibert, F., Hoheisel, J.D., Jacq, C., Johnston, M.*, et al.* (1996). Life with 6000 genes. Science *274*, 546, 563-547.

Henne, W.M., Buchkovich, N.J., and Emr, S.D. (2011). The ESCRT pathway. Dev Cell *21*, 77-91.

Hirasaki, M., Horiguchi, M., Numamoto, M., Sugiyama, M., Kaneko, Y., Nogi, Y., and Harashima, S. (2011). Saccharomyces cerevisiae protein phosphatase Ppz1 and protein kinases Sat4 and Hal5 are involved in the control of subcellular localization of Gln3 by likely regulating its phosphorylation state. J Biosci Bioeng *111*, 249-254.

Lin, C.H., MacGurn, J.A., Chu, T., Stefan, C.J., and Emr, S.D. (2008). Arrestin-related ubiquitin-ligase adaptors regulate endocytosis and protein turnover at the cell surface. Cell *135*, 714-725.

Merchan, S., Pedelini, L., Hueso, G., Calzada, A., Serrano, R., and Yenush, L. (2010). Genetic alterations leading to increases in internal potassium concentrations are detrimental for DNA integrity in Saccharomyces cerevisiae. Genes Cells *16*, 152-165.

Mulet, J.M., Leube, M.P., Kron, S.J., Rios, G., Fink, G.R., and Serrano, R. (1999). A novel mechanism of ion homeostasis and salt tolerance in yeast: the Hal4 and Hal5 protein kinases modulate the Trk1-Trk2 potassium transporter. Mol Cell Biol *19*, 3328-3337.

Munoz, I., Ruiz, A., Marquina, M., Barcelo, A., Albert, A., and Arino, J. (2004). Functional characterization of the yeast Ppz1 phosphatase inhibitory subunit Hal3: a mutagenesis study. J Biol Chem *279*, 42619-42627.

Nikko, E., and Pelham, H.R. (2009). Arrestin-mediated endocytosis of yeast plasma membrane transporters. Traffic *10*, 1856-1867.

Posas, F., Camps, M., and Arino, J. (1995). The PPZ protein phosphatases are important determinants of salt tolerance in yeast cells. J Biol Chem *270*, 13036-13041.

Prosser, D.C., Whitworth, K., and Wendland, B. Quantitative analysis of endocytosis with cytoplasmic pHluorin chimeras. Traffic *11*, 1141-1150.

Ruiz, A., Gonzalez, A., Munoz, I., Serrano, R., Abrie, J.A., Strauss, E., and Arino, J. (2009). Moonlighting proteins Hal3 and Vhs3 form a heteromeric PPCDC with Ykl088w in yeast CoA biosynthesis. Nat Chem Biol *5*, 920-928.

Sakumoto, N., Matsuoka, I., Mukai, Y., Ogawa, N., Kaneko, Y., and Harashima, S. (2002). A series of double disruptants for protein phosphatase genes in Saccharomyces cerevisiae and their phenotypic analysis. Yeast *19*, 587-599.

Sakumoto, N., Mukai, Y., Uchida, K., Kouchi, T., Kuwajima, J., Nakagawa, Y., Sugioka, S., Yamamoto, E., Furuyama, T., Mizubuchi, H.*, et al.* (1999). A series of protein phosphatase gene disruptants in Saccharomyces cerevisiae. Yeast *15*, 1669-1679.

Smillie, K.J., and Cousin, M.A. (2012). Akt/PKB Controls the Activity-Dependent Bulk Endocytosis of Synaptic Vesicles. Traffic.

Stark, M.J. (1996). Yeast protein serine/threonine phosphatases: multiple roles and diverse regulation. Yeast *12*, 1647-1675.

Yenush, L., Merchan, S., Holmes, J., and Serrano, R. (2005). pH-Responsive, posttranslational regulation of the Trk1 potassium transporter by the type 1-related Ppz1 phosphatase. Mol Cell Biol *25*, 8683-8692.

Yenush, L., Mulet, J.M., Arino, J., and Serrano, R. (2002). The Ppz protein phosphatases are key regulators of K+ and pH homeostasis: implications for salt tolerance, cell wall integrity and cell cycle progression. EMBO J *21*, 920-929.

Chapter 4

Golgi-to-PM Trafficking is Required for the Endocytic Targeting of Specific Cargoes

INTRODUCTION

Regulation of cellular localization is a key regulatory mechanism for controlling protein function. In mammalian cells, β-arrestin translocates from the cytosol to the plasma membrane (PM) following stimulation of GPCRs (Shenoy and Lefkowitz, 2005). In yeast, Art1 normally localizes to the cytoplasm, Golgi puncta, and the PM (Lin et al., 2008b). However, following stimulation or in the absence of inhibitory factors (like the Npr1 kinase (demonstrated in chapter 2)), Art1 PM localization is significantly increased (Figure 2.9 C and D). Given the localization pattern of Art1 in steady state, I hypothesized two reasonable models for Art1 translocation to the PM: (i) cytosol-to-PM translocation, and (ii) Golgi-to-PM translocation by a mechanism such as secretion.

Protein translocation from cytosol to the PM is mainly achieved by simple diffusion, while the translocation from Golgi apparatus to the PM requires different machineries. It has been reported that Arf1, a small GTPase, plays important roles in many general membrane trafficking pathways at the Golgi apparatus (Palmer et al., 1993). In addition, Sec7, a guanine nucleotide exchange factor (GEF), has been shown to activate Arf1 to recruit different secretion machineries to the TGN, which is critical for delivery of cargoes to the PM (Sata et al., 1998). One of the machinery that is regulated by Arf1 is the exomer coat complex. The exomer coat complex is composed of a core protein, Chs5, and four other subunits named Chs5p-Arf1p

binding proteins (ChAPs) with the function of transporting proteins from the trans-Golgi network (TGN) to the PM (Trautwein et al., 2006; Wang et al., 2006). Several cargoes, including Chs3 and Fus1, have been reported to be transported by the exomer complex from TGN to the PM (Barfield et al., 2009; Sanchatjate and Schekman, 2006). Although some of the ChAPs have been studied, a clear function for some ChAPs is still unknown. Although people have already understood how exomer complex is activated by Arf1, further studies are still required for finding novel exomer cargos.

In this chapter, I explore potential mechanisms of Art1 PM translocation. My findings suggest that the exomer complex, especially Chs5-Bch1 complex, plays an important role for Art1 TGN-to-PM translocation.

MATERIAL AND METHODS

Plasmids, Strains and Yeast Plating Assays

All plasmids and yeast strains used in this study are listed in Table S1 and Table S2, respectively. Canavanine plating assays were performed as previously described (Lin et al., 2008a). Briefly, yeast cultures grown overnight in YPD were normalized to 1 OD/mL, serially diluted and plated onto SCD plates using a pin-frogger. The following concentrations of canavanine were tested in each experiment: 0 μg/mL, 0.6 μg/mL, 0.8 μg/mL, 1.0 μg/mL, 2.0 μg/mL, 4.0 μg/mL and 6.0 μg/mL.

SILAC and Quantitative Mass Spectrometry

All quantitative mass spectrometry analysis was performed using SILAC labelling of yeast strains auxotrophic for lysine and arginine. Cells with or without chromosomal tagged Art1-HTF were grown to mid-log phase in the presence of heavy or light isotopes, respectively, (lysine and arginine). 0.5 mg/mL DSP was added prior to cell harvesting and affinity purification was performed by using flag M2 beads (Sigma). Heavy and light purified samples were mixed and digested with 1μg of trypsin for 2 hours at 37˚C. For phosphoprofiling experiments, phosphopeptides were purified using IMAC chromatography as previously described (Albuquerque et al., 2008). Purified peptides were dried, reconstituted in 0.1% trifluoroacetic acid, and analysed by LC-MS/MS using an Orbitrap XL mass spectrometer. Database search and SILAC quantitation was performed using Sorcerer software.

Recombinant Protein Expression and Purification

Full length Art1-6xHis-FLAG (pJAM583) and Rsp5-StrepII (pJAM587) were transformed into Rosetta2 competent cells (EMD Chemicals USA). 1L cultures were grown to mid-log phase (OD_{600}=0.7) at 37°C. 1mM IPTG was added to bacteria cultures to induce protein expression at 16°C for 20 hours. Cells were lysed by sonication in PBS with protease inhibitors. For Art1 purification, TALON Metal Affinity Resin beads (Clontech) were added to cleared lysates and rotated for 1 hour at 4 °C. Beads were washed in PBS, and then eluted in elution buffer (PBS with 200mM imidazole). For Rsp5 purification, I followed the protocol of Strep-tag Protein purification kit (Qiagen).

***In vitro* Liposome Binding Assays**

For nucleotide stripping, 20 μl of 1 mM major-minor liposomes with DiR dye and 1 μl 0.05 M EDTA was incubated with 6 μg of purified Arf1 and 1 μl of 10 mM nucleotide (GDP or GMPPNP) for 30 minutes at room temperature. 6 μg of Chs5 and Bch1 were added to the nucleotide stripping reaction. 1 μl of 2 M $MgCl_2$ was added to each reaction and incubated for 1 hour at room temperature for liposome binding reaction. 6 μg of Art1 and Rsp5 were added to the exomer liposome reaction and brought the final volume to 80 μl with HK buffer (20 mM HEPES pH 7.4, 150 mM KOAc) for 1 hour at room temperature. 50 μl of 2.5 M sucrose in HKM (HK buffer plus 1 mM $MgCl_2$) was added to each binding reaction and mixed well. 100 μl of the binding reactions were transferred to Beckman 7x20 mm PC ultracentrifuge tube and the remainder was saved as input samples. 100 μl of 0.75 M sucrose in HKM and 20 μl HKM was overlaid on top of the binding reaction. The sucrose gradient ultracentrifugation was performed at 100 krpm at 20˚C for 20 minutes. 30 μl of the

top gradient was withdrawn. The lipid recovery was estimated by mixing 48 μl of 0.1% Triton X-100 with 2 μl float fraction and quantified by the LiCor system. Normalized samples were loaded to SDS-PAGE and Western blot was performed to detect proteins in each reaction.

Additional related material and methods are the same as described in Chapter 2

RESULTS

Art1 Interacts with Specialized Secretion Machinery at the Golgi Complex

In an attempt to identify factors important for Art1 translocation to the PM, we used SILAC combined with quantitative mass spectrometry to identify Art1 interacting proteins. However, the only Art1 interacting protein identified from this analysis was Rsp5 (data not shown). In order to capture weak or transient Art1-interacting proteins, we added cross-linkers into the media shortly before harvesting the cells. As shown in Figure 4.1(A), addition of crosslinkers resulted in the identification of additional Art1 interacting proteins. One of the top hits identified in this analysis is Bch1, a subunit of the exomer complex that localizes to the trans-Golgi network (TGN) (Trautwein et al., 2006).

To confirm this interaction, we analyzed the subcellular localization of both Art1 and exomer complex by tagging the proteins with GFP and mCherry, respectively (Figure 4.1B). As shown previously, Art1-GFP localized to the PM and the cytoplasm (Lin et al., 2008b). Moreover, consistent with the Art1 interactome experiment result, we detected a strong co-localization of Art1 and exomer at the Golgi. These results are consistent with our observation that Art1 physically interacts with exomer, and suggests that this interaction occurs at the TGN.

The Exomer Complex Plays a Role in Art1-mediated Cargo Endocytosis

I wanted to better understand if interaction with exomer is required for Art1 function. I hypothesized that if the exomer complex is required for Art1 function, we would see canavanine sensitive phenotype in the exomer mutant, as Art1 can no

A

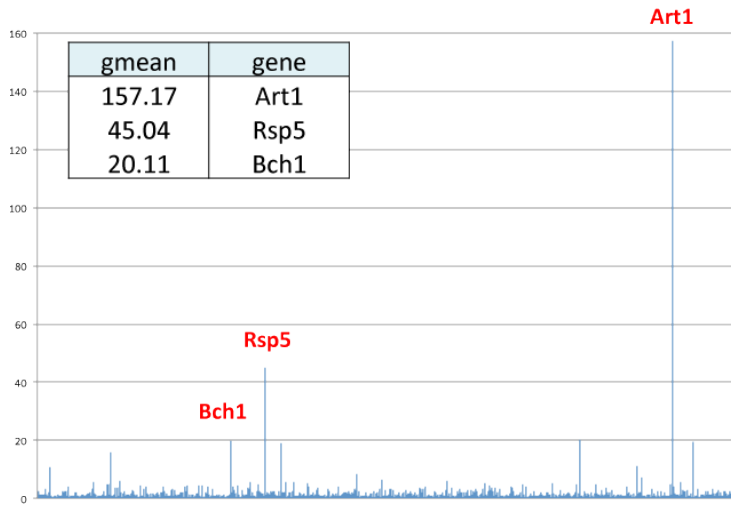

gmean	gene
157.17	Art1
45.04	Rsp5
20.11	Bch1

B

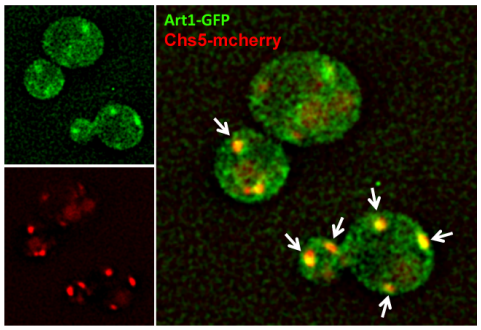

Figure 4-1

Figure 4.1. Art1 interacts with proteins in the secretion machinery at the Golgi apparatus (A) Art1 SILAC interactome experiment with cross-linker. X-axis represents different proteins and Y-axis represent gmean of each protein. WT (labeled with light isotope) and Art1-FLAG tagged cells (labeled with heavy isotope) were collected and analyzed by FLAG immunoprecipitation. Samples were subjected to SILAC and quantitative mass spectrometry. We made the gmean cutoff line at 20 to rule out some less strong bindings (Emi2, Car1, Hxk1 and Aro4) and found that besides the known Art1 interacting protein Rsp5, Bch1, the ChAP of exomer complex, also showed physical interaction with Art1. The inset table shows proteins containing peptides with more than a 20-fold increase in Art1-FLAG tagged cells compare to WT cells. (B) WT cells expressing both Art1-GFP and Chs5-mCherry were grown to midlog phase and subjected to microscopy imaging (arrows show the co-localization of the two proteins).

longer be recruited to the PM to turnover Can1. By using the canavanine plating assay in the exomer mutants, we tested whether Art1 PM trafficking is dependent on the exomer complex. As shown in Figure 4.2A, Δ*chs5* mutant shows a canavanine sensitive phenotype, suggesting that the exomer complex is required for Art1 function. Moreover, Δ*bch1* mutant shows a canavanine sensitive phenotype while Δ*chs6* mutant grows just like WT. This result is consistent with our Art1 SILAC interactome experiment, which demonstrates that Bch1 is the major ChAP that binds to Art1. Furthermore, the Δ*bud7* mutant also shows a canavanine sensitive phenotype, though it is not as severe as Δ*bch1* mutant. As previously reported, Bch1 and Bud7 have the highest sequence similarity among all the ChAPs (Barfield et al., 2009; Sanchatjate and Schekman, 2006). This result suggests the redundancy of Bch1 and Bud7 in regulating Art1 function.

To further explore Art1 function in exomer mutants, we directly measured arginine uptake by Can1 (Figure 4.2B). Consistent with the canavanine plating assay, Can1 is more activated to transport arginine in the Δ*chs5* mutant compare to WT cells, suggesting that there are more functional Can1 at the PM in the exomer mutants. Can1 activity in the Δ*bch1* mutant is also higher than the WT, although it is not as high as the Δ*chs5* mutant, which is probably due to the redundancy of Bch1 and Bud7.

Since both the exomer and Art1 mutants are hypersensitive to canavanine, we examined the effect of Art1 overexpression in exomer mutants (Figure 4.2C). Overexpression of Art1 in WT cells leads to a canavanine resistant phenotype in

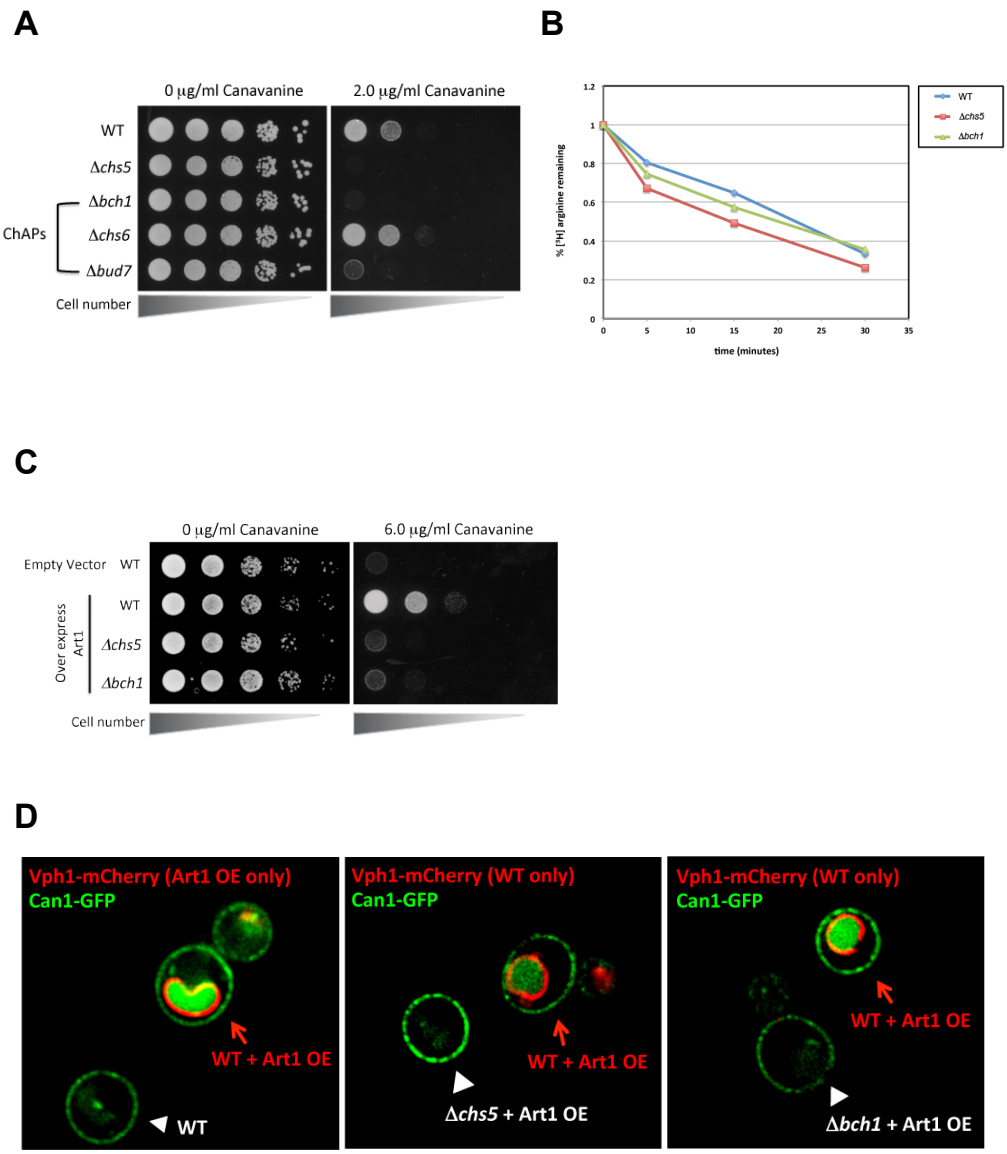
A
0 μg/ml Canavanine
2.0 μg/ml Canavanine
WT
Δchs5
Δbch1
ChAPs
Δchs6
Δbud7
Cell number
B
% [³H] arginine remaining
time (minutes)
WT
Δchs5
Δbch1
C
0 μg/ml Canavanine
6.0 μg/ml Canavanine
Empty Vector
WT
Over express Art1
WT
Δchs5
Δbch1
Cell number
D
Vph1-mCherry (Art1 OE only)
Can1-GFP
WT + Art1 OE
WT
Vph1-mCherry (WT only)
Can1-GFP
WT + Art1 OE
Δchs5 + Art1 OE
Vph1-mCherry (WT only)
Can1-GFP
WT + Art1 OE
Δbch1 + Art1 OE

Figure 4-2

Figure 4.2. Exomer complex is required for Art1-mediated Can1 endocytosis (A) WT (background BY4741) cells , as well as exomer core protein (Chs5) and ChAPs (Bch1, Chs6, and Bud7) mutants from the yeast deletion collection were plated on canavanine plates to score for Can1 endocytosis defect. (B) WT (blue), Δ*chs5* (red), and Δ*bch1* (green) cells were grown to midlog phase and subjected to [^{3}H] arginine. Samples were collected at 5, 15, and 30 minute time points. (C) WT cells expressing empty vector, as well as WT, Δ*chs5*, and Δ*bch1* cells carrying Art1 overexpression plasmids (driven by a TDH3 promoter) were plated on canavanine plates to score for the ability of Art1-mediated Can1 endocytosis. (D) Can1-GFP was imaged in WT cells expressing empty vector or Art1 over-expression (Art1 OE) plasmids (with chromosomal tagged Vph1-mCherry) in the left panel. Can1-GFP was imagined in both WT cells (marked by chromosomal tagged Vph1-mCherry) and exomer mutants (Δ*chs5* and Δ*bch1* cells for the middle and the right panels, respectively) carrying Art1 OE plasmids.

comparison to WT cells carrying empty vector. However, this canavanine resistant phenotype is dependent on the presence of both Chs5 and Bch1, suggesting that Art1-mediated Can1 endocytosis is dependent on the function of exomer complex. In addition, Can1 trafficking to the vacuole upon Art1 overexpression is dependent on the exomer complex. (Figure 4.2D, middle and right panel, respectively). This result is consistent with the canavanine plating assay and suggests that the exomer complex is required for Art1 regulation of Can1 endocytosis.

The Exomer Complex Mediates Art1 PM Recruitment and Phosphorylation

Given our observations that exomer plays a role in Art1 function, we wanted to decipher the molecular mechanism by which exomer positively mediates cargo turnover. Because one major function of the exomer complex is to transport proteins from the TGN to the PM, we hypothesized that the exomer complex may recruit Art1 to the PM during stimulation. To test this hypothesis, we expressed Art1-GFP in both WT (marked by chromosomal tagged Mup1-mCherry) and Δ*chs5* cells and subsequently treated the cells with CHX for 15 minutes to trigger Art1 PM translocation (Figure 4.3A). After stimulation, Art1-GFP was recruited to the PM in the WT cells. However, this PM recruitment is diminished in the Δ*chs5* mutants, suggesting that the exomer complex is required for efficient translocation of Art1 to the PM. This result suggests that exomer plays a specific role in translocation of Art1 to the PM, and is consistent with the endocytic defects observed in exomer mutants.

Previously, we reported that Npr1 phosphorylates Art1 at the PM, and this

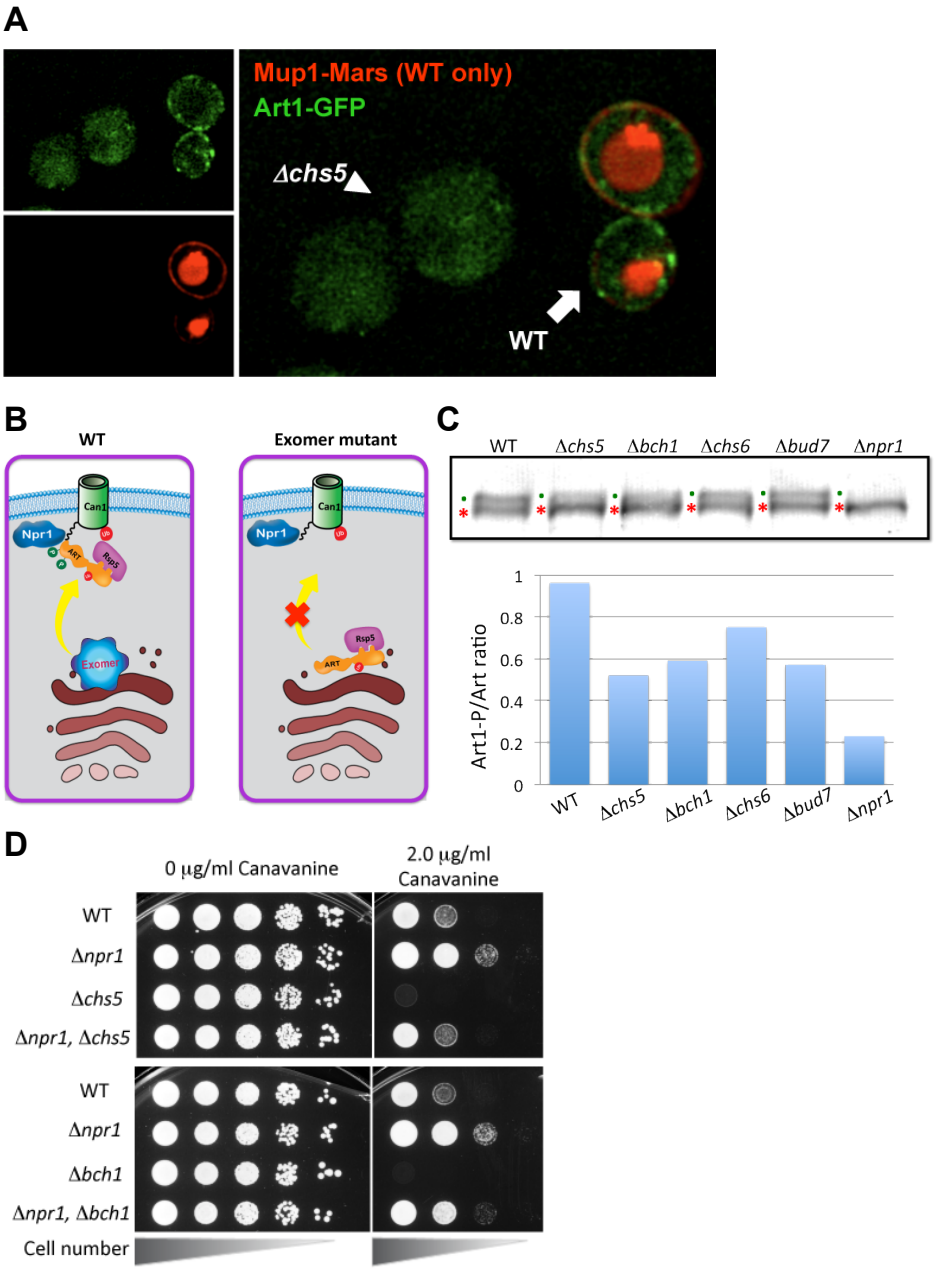
A
Mup1-Mars (WT only)
Art1-GFP
Δchs5
WT
B
WT
Exomer mutant
Can1
Npr1
Art1
Rsp5
Exomer
ART
C
WT
Δchs5
Δbch1
Δchs6
Δbud7
Δnpr1
Art1-P/Art ratio
1
0.8
0.6
0.4
0.2
0
D
0 μg/ml Canavanine
2.0 μg/ml Canavanine
WT
Δnpr1
Δchs5
Δnpr1, Δchs5
WT
Δnpr1
Δbch1
Δnpr1, Δbch1
Cell number

Figure 4-3

Figure 4.3. Art1 PM recruitment and phosphorylation is partially dependent on the exomer complex (A) WT (marked by chromosomal tagged Mup1-Mars) and Δ*chs5* cells were grown to midlog phase and then treated with cycloheximide (50mg/ml) for 15 minutes. Art1-GFP PM recruitment was imaged in both WT and D*chs5* cells. (B) Model for exomer-mediated Art1 PM recruitment and phosphorylation. In WT cells, the exomer translocates Art1 from Golgi to the PM where it is phosphorylated by Npr1 (left panel). However, in the exomer mutant, Art1 is unable to reach the PM (right panel). PM localization of Art1 is critical for its phosphorylation by Npr1 (C) Western blot of Art1 band-shift in WT, exomer mutants, and Δ*npr1* cells. The ratio of phosphorylated Art1 to dephosphorylated Art1 is quantified in the lower panel. (D) WT, Δ*npr1* Δ*chs5* and Δ*npr1* Δ*bch1* cells were plated on canavanine plates to test for genetic interactions between Npr1 and the exomer.

phosphoregulation is important to inhibit Art1 activity (demonstrated in chapter 2). Moreover, provided that the exomer complex plays a role in Art1 PM recruitment, we hypothesized that Npr1-mediated phosphorylation of Art1 should not takes place in exomer mutants (model is illustrated in Figure 4.3B). To test this hypothesis, we performed the Art1 band-shift assay to see if there is any Art1 phosphorylation change in the exomer mutants (Figure 4.3C). Using this approach, we found a reduction in Art1 phosphorylation in exomer mutants compared to WT cells. Additionally, Δ*chs5*, Δ*bch1*, and Δ*bud7* mutants showed less Art1 phosphorylation in comparison to Δ*chs6* mutants, which supports our previous finding that the Bch1 exomer complex is the major exomer complex responsible for Art1 PM recruitment. Nevertheless, none of the exomer mutants showed complete Art1 dephosphorylation as Δ*npr1* mutants showed. This result shows that exomer mutants cannot completely block Art1 phosphorylation and may suggests the existence of perhaps a secondary Art1 PM translocation route in addition to the exomer complex.

To better understand the genetic interaction between the exomer complex and Npr1, the Δ*npr1*Δ*chs5* and Δ*npr1*Δ*bch1* double knockouts were made and tested by the canavanine plating assay. If the exomer complex is required for Art PM translocation, I proposed the model shown in Figure 4.3B. In this model, the double knockouts should lead to canavanine sensitive phenotype because of a reduction in PM localized Art1. However, although the double knockouts were more sensitive to canavanine compare to Δ*npr1* mutants, they grew similar to or a little better than the WT cells. These results suggest that the exomer complex may not be the only

pathway to recruit Art1 to the PM. Thus, Art1 may be recruited to the PM via additional pathways, which will be discussed more in the DISCUSSION.

Art1 Interacts with the Exomer Liposome *in vitro*

In order to confirm the observed *in vivo* interaction between Art1 and exomer, and to prove that it is not through an indirect binding or an artifact of crosslinking, we examined Art1 binding to exomer using an *in vitro* liposome binding assay. First, we purified the recombinant Art1-6xHis from *E. coli* and then checked the protein expression by coomassie blue staining (Figure 4.4A). Although we observed some protein degradation during the purification process, the major band in the elution was the full length Art1. Since Art1 and Rsp5 form a complex in the cell, we reasoned that the formation of the complex might be important for Art1 protein stabilization or for Art1 function. Thus, we also purified the recombinant Rsp5-StrepII from *E. coli* and checked the protein expression by coomassie blue staining (Figure 4.4B). Compared to recombinant Art1, Rsp5 was relatively stable. In order to measure the amount of the purified Art1 and Rsp5, both proteins were stained by coomassie blue and subjected to quantification by the Odessey imaging system (Figure 4.4C).

It has been reported that the exomer complex can be recruited to liposomes via activated Arf1 (Wang et al., 2006). We wanted to determine whether the exomer complex has the ability to recruit Art1 to liposomes. To do this, we first incubated liposomes with activated (GDPPNP was added) and inactivated (GDP was added) Arf1 and then incubated these Arf1 liposomes with Chs5-Bch1 exomer complex.

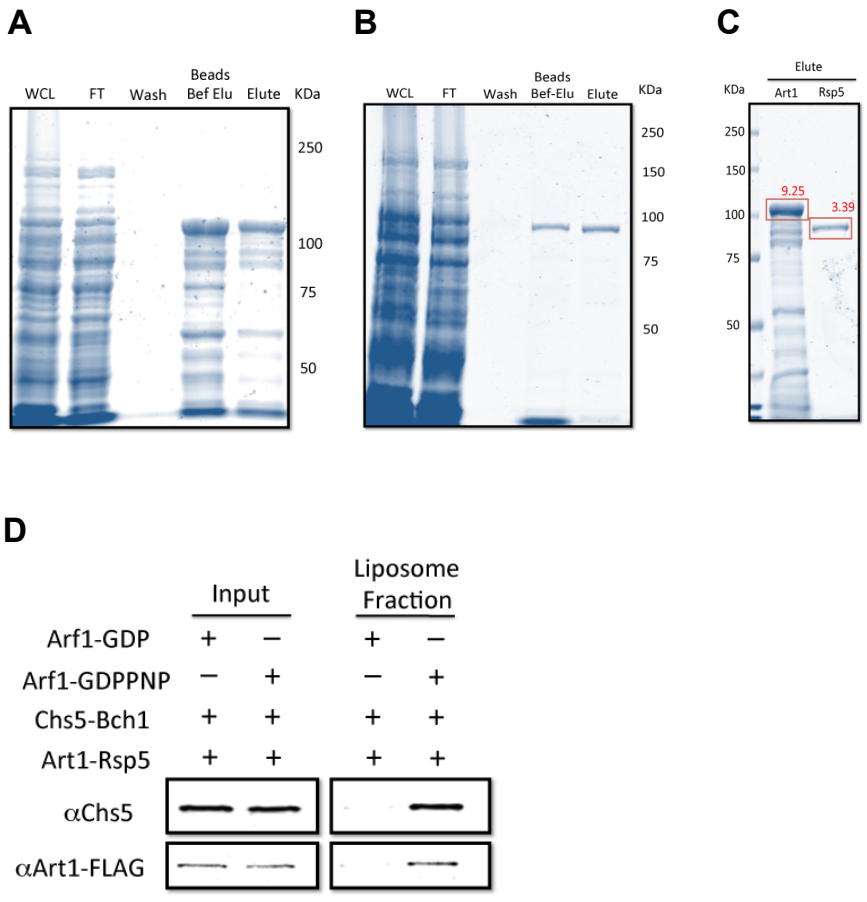
A
WCL
FT
Wash
Beads
Bef Elu
Elute
KDa
250
100
75
50
B
WCL
FT
Wash
Beads
Bef-Elu
Elute
KDa
250
150
100
75
50
C
Elute
KDa
Art1
Rsp5
250
150
100
75
50
9.25
3.39
D
Input
Liposome Fraction
Arf1-GDP
Arf1-GDPPNP
Chs5-Bch1
Art1-Rsp5
αChs5
αArt1-FLAG

Figure 4-4

Figure 4.4. Art1 is recruited to the exomer liposome *in vitro* (A) Recombinant Art1-His-tagged-FLAG was purified from E. coli and stained by Coomassie blue in the 6% SDS-PAGE. (WCL: whole cell lysate, FT: flow through, Beads Bef Elu: beads before elute). (B) Recombinant Rsp5-StrepII was purified from E. coli and stained by Coomassie blue in the 6% SDS-PAGE. (C) Purified Art1 and Rsp5 were subjected to 6% SDS-PAGE and the intensity of the bands were measured by Odyssey imaging system. (D) Purified recombinant proteins (Chs5, Bch1, Art1, and Rsp5) were incubated with liposomes with and without activated Arf1, GDPPNP- and GDP-bound respectively. Liposome fractions were analyzed by Western blot to detect the liposome binding ability of Chs5 and Art1.

After obtaining exomer-bound liposomes, recombinant Art1-Rsp5 (with 1:1 ratio) was added and liposomes were isolated by flotation. As Figure 4.4D shows, Chs5 can only bind to the activated Arf1 (GDPPNP bound form), which is a positive control for this *in vitro* binding assay. Consistent with our *in vivo* binding result, Art1 binds the activated Arf1 liposome with Chs5-Bch1 complex while we cannot detect the binding of Art1 to the Arf1 inactivated liposome. Taken together, these results confirm our *in vivo* binding result and demonstrate that Art1 can be recruited to the liposome through direct binding to the Arf1-exomer complex.

DISCUSSION

We have uncovered a possible role of the exomer complex in transporting Art1 from TGN to the PM (Figure 4.5). Specifically, we have shown that (1) the exomer complex plays a role in Art1-mediated cargo endocytosis and (2) the exomer complex is implicated in Art1 PM recruitment. These findings not only demonstrate the regulatory mechanism of Art1 function by the exomer complex but also establish the foundation to understand why Art1 localizes to the Golgi apparatus and how Art1 maintains its PM localization after stimulation.

Art1 can be Recruited to the PM via an Exomer-independent Mechanism

The results from the Art1 band-shift assay in the exomer mutants (Figure 4.3C) and Npr1 exomer double knockout canavanine plating assay (Figure 4.3D) suggest that the exomer machinery may not be the only mechanism for Art1 PM recruitment. Given our analysis of Art1 subcellular localization, Art1 can be recruited to the PM from either the cytosol or the Golgi apparatus. As such, three possible routes of PM translocation include: 1) direct targeting of Golgi vesicles to the PM; 2) indirect targeting from the Golgi apparatus to the PM via trafficking to and sorting at endosomes; 3) direct recruitment of cytosolic Art1 to the PM by diffusion. The first two possibilities require vesicle trafficking and thus can be tested using mutant strains defective for secretion from the Golgi apparatus (*sec1*^{ts}, *sec7*^{ts}, and *pik1*^{ts}) (Strahl and Thorner, 2007); (Wang et al., 2006), Golgi-to-endosome traffic (Δ*gga1*Δ*gga2,* Δ*laa1*) (Bonifacino and Hurley, 2008), or general membrane traffic (*sec18*^{ts}).

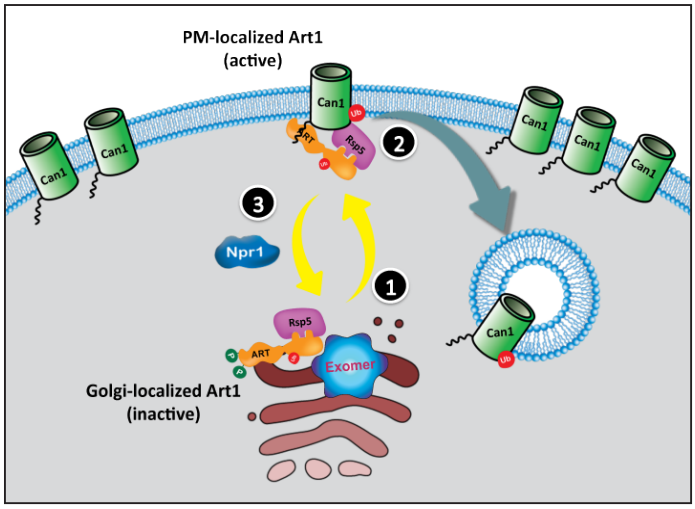
PM-localized Art1
(active)
Can1
Can1
Can1
Can1
Can1
Can1
Rsp5
ART
2
3
Npr1
1
Rsp5
ART
Exomer
Golgi-localized Art1
(inactive)
Can1

Figure 4-5

Figure 4.5. A functional model for the exomer complex mediation of Art1 subcellular localization. (1) Under unstimulated condition, the Art1-Rsp5 complex is inactive and localizes at the cytosol and Golgi apparatus. Following stimulation, the exomer complex recruits the Art1-Rsp5 complex to the TGN and transports it the PM. (2) After reaching the PM, the Art1-Rsp5 complex ubiquitinates cargoes, such as Can1, and targets them for endocytic degradation. Through binding to $PI(4,5)P_2$ at the PM, the Art1-Rsp5 complex maintains its PM localization and triggers more cargo endocytosis locally. (3) In order to dampen this endocytic signal, Npr1 can then be activated and recruited to the PM to phosphorylate Art1. Inactivated Art1-Rsp5 complex releases from the PM, thus finishing this regulatory cycle.

However, if Art1 PM translocation is shown to be independent of membrane trafficking in the cell, we can then test the role of the cytoskeleton. By using pharmacological inhibitors of cytoskeletal dynamics such as latrunculin and nocodazole, we can determine if actin or microtubule polymerization are required for Art1 localization to the PM or the Golgi apparatus. If the results indicate that Art1 PM recruitment is independent of membrane trafficking and cytoskeletal dynamics, then we may consider the possibility that Art1 diffuses directly from the cytosol to the PM. Since cytosolic diffusion of Art1 should be constant, it is possible that PM recruitment may result from a decreased off rate of Art1 from the PM during stimulation. Although we have shown that Npr1 is important for releasing Art1 from the PM, the detailed mechanism is still unknown. One possibility is that the massive amount of Art1 N-terminal phosphorylations by Npr1 can create a lot of negative charges, which may subsequently increase the repulsion force of Art1 off the PM. However, further studies are needed to dissect the mechanism of how both Npr1 and the exomer complex regulate Art1 PM localization.

Arf1 is Required for Art1-mediated Cargo Endocytosis

Based on the results of our *in vitro* exomer liposome binding assay (Figure 4.3D) and other publications (Wang et al., 2006), we can conclude that Arf1 is required for activating exomer complex. Therefore, we hypothesize that Arf1 is also required for Art1-mediated cargo endocytosis since Arf1 is an upstream regulator of the exomer complex. By testing canavanine sensitivity of the Δ*arf1* mutant, we found that the mutant showed the same sensitive phenotype as did exomer mutants (data not shown), suggesting that Arf1 plays a role in Can1 mediated endocytosis.

Furthermore, we tested whether Arf1 activity is essential for Art1-mediated cargo endocytosis by performing a genetic test of Art1 and Arf1. In brief, we over-expressed Art1 in both WT and Δ*arf1* mutant cells, and then plated them on canavanine plates. Similar to the exomer mutants, the Δ*arf1* mutant blocked the Art1 over-expressed canavanine resistant phenotype (data not shown). This result suggests that Arf1 may function upstream of Art1 and may positively regulate Art1 function. Additionally, we detected less phosphorylation in the Δ*arf1* mutant compare to WT cells (data not shown), indicating that Art1 PM recruitment is inhibited. All together, these results indicate that Arf1, like exomer complex, is required for Art1 PM recruitment and phosphorylation.

Dissect the Molecular Mechanism of Art1 Membrane Recruitment and Maintenance

Although we have shown that Art1 can be recruited to the exomer liposome, we do not know if all the elements tested in our experiment are required (Figure 4.3D). For example, Art1 might bind to the exomer liposome even without forming the complex with Rsp5 and could be recruited to the liposome in the absence of the Chs5-Bch1 complex. By testing Art1's ability to bind to different exomer complexes (such as Chs6 and Bud7) *in vitro*, we can confirm that Art1 binds to the Bch1 exomer complex but not to the Chs6 exomer complex. To address these questions, further experiments are required to clarify the Art1 liposome binding mechanism.

It is possible that Art1 membrane association could be dependent on lipids binding. First, we can test the binding of Art1 to the PIPs. We can also use yeast genetics to test the role of other lipids, such as ergosterol or sphingolipids, in Art1

membrane association. Alternatively, Art1 may associate with membranes through protein-protein interactions. To explore the possible role of other proteins in Art1 localization, we can determine if Art1 co-localizes with other known patch structures at the PM, including actin patches, PIK patches, and Osh patches.

Although there is no exomer homolog in the mammalian cells, Arf1 is highly conserved from yeast to mammalian cells. This study may provide a novel pathway to decipher how Arf1 can function as a transport machinery to recruit arrestin proteins to the PM in order to efficiently regulate membrane protein turnover.

REFERENCES

Albuquerque, C., Smolka, M., Payne, S., Bafna, V., Eng, J., and Zhou, H. (2008). A multidimensional chromatography technology for in-depth phosphoproteome analysis. Mol Cell Proteomics *7*, 1389-1396.

Barfield, R.M., Fromme, J.C., and Schekman, R. (2009). The exomer coat complex transports Fus1p to the plasma membrane via a novel plasma membrane sorting signal in yeast. Mol Biol Cell *20*, 4985-4996.

Bonifacino, J.S., and Hurley, J.H. (2008). Retromer. Curr Opin Cell Biol *20*, 427-436.

Lin, C., MacGurn, J., Chu, T., Stefan, C., and Emr, S. (2008a). Arrestin-related ubiquitin-ligase adaptors regulate endocytosis and protein turnover at the cell surface. Cell *135*, 714-725.

Lin, C.H., MacGurn, J.A., Chu, T., Stefan, C.J., and Emr, S.D. (2008b). Arrestin-related ubiquitin-ligase adaptors regulate endocytosis and protein turnover at the cell surface. Cell *135*, 714-725.

Palmer, D.J., Helms, J.B., Beckers, C.J., Orci, L., and Rothman, J.E. (1993). Binding of coatomer to Golgi membranes requires ADP-ribosylation factor. J Biol Chem *268*, 12083-12089.

Sanchatjate, S., and Schekman, R. (2006). Chs5/6 complex: a multiprotein complex that interacts with and conveys chitin synthase III from the trans-Golgi network to the cell surface. Mol Biol Cell *17*, 4157-4166.

Sata, M., Donaldson, J.G., Moss, J., and Vaughan, M. (1998). Brefeldin A-inhibited guanine nucleotide-exchange activity of Sec7 domain from yeast Sec7 with yeast and mammalian ADP ribosylation factors. Proc Natl Acad Sci U S A *95*, 4204-4208.

Shenoy, S.K., and Lefkowitz, R.J. (2005). Receptor-specific ubiquitination of beta-arrestin directs assembly and targeting of seven-transmembrane receptor signalosomes. J Biol Chem *280*, 15315-15324.

Strahl, T., and Thorner, J. (2007). Synthesis and function of membrane phosphoinositides in budding yeast, Saccharomyces cerevisiae. Biochim Biophys Acta *1771*, 353-404.

Trautwein, M., Schindler, C., Gauss, R., Dengjel, J., Hartmann, E., and Spang, A. (2006). Arf1p, Chs5p and the ChAPs are required for export of specialized cargo from the Golgi. EMBO J *25*, 943-954.

Wang, C.W., Hamamoto, S., Orci, L., and Schekman, R. (2006). Exomer: A coat complex for transport of select membrane proteins from the trans-Golgi network to the plasma membrane in yeast. J Cell Biol *174*, 973-983.

Chapter 5

Conclusions and Future Directions

CONCLUSIONS

Regulated endocytosis is critical to many cellular processes including cell growth, cell differentiation, and protein quality control. Previously, we demonstrated that a family of proteins in yeast called ARTs function to target ubiquitin ligase activity to specific plasma membrane (PM) proteins in order to regulate endocytosis. Here, we show that Art1 activity is mediated by a phosphoregulatory cycle, including 1) phosphoinhibition by a sequential repression mechanism involving TORC1-Npr1 kinases signaling pathway and 2) dephosphoactivation by Ppz phosphatases. In this negative kinase cascade, Art1 phosphoinhibition is mediated by the Npr1 kinase, which is itself negatively regulated by the activity of the TORC1 kinase. TORC1 inactivation results in dephosphorylation and PM recruitment of Npr1, where it co-localizes with Art1. Npr1 inhibits endocytosis by phosphorylation of the N-terminus of Art1, a modification which prevents Art1 PM recruitment. Thus, TORC1 tunes the abundance of transporters at the PM in response to changes in nutrient availability, demonstrating how signaling networks coordinate complex cellular processes to regulate cell growth. On the other hand, Ppz phosphatases are required for Art1-mediated PM cargo turnover. Depletion of Ppz phosphatases causes inhibition of Art1 dephosphorylation and leads to delayed cargo ubiquitination and endocytosis during stimulation conditions. Moreover, we demonstrate that Art1 translocation from tans-Golgi network (TGN) to PM by the exomer machinery is important for

Art1 activation. Art1 PM translocation and Art1-mediated cargoes endocytosis are inhibited in the exomer mutants. These findings reveal the phosphoregulatory cycle and subcellular localization regulation are important for Art1 function and provide the foundation for studying the regulation of ART family proteins.

MATERIAL AND METHODS

In vitro Protein-lipid Overlay PIP Blot Assays

Different PIPs were suspended in the resuspension buffer (250 μl Chloroform, 500 μl MeOH and 200 μl water). 2 μl of different PIPs were mixed with 8 μl spot buffer (250 μl Chloroform, 500 μl MeOH, 200 μl of 50 mM HCl and 2 μl Ponceau S) and spotted 1 μl of each PIP solution on the nitrocellulose membrane. PIP membrane was dried at 4°C in dark room overnight. The PIP membrane was incubated with blocking solution (5% non-fat dry milk in TBS with 0.1% Tween 20) for 1 hour at room temperature. After blocking, 20 μg of purified Art1 and Rsp5 in primary antibody solution (0.5% fatty-acid free BSA (Sigma) in TBS with 0.1% Tween 20) was added to the membrane and incubated overnight at 4°C. Membrane was washed by wash buffer (TBS with 0.1% Tween 20) for 5 times and incubated with primary antibody solution with αFlag M2 antibody overnight at 4°C. After 5 times of membrane washing by wash buffer, membrane was incubated with secondary antibody in blocking buffer for 1 hour at room temperature and washed 5 times with wash buffer. The blot was visualized by the Super-Signal chemiluminescent kit (Pierce).

Additional related material and methods are the same as described in Chapter 2 and Chapter 4

FUTURE DIRECTIONS

Endocytosis as an Effector of TORC1-mediated Growth Control

In the chapter 2, we elucidate a mechanism by which TORC1 controls the abundance of the Can1 arginine transporter at the PM. Importantly, by regulating the abundance of amino acid transporters at the plasma membrane, TORC1 can finely tune amino acid influx in response to various cellular signals and environmental conditions. For example, the prototype mechanism described in this study affords the cell very fine control over intracellular arginine concentration: Can1 is stabilized at the PM during starvation conditions but Can1 endocytosis is activated when the cell is nutrient replete. Additional studies will be required to determine how signals upstream of TORC1 are integrated to control endocytosis, but the reported canavanine and thialysine hypersensitivity phenotypes reported for *Δrheb1* yeast strains indicate that the signals are integrated upstream of Rheb (Holz et al., 2005; Urano et al., 2000). Furthermore, proteomic analysis of Npr1 indicates that it can interact not only with TORC1 but also with Snf1 (Breitkreutz et al., 2010), suggesting that Npr1 function may integrate several modes of regulation. Thus, although our results demonstrate that regulation of endocytosis is an important branch of the TORC1 response, future studies will be required to determine how signals upstream of TORC1 as well as orthogonal signals are integrated to mediate this endocytic downregulation response.

It is intriguing to consider how the regulation of endocytosis contributes to the adaptive growth strategies mediated by TORC1 signaling. Interestingly, recent work in mammalian cells has demonstrated that nutrient transporters at the cell surface

that facilitate the influx of leucine are required for TORC1 activity (Nicklin et al., 2009). Thus, it is possible that TORC1-mediated endocytosis of amino acid transporters provides an autoinhibitory feedback loop that limits TORC1 activation (Figure 5.1A), consistent with our analysis of TORC1 signaling during a YPD shift timecourse (Figure 5.1B and C). Furthermore, the ability of TORC1 to sense misfolded proteins and respond by activating endocytosis could promote the turnover of misfolded or damaged proteins at the PM. Additionally, the role of TORC1 signaling as both a positive regulator of endocytosis and a negative regulator of autophagy is intriguing. In such an inversely-coordinated system, dampened TORC1 signaling during starvation conditions simultaneously activates autophagy and inhibits endocytosis of the arginine transporter at the PM, both of which contribute to the availability of amino acids. TORC1 coordination of two distinct membrane trafficking pathways towards a cooperative outcome is an elegant example of how signaling networks can harness complex cellular processes to regulate cell growth.

Investigate Cargo Phosphorylation as a Determinant of Art1 Recognition

We demonstrate that the phosphorylation of Art1 by Npr1 is governed by global stress response signaling pathways in order to regulate the turnover of many PM cargos. However, Art1 phosphorylation does not seem to play a role in methionine-induced uptake of another Art1 target, the methionine transporter Mup1. We hypothesize that in cases of such "acute" stimulation, cargo phosphorylation may also serve to regulate Art1 activity. It has been demonstrated that the translational

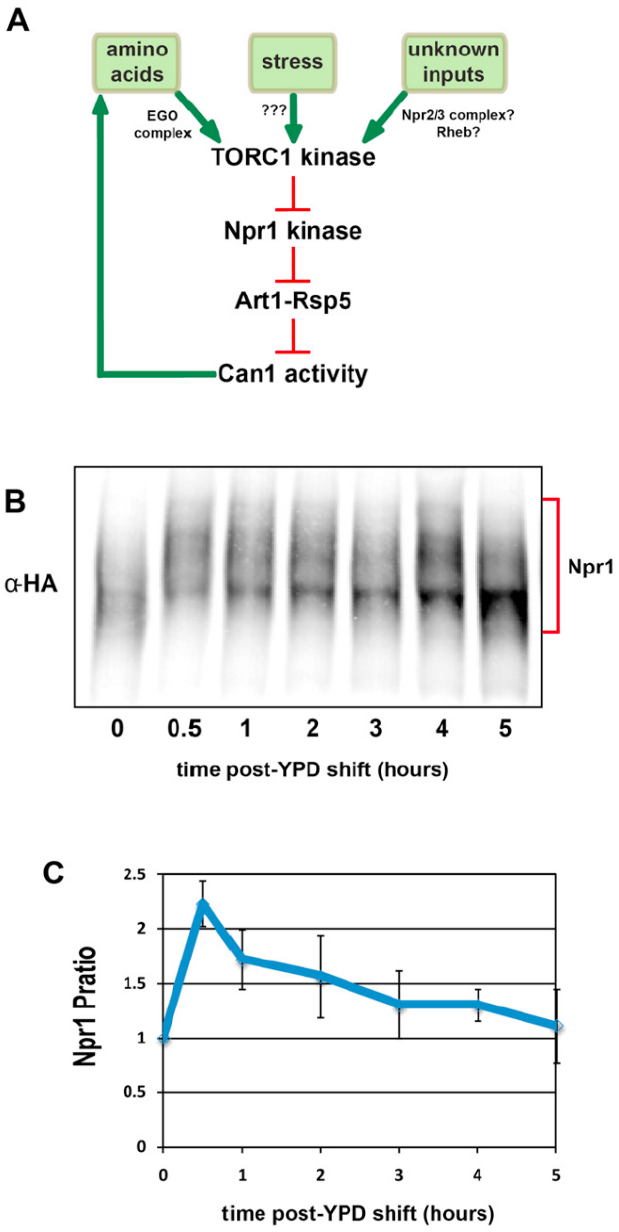
A
amino acids
stress
unknown inputs
EGO complex
???
Npr2/3 complex? Rheb?
TORC1 kinase
Npr1 kinase
Art1-Rsp5
Can1 activity
B
α-HA
Npr1
0 0.5 1 2 3 4 5
time post-YPD shift (hours)
C
Npr1 Pratio
2.5
2
1.5
1
0.5
0
0 1 2 3 4 5
time post-YPD shift (hours)

Figure 5-1

Figure 5.1. A potential model for feedback in the TORC1-Npr1-Art1 pathway (A) A model for the TORC1-Npr1-Art1 pathway that highlights a potential feedback mechanism. By this model, Can1-mediated amino acid influx would activate TORC1 signaling. Such a feedback mechanism could facilitate a highly adaptive circuit: increased TORC1 activity would trigger increased Art1 activation, which in turn would decrease influx of amino acids and thus decrease TORC1 signaling. In the other direction, loss of TORC1 activity would inactivate Art1, causing a stabilization of amino acid transporters at the surface with the potential to increase amino acid uptake and activate TORC1 signaling. (B) Analysis of Npr1 phosphorylation in response to a YPD shift timecourse. (C) Quantitation of results in (B).

control of Gap1 plays a minor role for its response to stimuli while posttranslational control is the key regulatory mechanism (Stanbrough and Magasanik, 1995). Furthermore, in the previous reports, different posttranslational modifications after cargo stimulation have been observed (Kelm et al., 2004) and phosphorylation is a prerequisite for endocytosis of these cargoes (Hicke et al., 1998).

To examine the relationship between cargo phosphorylation and Art1 recognition during acute stimulation, we will first perform phosphoprofiling analysis of cargo proteins during stimulated uptake. If candidate phosphosites are identified, we will perform functional analysis and trafficking assays on phospho-point mutants of the cargo. Finally, if candidate phosphosites on cargo are identified, we will perform biochemical experiments to determine if cargo phosphorylation specifies ART interaction. This will be done either by co-immunoprecipitation, yeast two-hybrid, or protein complementation assays.

In addition, the Art1 recognition element lies in the N-terminal cytosolic tail of Can1 (Lin et al., 2008). If cargo phosphoprofiling does not reveal candidate phosphosites, we will mutate all Ser/Thr residues in the N-terminal cytosolic tail to determine if phosphorylation may be required for cargo turnover. If crucial phosphosites are identified in cargo and shown to mediate ART interaction, then it will be important to identify the cargo protein kinase. To identify candidate cargo kinases, we will first test known permease kinases for their ability to phosphorylate specific cargo. Proteomic analysis of cargo interacting proteins can also be used to identify potential cargo kinases. These experiments may help identify specific cargo

protein kinases, which could ultimately provide another mechanism of ART-cargo specificity.

Two-step Phosphorylation of Art1

We demonstrated that loss of Npr1 *in vivo* causes a bandshift that cannot be reconstituted *in vitro* (Figure 2.4J). By using point mutagenesis, we were able to determine that the bandshift is the result of phosphorylation at a C-terminal residue, T619 (Figure 2.7I). T619 is a proline-directed phosphorylation site, and thus is not a substrate for Npr1 phosphorylation (Prosser et al., 2010). In addition, the alanine substitution of T619 gives a canavanine resistant phenotype (Figure 5.2A), which suggests that this residue is also important of Art1 activity regulation. However, phosphorylation at T619 is regulated by Npr1 (Figure 2.7C). We proposed two models that might explain these observations (Figure 5.2B). Based on our model, we will first try to identify this second Art1 regulating kinase. Since this Art1 C-terminal kinase is a proline-directed kinase and there are only limited amount of proteins in this kinase family, we can adapt the same strategy used in the phosphatase screen to identify the potential Art1 C-terminal kinase. After identifying and characterizing the kinase, we will also be interested in understanding whether there is cross talk between the N-terminus and C-terminus phosphorylations.

Art1-Rsp5 Complex Binds to PI(4,5)P_2 *in vitro*

Although our results suggest that the exomer complex may play a role in transporting Art1 from the TGN to the PM, how Art1 maintains its PM localization is

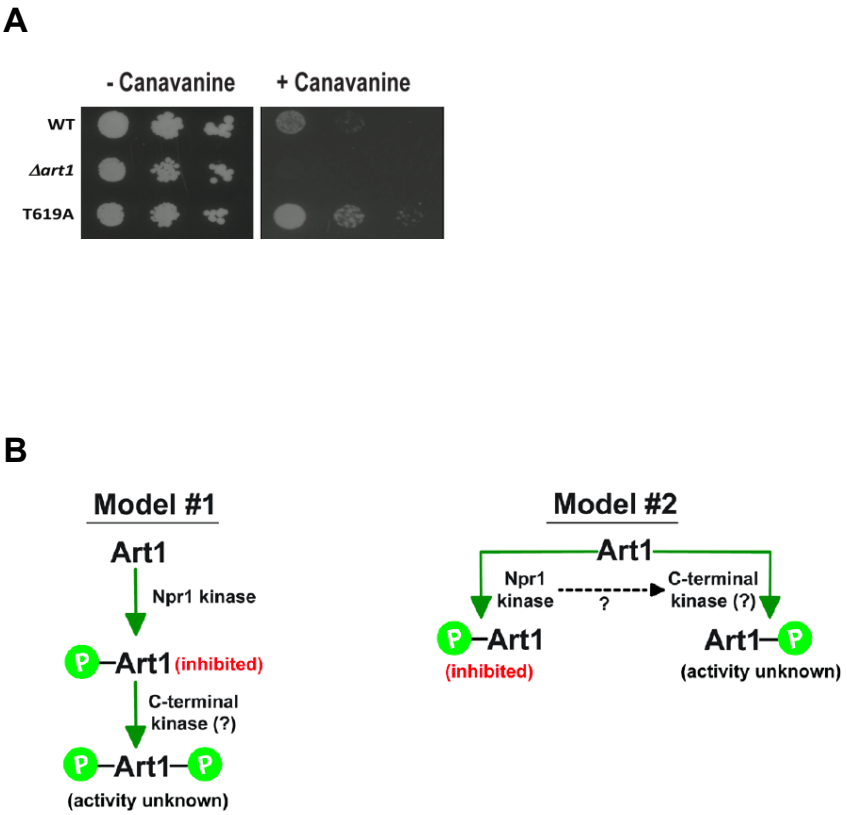
A
- Canavanine
+ Canavanine
WT
Δart1
T619A
B
Model #1
Art1
Npr1 kinase
P–Art1 (inhibited)
C-terminal kinase (?)
P–Art1–P
(activity unknown)
Model #2
Art1
Npr1 kinase
?
C-terminal kinase (?)
P–Art1
(inhibited)
Art1–P
(activity unknown)

Figure 5-2

Figure 5.2. Art1 is regulated by 2 kinases (A) Thr619 alanine substitution mutant allele of Art1 and Δ*art1* were analyzed for growth in the presence of canavanine. (B) Two potential models for Art1 2-step phosphorylation: 1) Followed by Npr1 kinase-mediated N terminus phosphorylation of Art1, another C terminus kinase then can phosphorylate Art1; 2) Art1 can be phosphorylated by two kinases at N and C terminus independently. However, the N terminus Npr1 kinase may have crosstalk to the C terminus phosphorylation.

still largely unknown. Upon stimulation, Art1 traffics to the PM and forms small transient patches. These Art1 patches differ from PM subdomains that contain Can1 (Pil patches) or endocytic machinery (Ede1 patches) in terms of size, localization, and stability (data not shown), suggesting the Art1 PM association occurs independent of these subdomains. In mammalian cells, β-arrestin and arrestin3 can bind to phosphoinositides, an interaction that appears to be required for β_2-adrenergic receptor endocytosis (Gaidarov et al., 1999). Based on these observations, we hypothesized that Art1 interacts with phosphoinositides and that such an interaction could play a role for Art1 association with the PM.

It is well-established that phosphoinositides (PIPs) are produced by specific PI-kinases that localize to specific membrane compartments in the cell (Behnia and Munro, 2005). Abolishing these kinases can spatially deplete PIPs in a compartment-specific manner. To test if Art1 membrane association is PIP-dependent, I adopted a genetic approach by taking advantage of temperature-sensitive alleles of yeast PI kinases known to control PIP levels on the Golgi (*pik1^{ts}*) and PM (*stt4^{ts}*, *mss4^{ts}*) (Baird et al., 2008). However, during heat-shock stimulation, Art1 will also be activated and recruited to the PM. Therefore, when we tested Art1 localization in these mutant strains under the non-permissive temperature, we could still see Art1 PM recruitment (data not shown). This result does not rule out the possibility that Art1 translocates to the PM before the PIPs are depleted from the cells.

To determine if Art1 could associate with the PM by binding to PIPs, I performed a PIP binding assay. PIP strips were incubated with Art1-Rsp5 complex

and subjected to immunoblot for detecting its PIP binding specificity. Among all the PIP species tested, Rsp5-Art1 complex binds to PI(4,5)P_2 specifically (Figure 5.3), suggesting the protein complex may associate with the PM through binding to PI(4,5)P_2. Additionally, neither the single Art1 nor Rsp5 has the ability to bind to any PIP, which suggests that the formation of the complex is critical for its PIP binding ability. These results also imply the existence of a conformational change that may expose the PIP binding domain of the protein to the membrane during the formation of the Art1-Rsp5 complex. We propose a model that under stimulation, exomer complex can transport Art1-Rsp5 complex from the TGN to the PM. After the Art1-Rsp5 complex reaches the PM, it starts to ubiquitinate and turnover the membrane proteins. By binding to PI(4,5)P_2, the complex can associate with the PM and locally triggers cargo endocytosis. In order to prevent excessive cargo endocytosis, Npr1 will then be recruited to the PM and phosphorylates Art1 to eject it from the PM to finish this regulatory cycle.

It has been reported that the N-terminus of Rsp5, the C2 domain, has the affinity to bind to all species of PIPs *in vitro* (Dunn et al., 2004). However in our PIP binding assay, Rsp5 bound very weakly to PI3P (Figure 4.5A). Based on these observations, I proposed that there might exist some auto-inhibitory domains in Rsp5 that serve to block its C2 domain from binding to PIPs. After binding to Art1 through the WW domains, which is in close proximity to the N terminal C2 domain (Lin et al., 2008), Rsp5 may not only exposes its C2 domain to the PIPs but also gains the binding specificity to PI(4,5)P_2. On the other hand, this PIP binding ability of the Art1-Rsp5

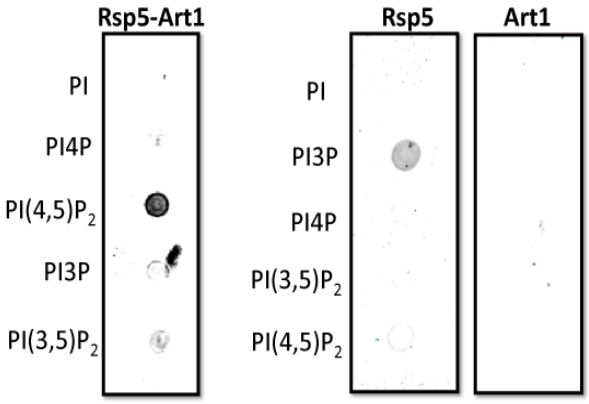
Rsp5-Art1
PI
PI4P
PI(4,5)P2
PI3P
PI(3,5)P2
Rsp5
Art1
PI
PI3P
PI4P
PI(3,5)P2
PI(4,5)P2

Figure 5-3

Figure 5.3. Art1-Rsp5 complex binds to PI(4,5)P_2 *in vitro.* Purified recombinant Art1, Rsp5 and Art1-Rsp5 complex were incubated with PIPs strips and then subjected to Western blot to detect the PIPs binding ability of each protein.

complex could be contributed by Art1, rather than Rsp5. Protein conformational changes could occur after forming the complex with Rsp5, which could promote its binding to $PI(4,5)P_2$. Further studies will be required for a better understanding of the mechanism of how Rsp5 and Art1 bind to $PI(4,5)P_2$.

Determine the Art1 Membrane Interaction Domain

Based on our results, Art1 can be divided into 3 general regions: the N terminus of Art1 (amino acids 1-134) which undergoes phosphoregulation by Npr1, the predicted arrestin domain (amino acids 135-397), and a C terminal region (amino acids 398-818) which includes the PY motifs and critical proline-directed phosphorylation sites. To determine if any of these regions are sufficient for membrane interaction, we will express these domains fused to GFP in yeast cells and score localization to both PM and Golgi. Once a minimal membrane interaction domain is established, we can use binding assays to test if specific lipids are sufficient to mediate the interaction. These results may help identify novel membrane interaction motifs within Art1. For any membrane interaction domain that is identified it will be interesting to assess the level of conservation within the ART family of proteins.

Given the fact that Art1 PM recruitment is highly regulated and may be subject to control by various signaling pathways, it is possible that we will not be able to isolate a fragment of Art1 sufficient for membrane recruitment. If this is the case, we will examine the functional consequences of adding lipid modification motifs (palmitoylation and/or myristoylation) to Art1, which should result in constitutive PM localization independent of cellular signals. Once established, I will determine

the functional effect of constitutive Art1 PM localization using canavanine sensitivity and cargo trafficking assays.

REFERENCES

Baird, D., Stefan, C., Audhya, A., Weys, S., and Emr, S.D. (2008). Assembly of the PtdIns 4-kinase Stt4 complex at the plasma membrane requires Ypp1 and Efr3. J Cell Biol *183*, 1061-1074.

Behnia, R., and Munro, S. (2005). Organelle identity and the signposts for membrane traffic. Nature *438*, 597-604.

Breitkreutz, A., Choi, H., Sharom, J., Boucher, L., Neduva, V., Larsen, B., Lin, Z., Breitkreutz, B., Stark, C., Liu, G.*, et al.* (2010). A global protein kinase and phosphatase interaction network in yeast. Science *328*, 1043-1046.

Dunn, R., Klos, D.A., Adler, A.S., and Hicke, L. (2004). The C2 domain of the Rsp5 ubiquitin ligase binds membrane phosphoinositides and directs ubiquitination of endosomal cargo. J Cell Biol *165*, 135-144.

Gaidarov, I., Krupnick, J.G., Falck, J.R., Benovic, J.L., and Keen, J.H. (1999). Arrestin function in G protein-coupled receptor endocytosis requires phosphoinositide binding. EMBO J *18*, 871-881.

Hicke, L., Zanolari, B., and Riezman, H. (1998). Cytoplasmic tail phosphorylation of the alpha-factor receptor is required for its ubiquitination and internalization. J Cell Biol *141*, 349-358.

Holz, M.K., Ballif, B.A., Gygi, S.P., and Blenis, J. (2005). mTOR and S6K1 mediate assembly of the translation preinitiation complex through dynamic protein interchange and ordered phosphorylation events. Cell *123*, 569-580.

Kelm, K.B., Huyer, G., Huang, J.C., and Michaelis, S. (2004). The internalization of yeast Ste6p follows an ordered series of events involving phosphorylation, ubiquitination, recognition and endocytosis. Traffic *5*, 165-180.

Lin, C.H., MacGurn, J.A., Chu, T., Stefan, C.J., and Emr, S.D. (2008). Arrestin-related ubiquitin-ligase adaptors regulate endocytosis and protein turnover at the cell surface. Cell *135*, 714-725.

Nicklin, P., Bergman, P., Zhang, B., Triantafellow, E., Wang, H., Nyfeler, B., Yang, H., Hild, M., Kung, C., Wilson, C., *et al.* (2009). Bidirectional transport of amino acids regulates mTOR and autophagy. Cell *136*, 521-534.

Prosser, D.C., Whitworth, K., and Wendland, B. (2010). Quantitative analysis of endocytosis with cytoplasmic pHluorin chimeras. Traffic *11*, 1141-1150.

Stanbrough, M., and Magasanik, B. (1995). Transcriptional and posttranslational regulation of the general amino acid permease of Saccharomyces cerevisiae. J Bacteriol *177*, 94-102.

Urano, J., Tabancay, A.P., Yang, W., and Tamanoi, F. (2000). The Saccharomyces cerevisiae Rheb G-protein is involved in regulating canavanine resistance and arginine uptake. J Biol Chem *275*, 11198-11206.

Table S1. Strains used in this study

Strain	Genotype	Source
SEY6210	*MATα leu2-3, 112 ura3-52 his3- Δ200 trp1-Δ901 lys2-801 suc2- Δ9*	Robinson et al., 1988
SEY6210.1	*MATa leu2-3, 112 ura3-52 his3- Δ200 trp1-Δ901 lys2-801 suc2- Δ9*	Robinson et al., 1988
BY4741	*MATa ura3-Δ0 his3-Δ1 leu2-Δ0 met15-Δ0*	ResGen™ Collection
Δtco89	*Δtco89::*KanMX6 (BY4741)	ResGen™ Collection
Δbit61	*Δbit61::*KanMX6 (BY4741)	ResGen™ Collection
Δavo2	*Δavo2::*KanMX6 (BY4741)	ResGen™ Collection
Δnpr1	*Δnpr1::*KanMX6 (BY4741)	ResGen™ Collection
Δnnk1	*Δnnk1::*KanMX6 (BY4741)	ResGen™ Collection
Δfmp48	*Δfmp48::*KanMX6 (BY4741)	ResGen™ Collection
Δrck1	*Δrck1::*KanMX6 (BY4741)	ResGen™ Collection
Δsky1	*Δsky1::*KanMX6 (BY4741)	ResGen™ Collection
Δksp1	*Δksp1::*KanMX6 (BY4741)	ResGen™ Collection
Δatg1	*Δatg1::*KanMX6 (BY4741)	ResGen™ Collection
JMY527	*Δnpr1::*HIS3MX6 (SEY6210)	This study
PHY501	*Δnpr1*::KanMX6 *Δtco89*::HIS3MX6 (BY4741)	This study
CLY461	*Δart1*::HIS3MX6 (SEY6210.1)	Lin et al., 2008
PHY1	*Δnpr1*::HIS3MX6 *Δart1*::TRP1MX6 (SEY6210)	This study
JMY827	*Δarg4::*KanMX6 *ART1::*6xHIS-TEV-3xFLAG-TRP1MX6 (SEY6210)	This study
JMY898	*Δnpr1::*HIS3MX6 (JMY827)	This study
Δppq1	*Δppq1::*KanMX6 (BY4741)	ResGen™ Collection
Δptc1	*Δptc1::*KanMX6 (BY4741)	ResGen™ Collection
Δppg1	*Δppg1::*KanMX6 (BY4741)	ResGen™ Collection
Δppz1	*Δppz1::*KanMX6 (BY4741)	ResGen™ Collection

Table S1. Strains used in this study (continued)

Strain	**Genotype**	**Source**
Δyvh1	*Δyvh1::*KanMX6 (BY4741)	ResGen™ Collection
Δhal3	*Δhal3::*KanMX6 (BY4741)	ResGen™ Collection
PHY147	*Δppz1*::HIS3MX6 (SEY6210)	This study
PHY151	*Δppz2*::TRP1MX6 (SEY6210)	This study
PHY647	*Δppz1*::HIS3MX6 *Δppz2::TRP1MX6* (SEY6210)	This study
NBY40	Mup1-pH*::*KanMX6 (SEY6210.1)	This study
PHY743	Mup1-pH*::*KanMX6 Δ*ppz1*::HIS3MX6 Δ*ppz2*::TRP1MX6 (SEY6210)	This study
PHY716	Δ*ppz1*::HIS3MX6 Δ*ppz2*::TRP1MX6 Δ*npr1*::HIS3MX6 (SEY6210.1)	This study
PHY726	Ppz1-GFP::TRP1MX6 (SEY6210)	This study
PHY727	*Δhal3*::HIS3MX6 (SEY6210)	This study
PHY728	*Δvhs3*::HIS3MX6 (SEY6210)	This study
PHY729	*Δvhs3*::HIS3MX6 *Δhal3::KanMX6* (SEY6210.1)	This study
JMY78	Mup1-HTF::TRP1MX6 (SEY6210)	This study
JMY212	Mup1-HTF::TRP1MX6 Δ*art1*::HIS3MX6 (SEY6210)	This study
PHY739	Δ*ppz1*::HIS3MX6 Δ*ppz2*::TRP1MX6 Mup1-HTF::TRP1MX6 (SEY6210.1)	This study
PHY746	Ppz1-MARS::TRP1MX6 (SEY6210)	This study
CFY207	Δ*chs5*::TRP1MX6 (SEY6210.1)	This study
CFY258	*Δbud7::*KanMX6 (SEY6210.1)	This study
Strain	Genotype	Source
CFY260	*Δbch1::*KanMX6 (SEY6210.1)	This study
CFY256	*Δchs6::*KanMX6 (SEY6210.1)	This study
PHY232	Δ*chs5*::TRP1MX6 Δ*npr1*::HIS3MX6 (SEY6210.1)	This study
PHY233	*Δbch1::*KanMX6 Δ*npr1*::HIS3MX6 (SEY6210.1)	This study

Table S2. Plasmids used in this study

Plasmid	Description	Source
pCHL571	pRS416-P$_{CAN1}$-*CAN1*-GFP	Lin et al., 2008
pCHL642	pRS416-P$_{MUP1}$-*MUP1*-GFP	Lin et al., 2008
pSR21	pRS416-P$_{FUR4}$-*FUR4*-GFP	Lin et al., 2008
pJAM463	pRS415-P$_{NPR1}$-*3xFLAG-NPR1*	This study
pJAM478	pRS415-P$_{NPR1}$-*3xFLAG-npr1 K467R*	This study
pJAM479	pRS415-P$_{NPR1}$-*3xFLAG-npr1 G581W*	This study
pJAM480	pRS415-P$_{NPR1}$-*3xFLAG-npr1 D561A*	This study
pJAM536	pRS415-P$_{CPY}$-*3xFLAG-NPR1*	This study
pJAM537	pRS415-P$_{ADH1}$-*3xFLAG-NPR1*	This study
pJAM538	pRS415-P$_{TDH3}$-*3xFLAG-NPR1*	This study
pCHL641	pRS416-P$_{ART1}$-*ART1*-3xHA	Lin et al., 2008
pJAM367	pRS416-P$_{ART1}$-*ART1*-3xFLAG	This study
pCHL582	pRS416-P$_{CAN1}$-*CAN1*-6xHis-TEV-3xFLAG	Lin et al., 2008
pJAM548	pRS415-P$_{ADH1}$-*3xFLAG-npr1 K467R*	This study
pJAM589	pRS416-P$_{ART1}$-*art1*-(S/T 79, 82-85, 96, 99, 100 A)-3xFLAG	This study
pCHL639	pRS416-P$_{ART1}$-*ART1*-GFP	Lin et al., 2008
pJAM599	pRS416-P$_{ART1}$-*art1*-(S/T 79, 82-85, 96, 99, 100 A)-GFP	This study
425-GFP-CPS	pRS425-P$_{CPS}$-GFP-CPS	This study
pJAM556	pRS415-P$_{TDH3}$-*ART1-HA*	This study